AD-A097 178 LAMONT-DOHERTY GEOLOGICAL OBSERVATORY PALISADES NY F/6 8/11
TECTONICS OF ASIA AND WAVEFORM STUDIES OF THE VELOCITY AND Q ST--ETC(U)
OCT 80 L R SYKES, L J BURDICK F49620-79-C-0021

UNCLASSIFIED AFOSR-TR-81-0285 NL

1 OF 2
AD A
097178

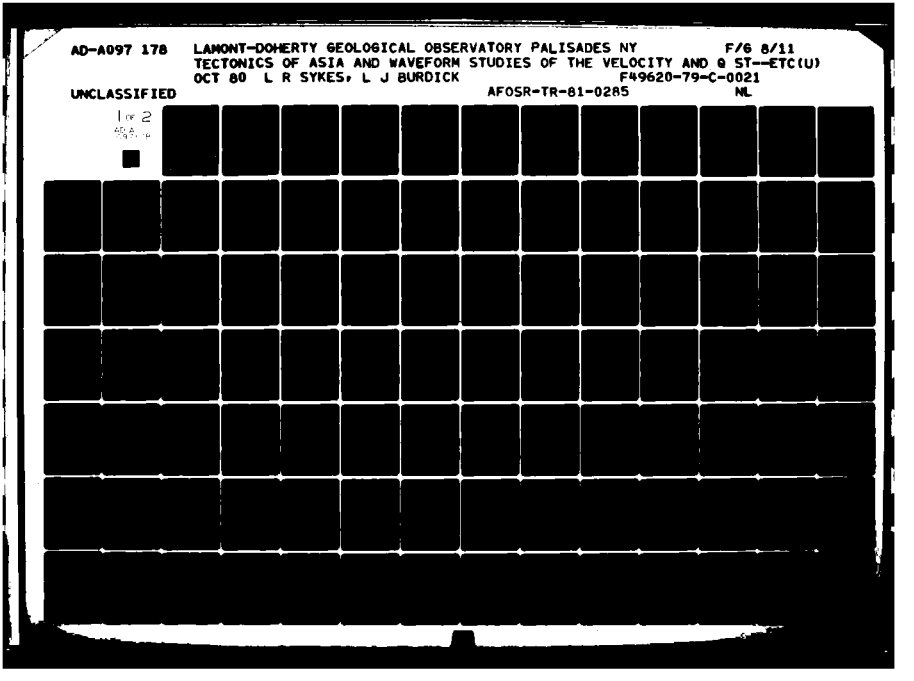

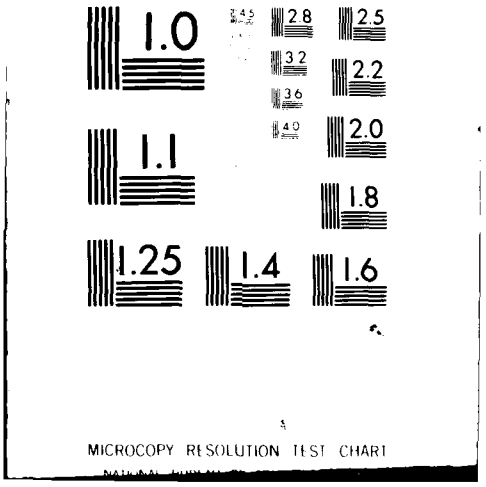
1.0
2.8
2.5
3.2
2.2
3.6
4.0
2.0
1.1
1.8
1.25
1.4
1.6
MICROCOPY RESOLUTION TEST CHART

AFOSR-TR- 81-0285

LEVEL II

7

ANNUAL TECHNICAL REPORT

AD A097178

ARPA Code Number:	3291-32
Program Code:	0D60
Name of Contractor:	Columbia University (Lamont-Doherty Geological Observatory)
Date of Contract:	1 September 1979
Contract Expiration Date:	31 October 1980
Amount of Contract:	$146,611
Contract Number:	F 49620-79-C-0021
Principal Investigators:	Dr. Lynn R. Sykes (914-359-2900) Dr. Lawrence J. Burdick (914-359-2900)
Short Title:	Part 1 - "Tectonics of Asia" Part 2 - "Velocity and Q Structure"

Supported by

Advanced Research Projects Agency (DOD)

and

Monitored by AFOSR Under Contract #F 49620-79-C-0021

DTIC
ELECTE
APR 2 1981
S D
D

DTIC FILE COPY

The views and conclusions contained in this document are those of the authors and should not be interpreted as necessarily representing the official policies, either expressed or implied, of the Defence Advanced Research Projects Agency, or the U.S. Government.

814 2 046

Approved for public release;
distribution unlimited.

TABLE OF CONTENTS

Accession For	
NTIS GRA&I	☒
DTIC TAB	☐
Unannounced	☐
Justification	
By	
Distribution/	
Availability Codes	
Dist	Avail and/or Special
A	

Part I: Tectonics and Wave Propagation in Central Asia

TECHNICAL SUMMARY

1. Surface-wave analysis proves to be an effective way of determining focal mechanisms for earthquakes with relatively small magnitudes. By comparing the surface waves of one event to another nearby event, the effects of the epicenter-to-station path can be largely reduced. This is true even when most paths cross or lie along zones of complicated deformation. Two events in the northern Arabian Sea have similar mechanisms and can be interpreted as earthquakes along transform features between the Indian and Arabian plates.

→ pg. 18

A. Focal Mechanisms of Small-Magnitude Earthquakes in Central Asia Determined from Surface-Wave Analysis

Determination of focal mechanisms for small-magnitude earthquakes in Central Asia aids in the understanding of the tectonic framework that characterizes this area. For earthquakes with magnitudes greater than about 5.5, a plot of first-motion data on a focal sphere usually provides adequate constraint on the nodal planes. For smaller magnitude events, however, first-motions are not well-recorded at a sufficient number of stations to give a well-determined solution. Surface waves, on the other hand, are usually well recorded to distances of approximately 70° for events with magnitudes as low as 4.5. As the surface waves contain information on the depth and source parameters, it is thus possible by proper

AIR FORCE OFFICE OF SCIENTIFIC RESEARCH (AFSC)
NOTICE OF TRANSMITTAL TO DDC
This technical report has been reviewed and is approved for public release IAW AFR 190-12 (7b).
Distribution is unlimited.
A. D. BLOSE
Technical Information Officer

analysis to determine the focal mechanisms and depths of earthquakes with relatively small magnitudes.

Under this contract an analysis was made of the focal mechanisms of two earthquakes located in the northern Arabian Sea. One event occurred at the northern end of the Owen fracture zone (30 March 1966, M_b = 5.3); the other occurred along the Murray ridge about 300 km to the east-northeast of the first event (9 November 1968, M_s = 5.1). These shocks are located in a region of complicated tectonics near the triple junction for the Indian, Arabian, and Eurasian plates. The results of the surface-wave analysis show that the nodal planes for the two events are similar.

Method of Analysis. The method of analysis used in this study is a comparative event technique. The observed difference in phase and the ratio of amplitude spectra between two nearby events are compared to theoretical values to determine simultaneously the strike, slip, dip, depth and moment of both events. In addition, the amplitude spectrum of each event should agree with the respective theoretical spectrum, and the final solution should not grossly violate whatever limited first-motion data are available. In this method, which has been most extensively developed by D. Weidner and A. Kafka (Weidner, 1972; Kafka and Weidner, 1979; Kafka, 1980), the effects of epicenter-to-station paths on the observed spectra are largely eliminated since the paths are nearly identical. If the focal mechanism of one of the two events being compared is independently known, this event in essence provides path corrections for the second event, and the method can be termed a master-event technique.

For each earthquake copies of seismograms were made from WWSSN film chips for stations with recorded surface waves. An attempt was made to

obtain records from the same station for both shocks in as many cases as possible. The seismograms were then digitized and interpolated at equal intervals of slightly less than 1 sec. Next the group velocity dispersion was determined using the technique of Dziewonski et al. (1969) and this information was used to filter the digitized record with a filter designed to pass those frequencies arriving at a particular time (i.e., time-variable filtering, Landisman et al., 1969). The values of amplitude and phase at 5 frequencies were obtained from the fourier transform of the filtered record. The values of amplitude are corrected for instrument response and attenuation ($\gamma = 1.5 \times 10^{-6}$); while values of phase are corrected for instrument response, propagation, and the origin time - digitization time delay.

To compare the observed values to theoretical values three parameters are defined:

$$\sigma_\phi^2 = \frac{\Sigma W_i (\Delta\phi_f^{obs} - \Delta\phi_f^{t})^2}{\Sigma W_i}$$

$$\sigma_A^2 = \frac{\Sigma W_i (\log A^{obs} - \log A^{t})^2}{\Sigma W_i}$$

$$\sigma_{A1,2}^2 = \frac{\Sigma W_i (\log (A_1^{obs}/A_2^{obs}) - \log (A_1^{t}/A_2^{t}))^2}{\Sigma W_i}$$

Superscripts obs and t refer to observed and theoretical values, respectively; Aj refers to the amplitude of the jth event; $\Delta\sigma$ is the differential focal phase; and the W's are weights. The summations are taken over the appropriate stations and periods. The weights are taken as proportional to the theoretical values of amplitude.

When the theoretical and observed values are close, the residual parameters defined above are small. The best solution is found by searching through the 8-dimensional space defined by the strike, slip, dip, and depth of both events to find that set of source parameters that minimizes the residual parameters.

Results for the Northern Arabian Sea. The two earthquakes that form the event-pair for the northern Arabian Sea are associated with the Owen fracture zone and the Murray ridge, respectively (Figure 1). Pertinent information on these events is listed in Table 1. The azimuthal distribution of stations at which records were obtained for these events is shown in Figure 2. The stations are well distributed except to the south in the Indian Ocean. Our theoretical calculations of Rayleigh wave radiation patterns are based on the work of Saito (1967), and we have used the oceanic earth model of Harkrider and Anderson (1966) for the source region in all cases. Several authors (e.g. Weidner, 1972; Patton, 1978) have found that variations in the assumed earth model do not seriously affect the Rayleigh wave radiation.

Event 1 has been previously studied by Sykes (1970). He determined a fault-plane solution based on first-motion readings and the polarization of S-waves. His solution, although classified as of poor quality, is consistent with predominantly strike-slip motion in a right-lateral sense along the Owen fracture zone. Figure 3a presents the limited first-motion data for this event.

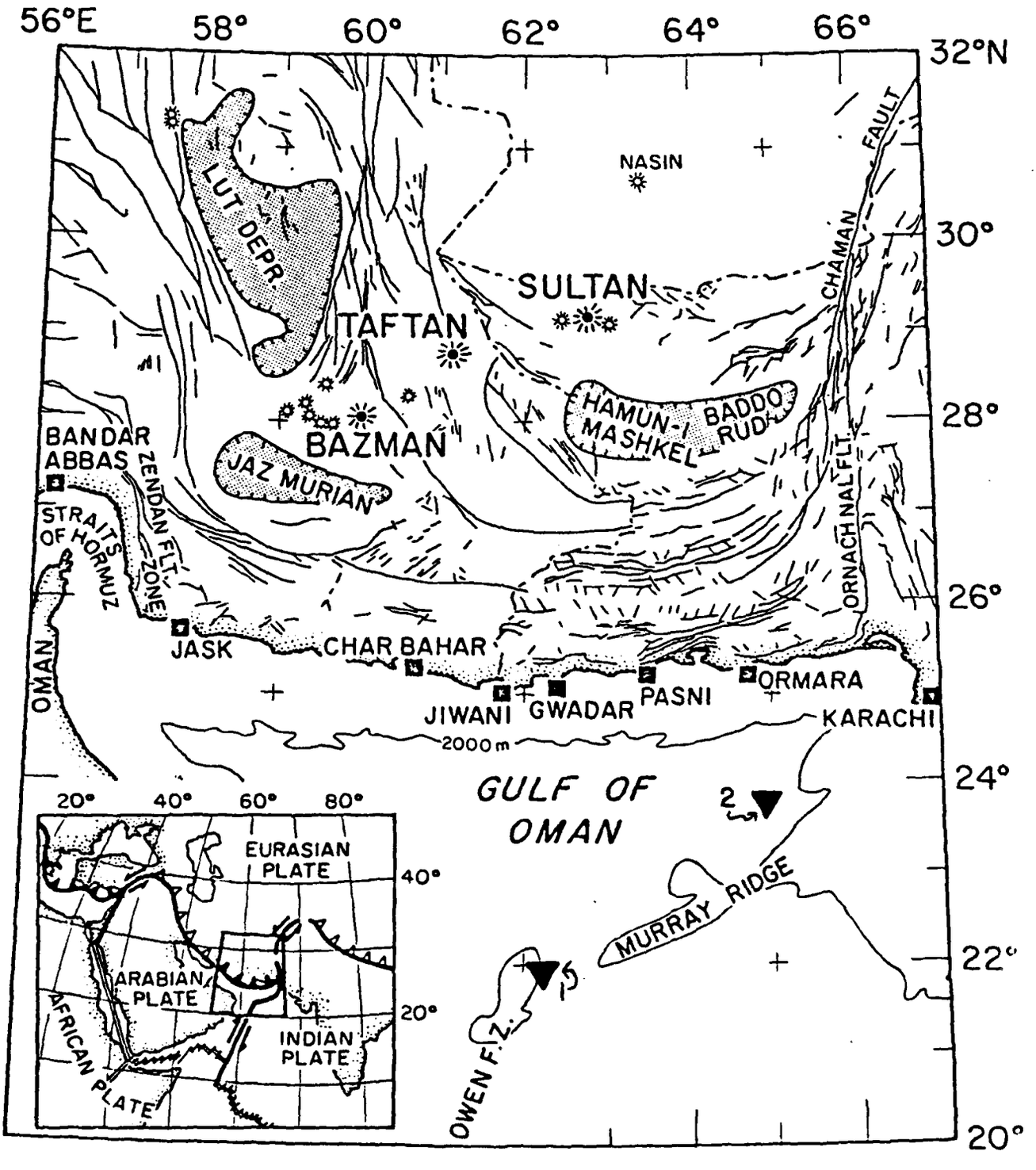

Figure 1. Tectonic setting for the two earthquakes studied. The locations of the events are indicated by the triangular symbols: 1- 30 March 1966, 2- 9 November 1968.

TABLE 1

Event	Date	Location	Depth (ISC) (km)	Magnitude
1	30 Mar 1966	Owen F.Z.; 21.87°N, 62.32°E	28	m_b = 5.3
2	9 Nov 1968	Murray Ridge; 23.79°N, 64.73°E	15	m_b = 5.1

TABLE 2

Event	Date	Depth (km)	Strike (deg)	Slip (deg)	Dip (deg)	Moment (x 10^{24} dyne-cm)
1	30 Mar 1966	20	20	345	60	5.6
2	9 Nov 1968	13	30	0	56	5.1

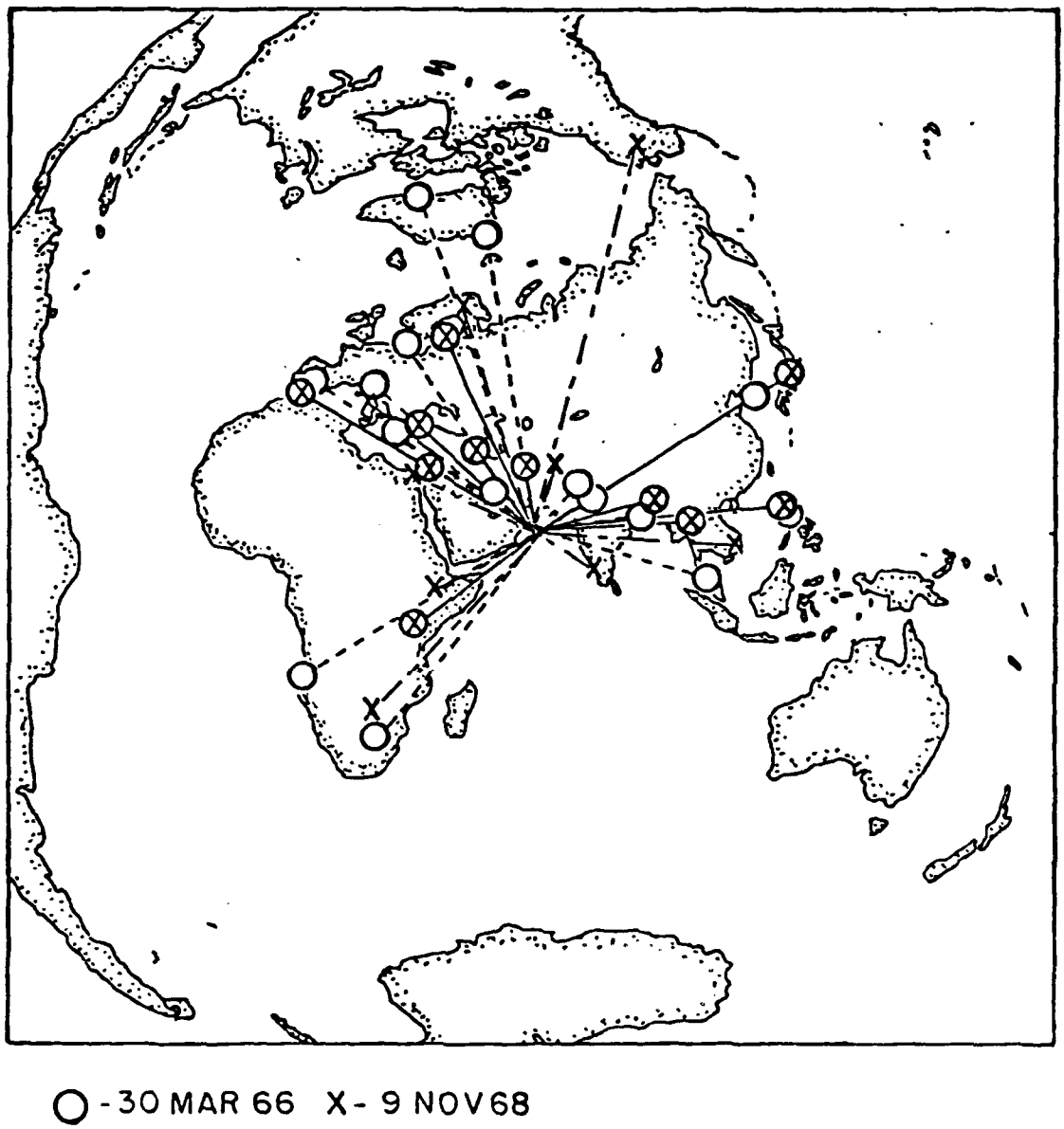

Figure 2. Locations of the stations for which seismograms were studied. The paths along which surface waves travelled to each station are shown by the dashed and solid lines. Note that many paths cross or lie along zones of complicated deformation.

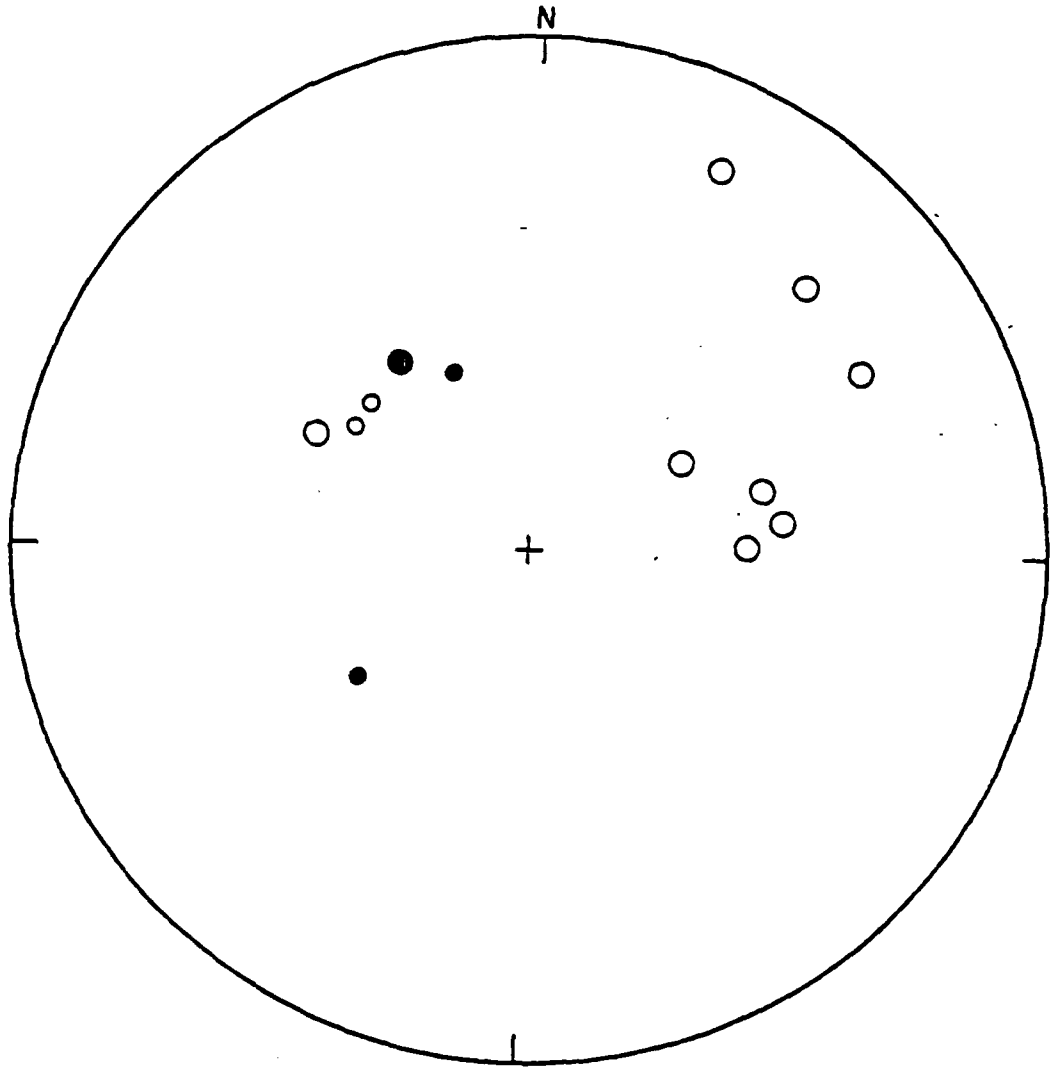

Figure 3. (a.) and (b.) Observed first-motions for the events studied. Solid symbols represent compressional first-motions while open symbols represent those with a dilatational character; crosses indicate nodal arrivals. Smaller symbols denote data of poorer quality. A lower-hemisphere projection is used.

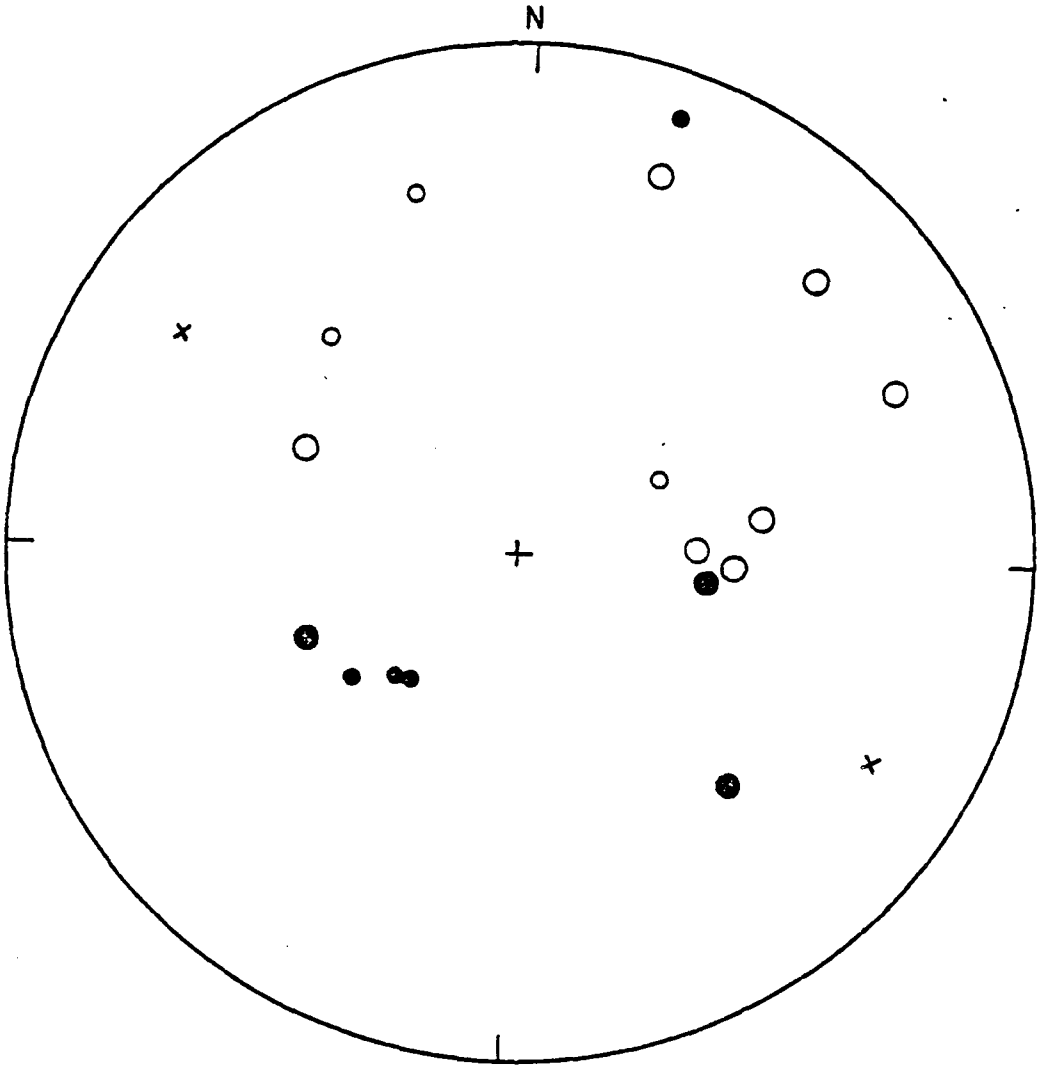

Figure 3. (b.)

The results for event 1 based on the surface wave analysis agree fairly well with Sykes' solution. Figure 4a shows the values of depth, strike, slip, and dip that minimize the three residual parameters. Most of the minima are well defined and occur at similar values for all three residual parameters. The phase information allows one to resolve the ambiguities in slip and dip that occur when only amplitude information is considered. In Figure 5 the observed amplitude as a function of azimuth at a period of 40 sec is compared to theoretical values. The agreement is good. Results for event 1 are summarized in Table 2.

The second event occurred along the Murray ridge. The Murray ridge is a bathymetric feature extending in a northeast direction from the northern end of the Owen fracture zone to the continental shelf of the Indian subcontinent. It is located in a region of complicated tectonics near the triple junction for the Arabian, Indian, and the Iranian portion of the Eurasian plates. Although the tectonic significance of the Murray ridge is not known, McKenzie and Sclater (1971) have speculated that there may be a component of spreading associated with the feature.

The results of the surface wave analysis for event 2 are shown in Figure 4b. The orientations of the nodal planes are similar to those for event 1. In Figure 6 the observed and theoretical values of amplitude are shown as a function of azimuth. As for the first event, the agreement is quite satisfactory.

In Figure 7 the observed differential phase between the two events is compared to theoretical values for the solutions derived from the surface wave data. The observed data matches well the theoretical values, especially considering that these events are separated by a distance ($\sim$ 350 km) that is large for the comparative-event style of analysis. A

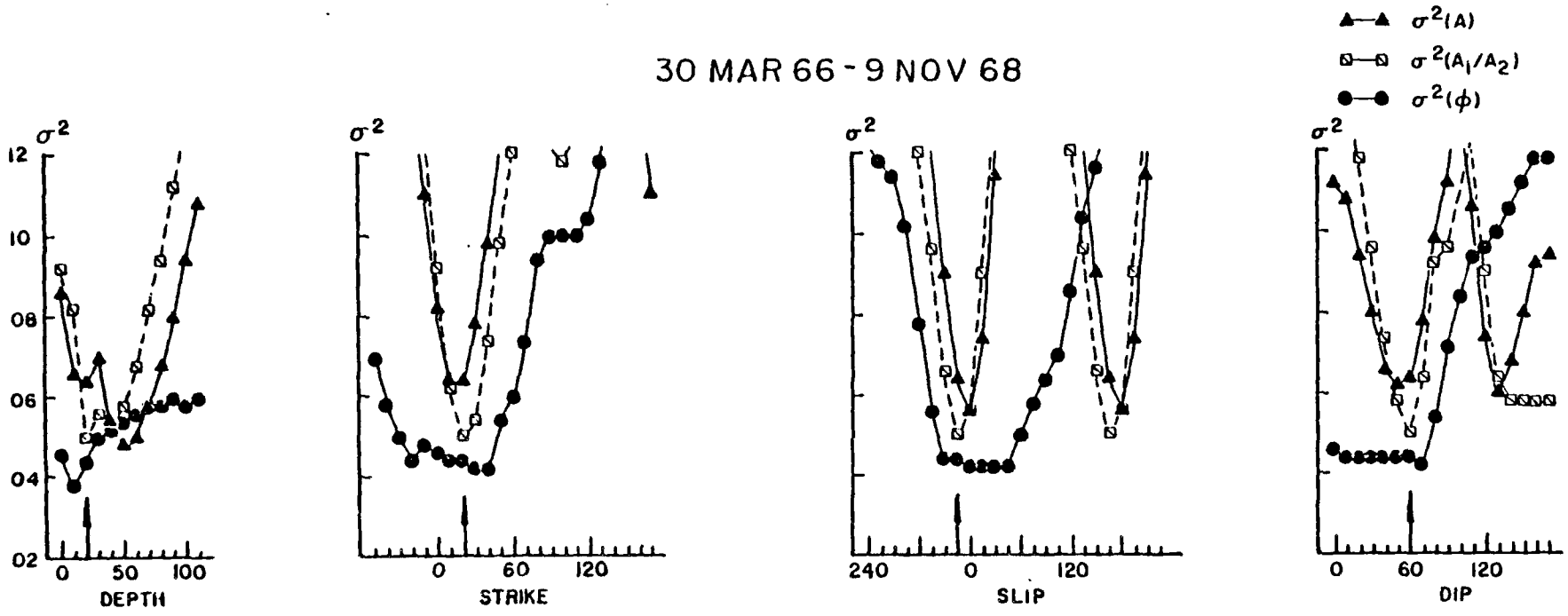

Figure 4. (a.) Variation of residual parameters as a function of depth, strike, slip and dip for the shock of 30 March 1966. See text for mathematical definition of the various residual parameters. The arrows indicate the final solution. Note how minima in the residual curves coincide near the chosen solution. The amplitude and relative amplitude data appear to have more resolving power than differential phase, but the phase data allow a choice to be made between alternate minima in the amplitude residuals for slip and dip.

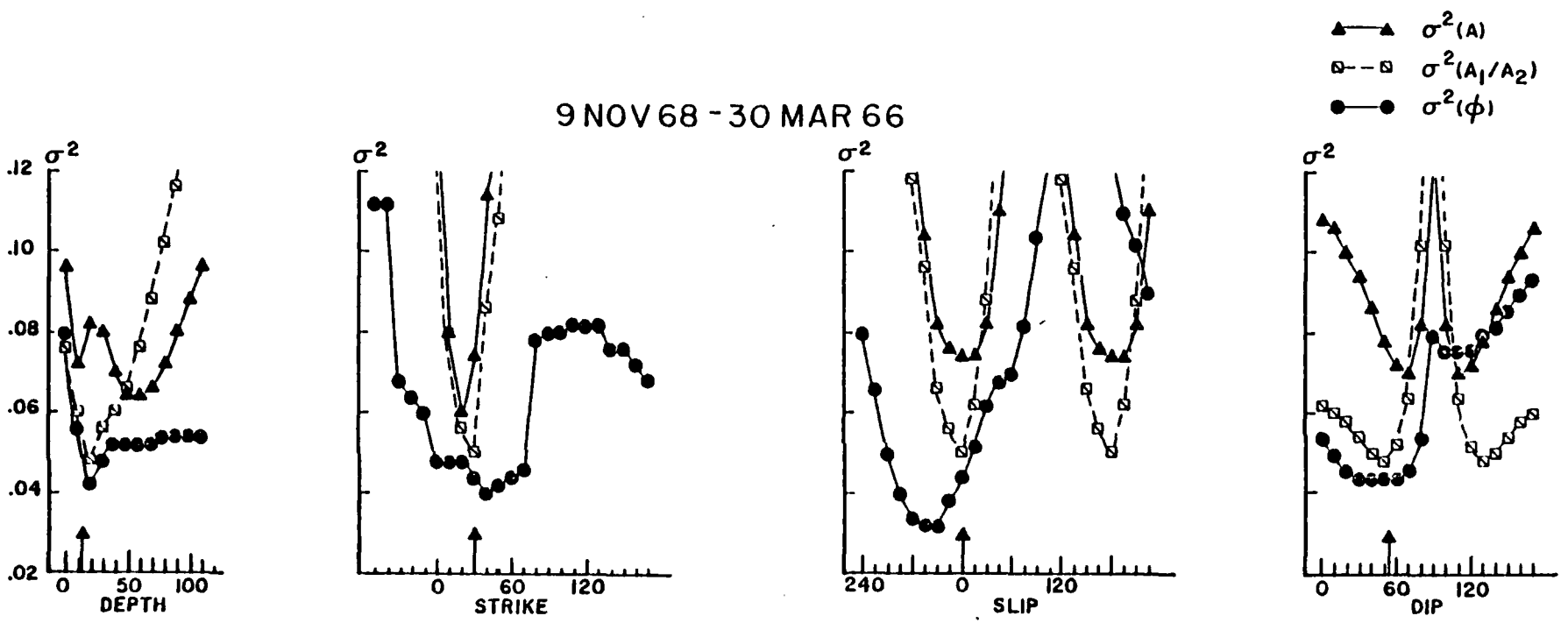

Figure 4. (b.) Same as (a) but for event of 9 November 1988. Note that the minima do not coincide quite as well for this shock indicating a solution of somewhat poorer quality.

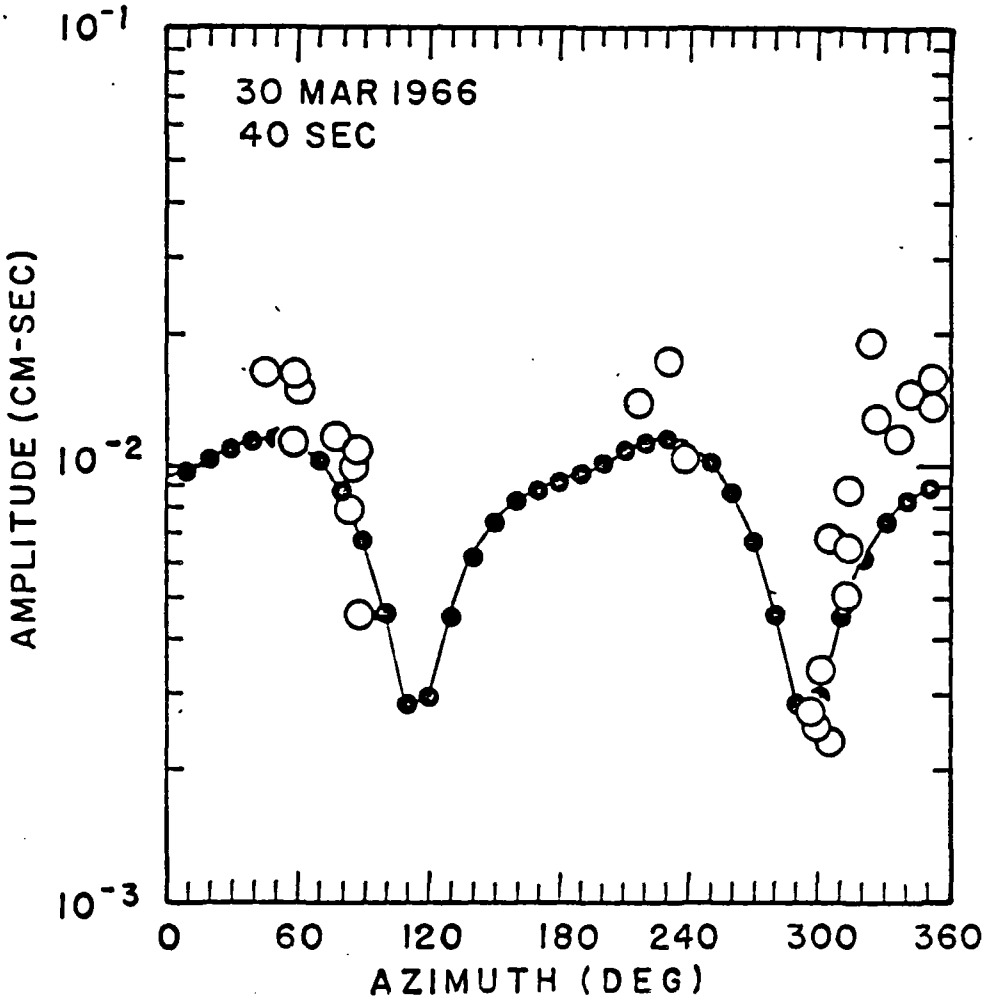

Figure 5. Comparison of the observed amplitude data with theoretical values for the final solution: 30 March 1966, 40 sec. The fit between observed and theoretical values is quite good. A better fit might be possible if more weight were given to the longer periods (40, 50 sec) at the expense of the shorter periods (20, 25, 30 sec) in the computation of residual parameters. The longer periods appear to be more stable and contain less noise.

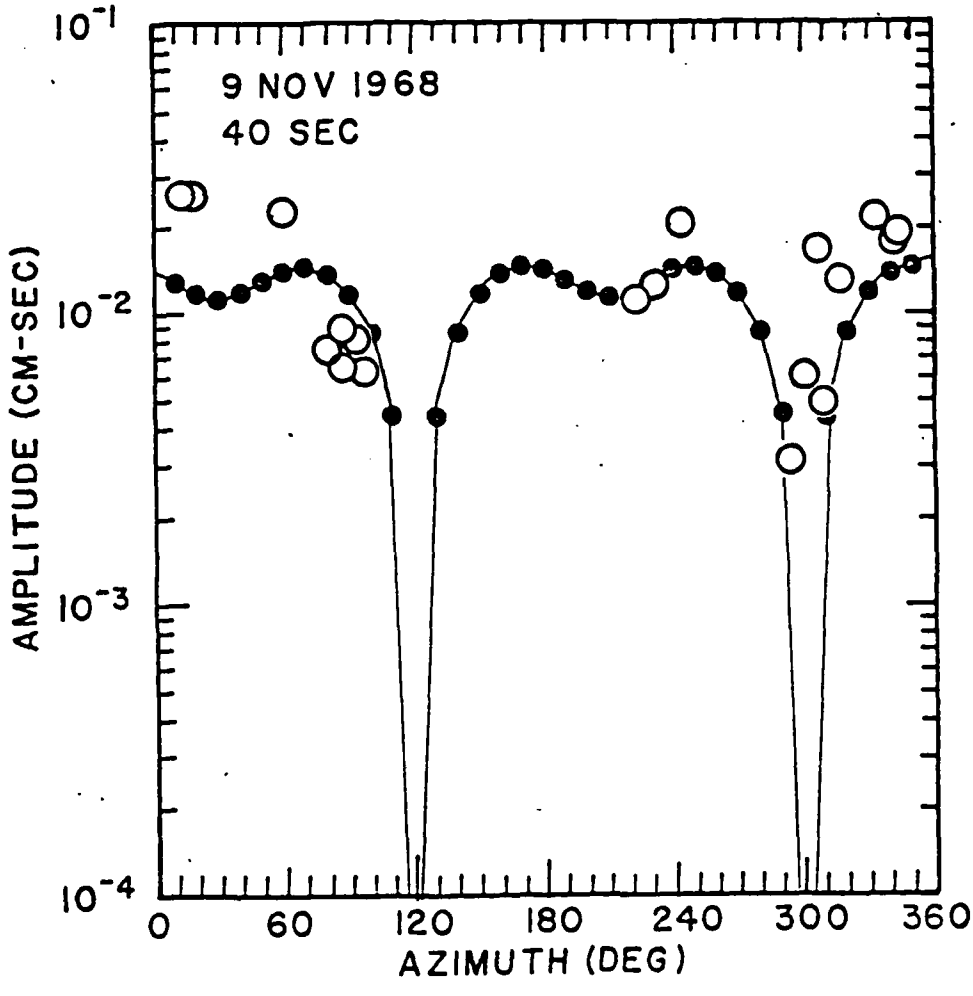

Figure 6..Comparison of the observed amplitude data with theoretical values for the final solution: 9 November 1968, 40 sec. The fit is satisfactory although not as good as for the earthquake of 30 March 1966.

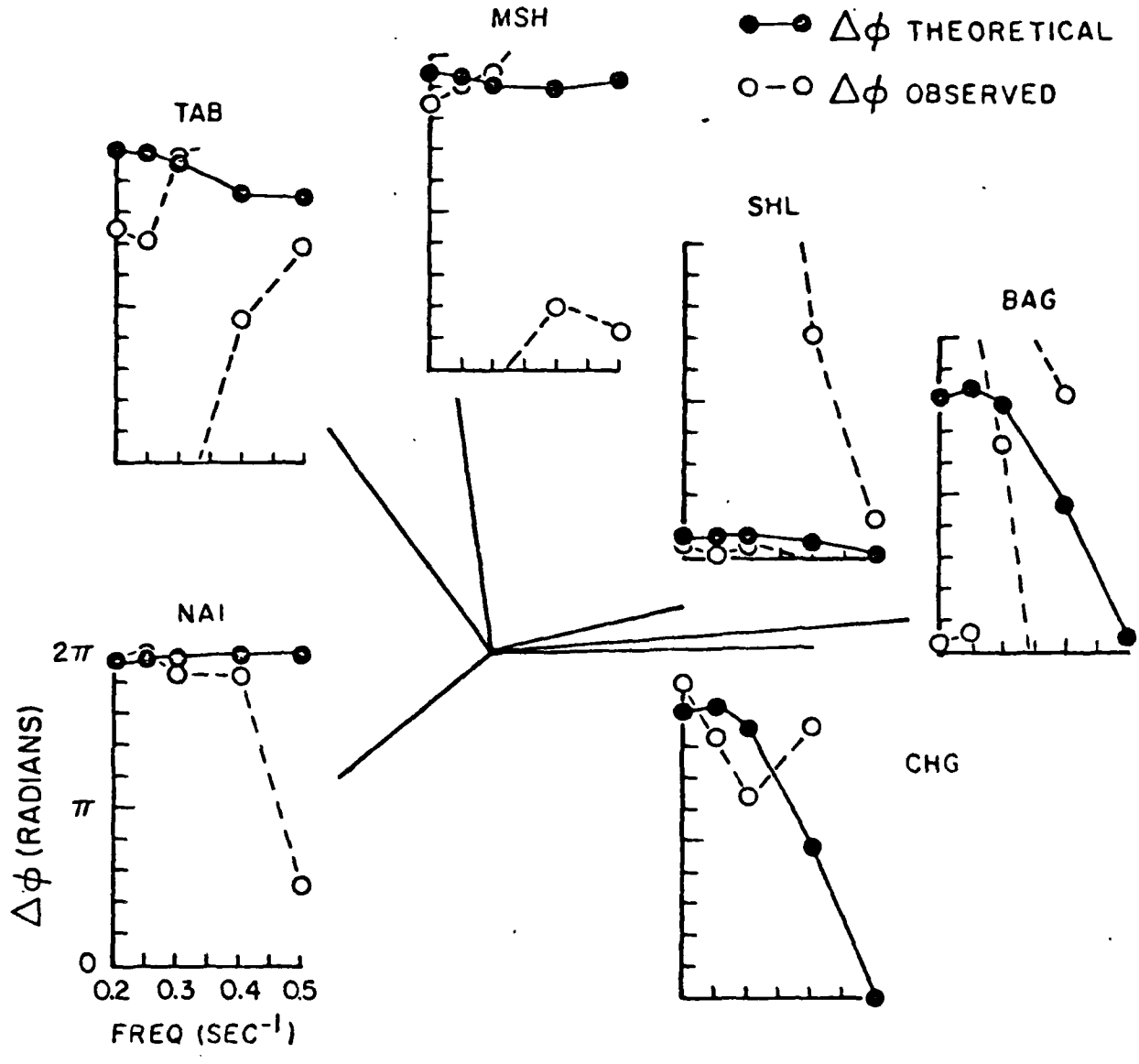

Figure 7. Observed and theoretical values of phase difference for the event-pair studied. At low frequencies (<0.3 sec^{-1}) the agreement between the two values is good. Phase difference values for five other stations are not stable and are not shown.

number of stations are not shown, however, as the scatter in the observed differential phase indicated that this parameter was not well resolved at those stations.

The observed values of amplitude ratio are compared in Figure 8 to those determined theoretically. The theoretical ratio is not widely varying, except at nodes, since the mechanisms are similar. It is difficult to determine visually the quality of the fit to the observed values, but this theoretical ratio does minimize the residual parameter for amplitude ratio (Figures 5 and 6).

Conclusions. The comparative-event technique for the use of surface waves to determine source parameters works adequately even when many of the epicenter-to-station paths cross regions of complicated tectonics. Almost all of the paths in this study either cross or fall along the Alpide-Himalayan belt of deformation. This is in contrast to the predominantly oceanic character of most paths used in previous studies.

The nature of the Murray ridge is not revealed on the basis of the one focal mechanism for this region. Although a mechanism indicating active spreading was not found, this possibility cannot be ruled out. The earthquake studied may represent movement on a transform fault connecting small segments characterized by spreading. In this interpretation the northeasterly trending nodal plane is considered the fault plane.

An alternative explanation involving left-lateral movement on the northwesterly trending nodal plane may also be possible. There are several short scarps (Figure 1) that have a strike similar to that of this nodal plane. The overall tectonics of the region, however, seems to favor the first interpretation.

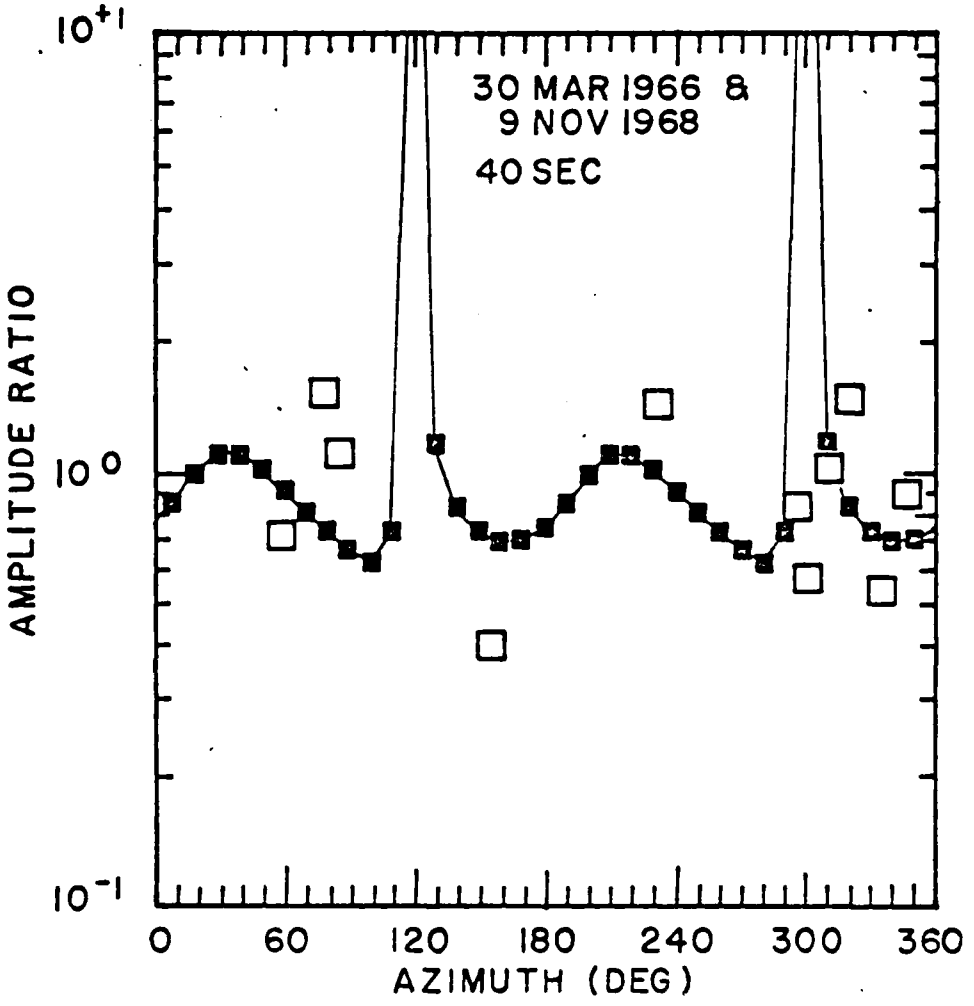

Figure 8. Comparison of observed and theoretical values of ratio amplitude for the event-pair studied. Note that the observed values scatter within a small range about a value of 1.0. This signifies that the two events have similar mechanisms. Any set of similar mechanisms will fit the data fairly well; thus, when the mechanisms are similar the ratio of amplitude is not useful for discriminating between different sets of similar mechanisms.

Part II: Waveform Studies of the Velocity and Q Structure of the Mantle

TECHNICAL SUMMARY

In recent years, the techniques of time domain waveform synthesis have permitted us to understand much more about seismic sources, about the seismic velocity structure of the earth and about seismic attenuation than ever before. In a second, separate program of study, which is described here, an effort is being made to apply these techniques to solution of the detection, discrimination and yield estimation problems. A variety of investigations have either been completed or are under way which are designed to derive as much information about the earth as possible from seismic body waves.

We present the final results of a study of the structure of the upper mantle beneath North America and Europe. Models of the velocity structure of the earth were developed which explain the major features of P wave propagation at ranges between 15° and 30°. Final results are presented on a study of the Gazli earthquakes in Uzbekistan, USSR. They occured in a region which is geographically convenient for sampling wave propagation within the Soviet Union. Consequently, they have already been studied by a number of investigators working on discrimination problems (Pearce, 1980; Pomeroy, 1980). The Gazli area had been relatively aseismic in recent times, but an analysis of the historic record shows that it is very probably a seismic zone with a long repeat time. A waveform analysis of the teleseismic body waves is also presented. Finally, interim reports are presented on investigations in progress of a major three dimensional

seismic feature of geographic importance to monitoring sources in the Soviet Union and of the frequency dependence of Q in the earth. In the former study, an analysis of the particle motion of WWSSN stations located on the collision boundary between the Indian and Eurasian continents has indicated that the plate boundary has a significant effect on long period body wave propagation. Further work is in progress to explain the phenomenon in terms of a tectonic model. In the latter study, investigations are being undertaken to determine how significant the frequency dependence of Q will be to waveform analysis techniques and also to determine what the frequency dependence of Q is.

A. A Comparison of the Upper Mantle Structure Beneath the US and Europe

The characteristics of body wave propagation to epicentral distances of 20° or more depends to a large extent on tectonic regime. The western US, eastern US and Europe are important test areas for understanding this dependence because they are well sampled by sources and stations and because they have already been extensively studied by many researchers. Some of the more significant investigations include the travel time studies of Hales (1972) and England and Worthington (1977); the apparent velocity studies of King and Calcagnile (1976), England, Kennett and Worthington (1978) and Johnson (1967); and the waveform analysis studies of Wiggins and Helmberger (1973), Dey Sarkar and Wiggins (1976) and Given and Helmberger (1980). Each method for determining mantle structure has provided some important information, but generally speaking, travel time studies have provided the roughest picture usually showing that tectonically active regions are slow with respect to stable continent. Apparent

velocity studies have led to more refined models and waveform analysis studies have resolved the finest detail. The new work presented here shows that all the different types of information need to be taken into account. Even though travel time data provides only rough constraints, it can be important. A complete report on the upper mantle study of North America and Europe is presented in Appendix I. It has been accepted for publication in the Journal of Geophysical Research.

In a parallel study to the one reported here Burdick and Helmberger (1978) completed an upper mantle study of the western US. They proceeded by first modeling several seismic sources very accurately and then by modeling the structure of the upper mantle using records from the known sources. The main new result of that work was the specific identification in long period body waves of pulses reflected from the upper mantle discontinuities. Figure 1 shows a particularly good example of a reflection (labeled D1) from the 670 km discontinuity in the mantle. In the course of their study they developed model T7 which, as shown in the figure, had some advantages over a previous model HWA. The data set used to arrive at model T7 did have a shortcoming, however, in that no observations were available from the back branch of the 670 km discontinuity. The back branch of the 400 km discontinuity was clearly identified in records from near 15° and its forward branch in records from near 23°. The forward branch of the 670 km discontinuity was clearly identified in records near 27° (Figure 1), but because appropriate records were not available from near 19°, model T7 was unconstrained with respect to the behavior of the forward branch of this triplication. Figure 2 shows several records from the new data set at ranges of 19° to 20° which do contain a small feature associated with the missing triplication branch.

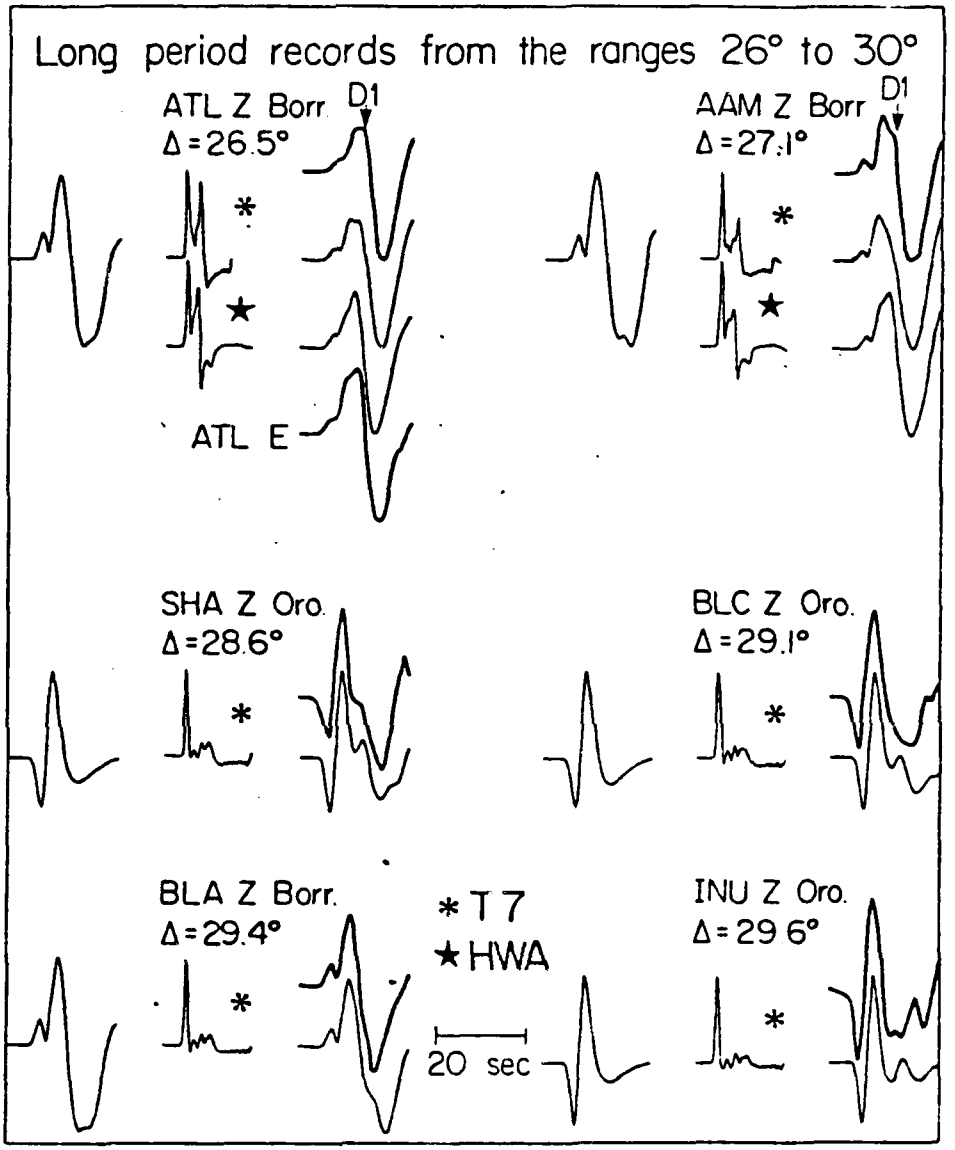

Figure 1 The long period records shown in the figure contain two arrivals. The second arrival which is marked as D1 is a reflection from the 670 km discontinuity (see Figure 3.4). The effective source function is shown on the left for each station. The filtered delta function response is next and, the synthetic seismogram is on the right in light line. The observed record is on the right in dark line. Model T7 appears to correctly predict the behavior of the reflection, but HWA does not.

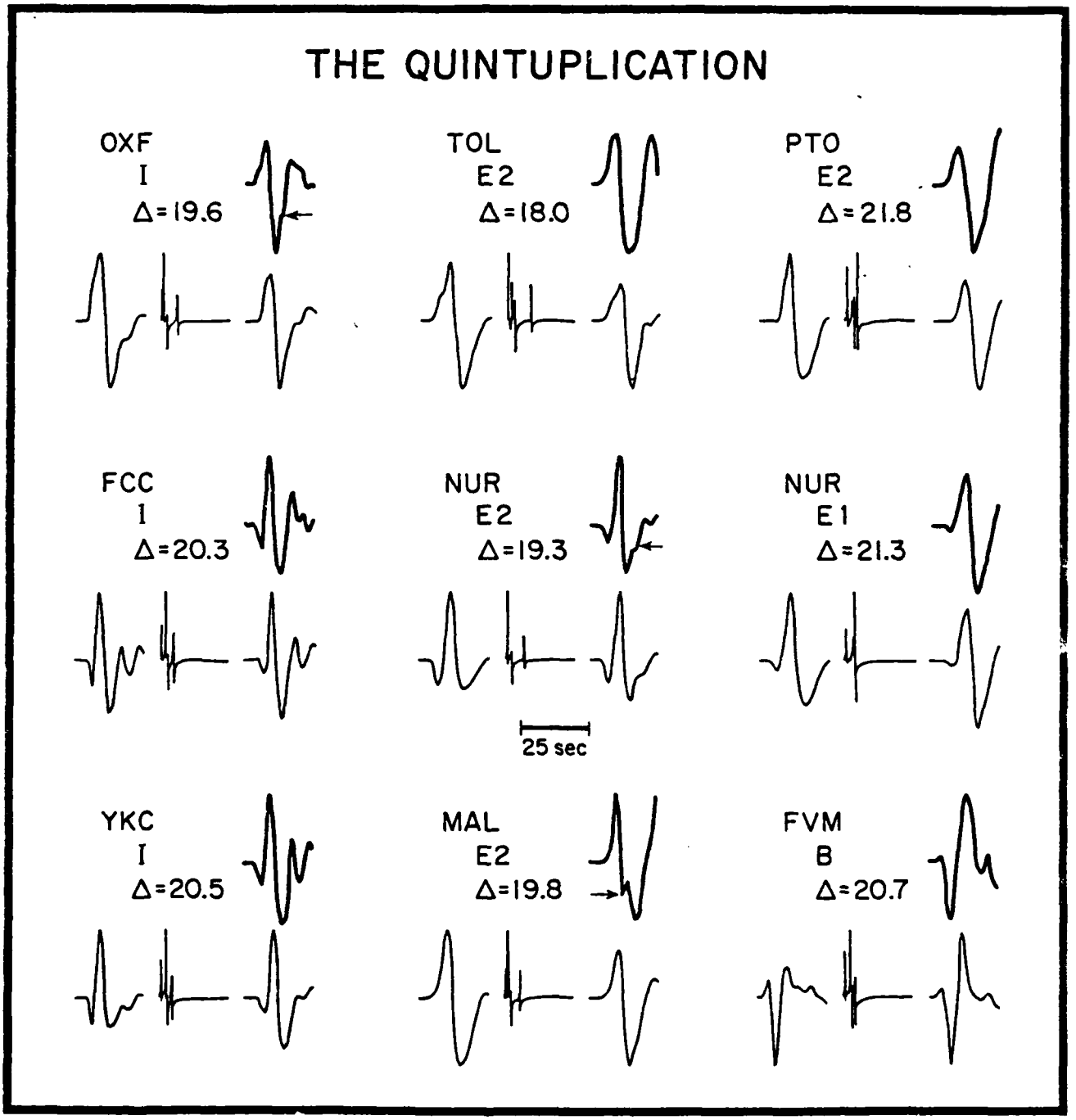

Figure 2 Figure arrangement is the same as figure 1. A further discussion is given in appendix I.

Model T9 is the new upper mantle model introduced in Appendix I to be consistent with the new data. The model fits the arrival at 19.3° and 19.6° and as discussed in the appendix can also fit the arrival at 19.8° if a different source is assumed. Figure 3 shows the two new upper mantle models T9 (tectonic continent) and S8 (stable continent). They appear to correctly predict the behavior of long period P wave propagation out to ranges of 30°. As has long been suspected from surface wave studies, the main difference between tectonic and stable continent appears to be simply the appearance or disappearance of a low velocity zone.

The second important new result of the new study is that there is a baseline difference in travel time between models for Northeast Eurasia (King and Calcagnile, 1976; Given and Helmberger, 1980) and models T9 and S8. The former models are tied to ISC origin times for Russian nuclear blasts, and the latter are tied to NTS origin times. Figure 4 compares the model of Given and Helmberger (1980) K8 to model S8. It is clear that most of the difference in travel time has been absorbed in a difference in depth to the major discontinuities. Other than this difference, the two models are very similar. The ISC times for the Soviet nuclear tests are generally several seconds before the minute. If this is a systematic error, then perhaps the depth to the major discontinuities does not vary as significantly as would be indicated by Figure 4. In any case, it would now appear that in the models of Given and Helmberger (1980), in T9 and in S8 we have developed very useful tools for understanding the properties of P wave propagation in the ranges 10° to 30°.

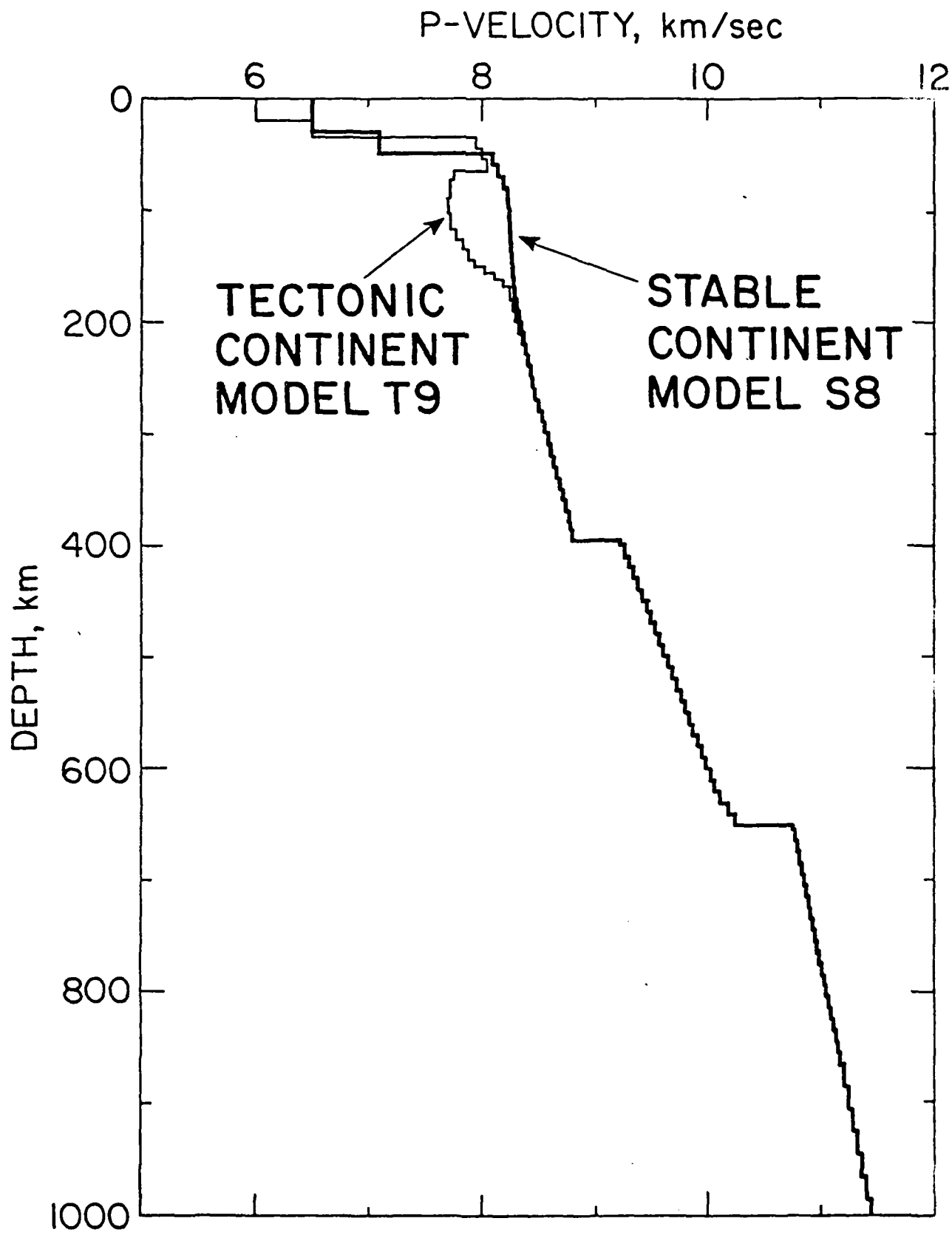
P-VELOCITY, km/sec
6
8
10
12
0
200
400
600
800
1000
DEPTH, km
TECTONIC
CONTINENT
MODEL T9
STABLE
CONTINENT
MODEL S8

Figure 3

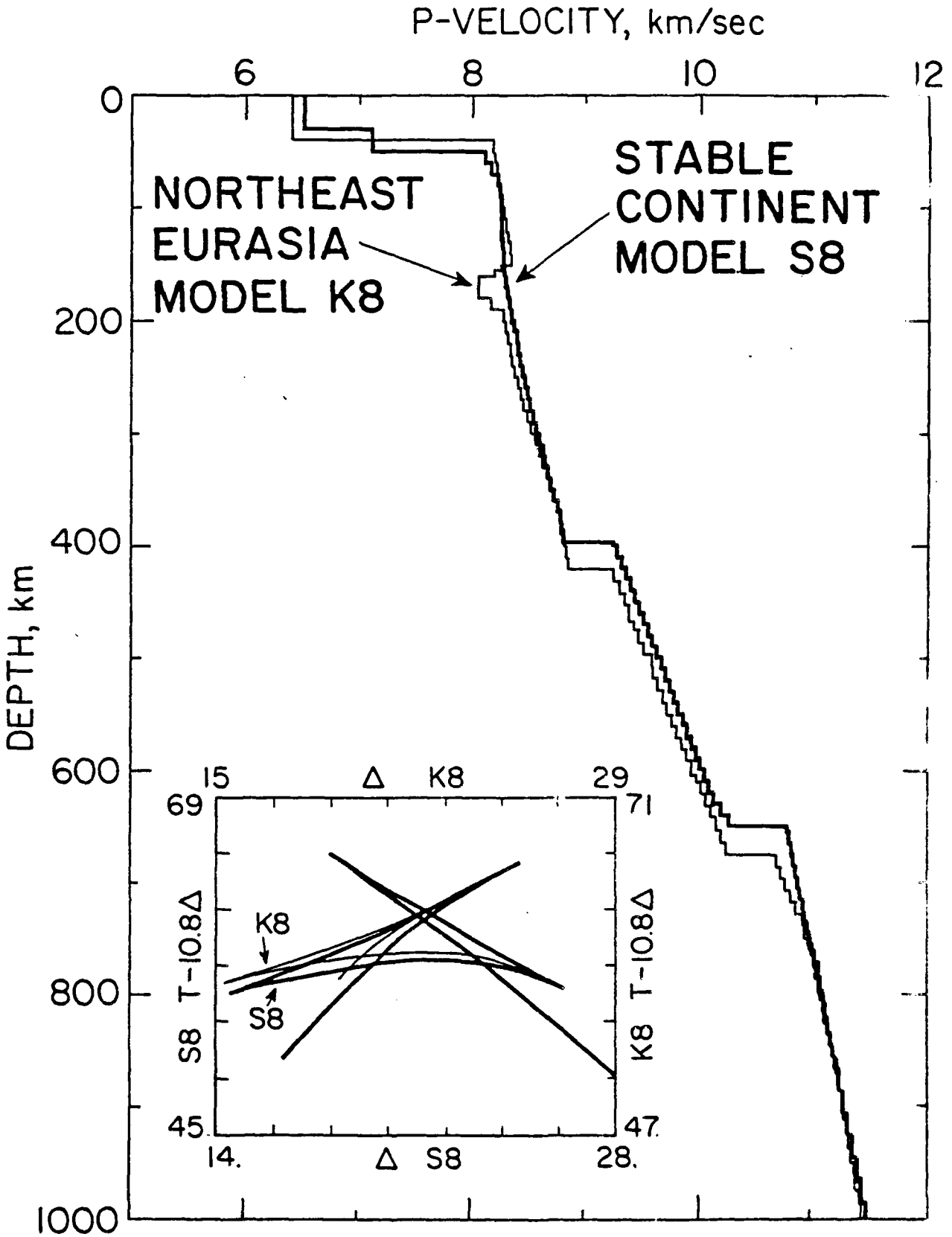
P-VELOCITY, km/sec
6
8
10
12
0
200
400
600
800
1000
DEPTH, km
NORTHEAST
EURASIA
MODEL K8
STABLE
CONTINENT
MODEL S8
15
Δ K8
29
69
71
S8 T-10.8Δ
K8 T-10.8Δ
K8
S8
45
47
14.
Δ S8
28.

Figure 4

B. The Focal Mechanisms of the Gazli Earthquakes

The Gazli sequence of earthquakes in Uzbekistan, USSR is a very important one because of its unique location. No comparable sequence has occurred since the advent of modern seismic recording. Pearce (1980) found the sequence to be very useful in testing his technique for source discrimination using array data. Pomeroy (1980) also used the sequence in a study of Lg propagation in the Soviet Union.

The Gazli sequence contained two major shocks, both of magnitude 7.1. Because of the overall importance of the sequence, we have undertaken a waveform analysis study of these two events to determine their focal mechanisms. We have also studied the historical seismicity records to attempt to determine why they happened where they did. A complete report is given in Appendix II. It has been published in the Bulletin of the Seismological Society of America. Figure 5 shows the locations of the Gazli earthquakes. Also shown as a shaded area is an arcuate region which underwent severe deformation in Hercynian times. The Gazli events appear to have occurred on this belt. This would support the suggestion of Sykes (1978) that intraplate earthquakes tend to occur on such belts. Figures 6 and 7 show the final focal mechanism solutions for the two events and the associated waveform fits. The most important observation is that the two events had substantially different mechanisms. It is often assumed that the large events in a sequence all occur on the same fault plane. As discussed in Appendix II, Aptekman et al. (1978) have suggested that this may not be true for thrust events. The evidence from Gazli tends to bear them out.

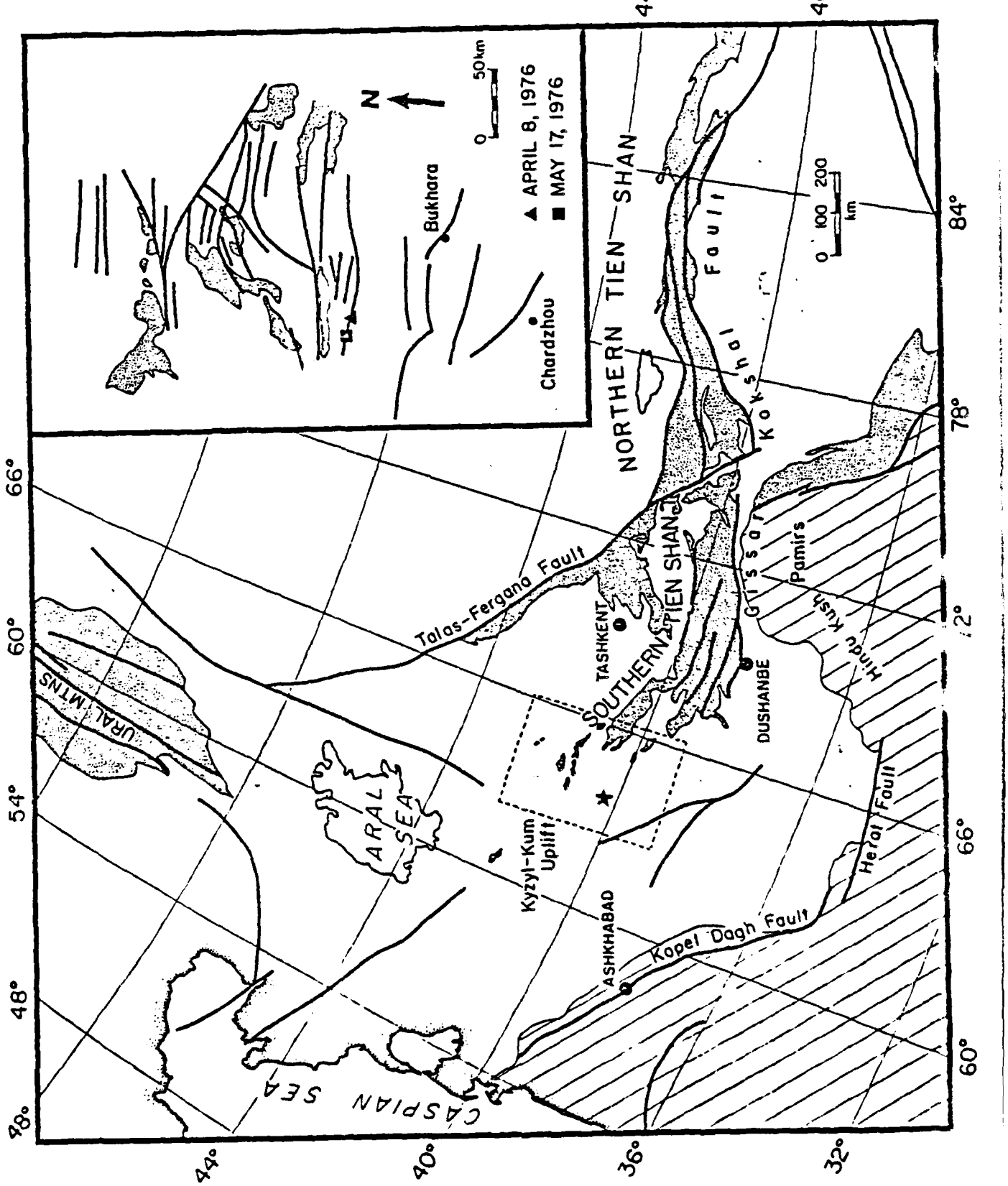
APRIL 8, 1976
MAY 17, 1976
Bukhara
Chardzhou
N
0 50km
NORTHERN TIEN SHAN
Fault
Kokshal
Talas-Fergana Fault
TASHKENT
SOUTHERN TIEN SHAN
Gissar
Pamirs
Hindu Kush
DUSHANBE
URAL MTNS
ARAL SEA
Kyzyl-Kum Uplift
ASHKHABAD
Kopet Dagh Fault
Herat Fault
CASPIAN SEA
0 100 200 km
84°
78°
66°
60°
54°
48°
42°
44°
40°
36°
32°

Figure 5

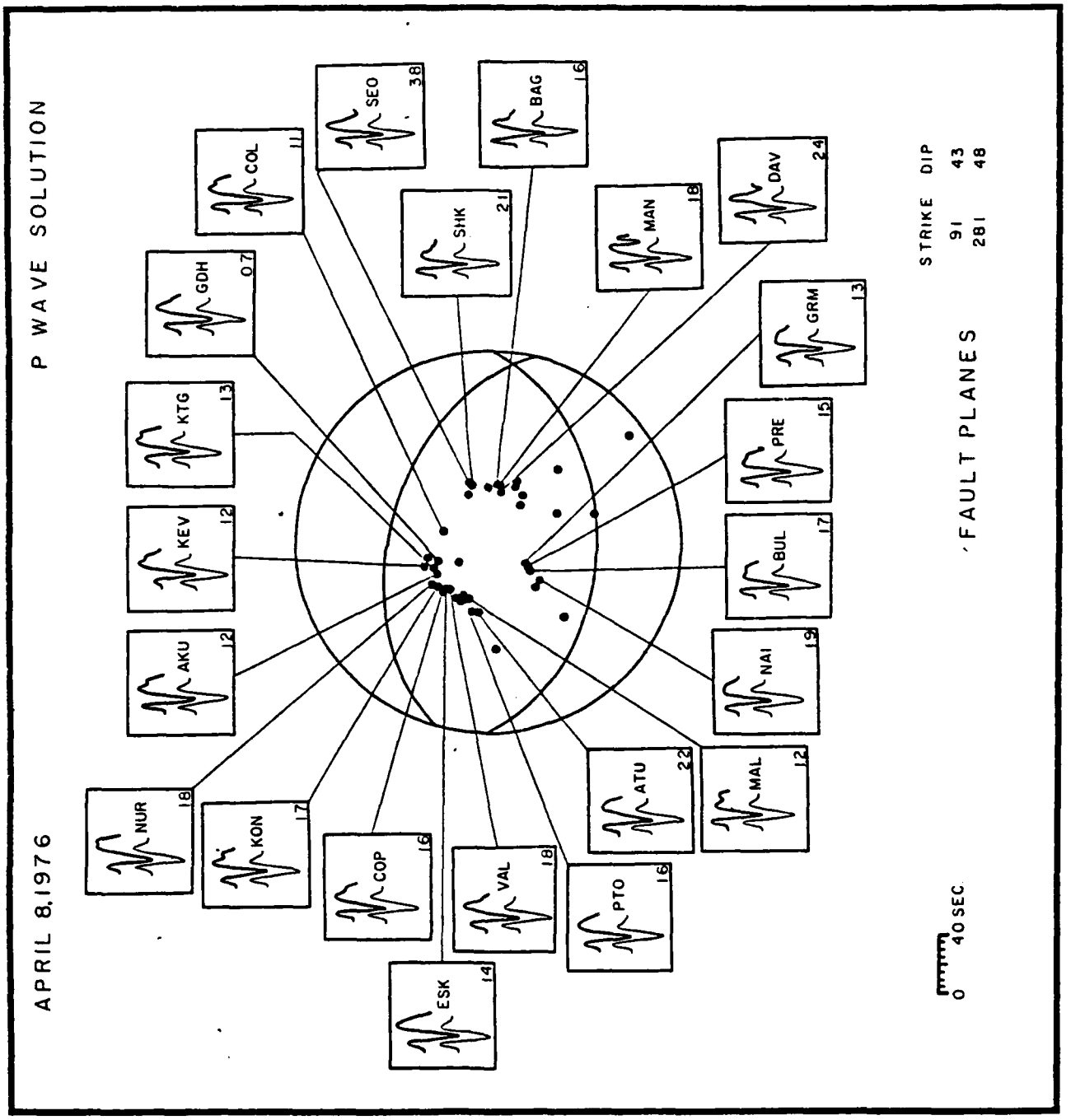
P WAVE SOLUTION
APRIL 8,1976
FAULT PLANES
STRIKE DIP
91 43
281 48
0 40 SEC
SEO 38
BAG 16
COL 11
SHK 21
MAN 18
DAV 24
GDH 07
GRM 13
KTG 13
PRE 15
KEV 12
BUL 17
AKU 12
NAI 19
ATU 22
MAL 12
NUR 18
KON 17
COP 16
VAL 18
PTO 16
ESK 14

Figure 6

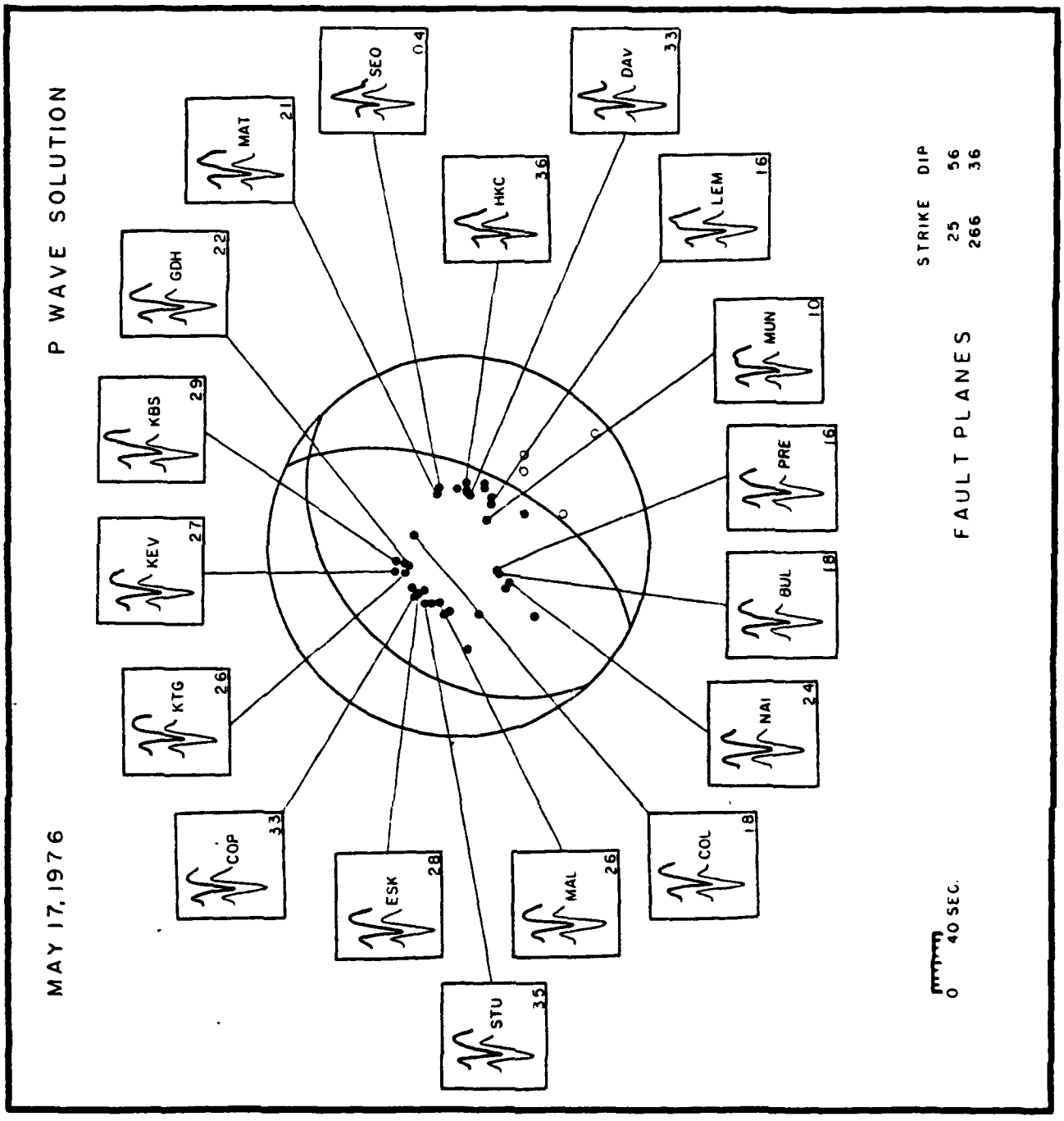
P WAVE SOLUTION
MAY 17, 1976
FAULT PLANES
STRIKE DIP
25 56
266 36
0 40 SEC.
SEO 04
DAV 33
MAT 21
HKC 36
LEM 16
GDH 22
MUN 10
KBS 29
PRE 16
KEV 27
BUL 18
KTG 26
NAI 24
COP 33
COL 18
ESK 28
MAL 26
STU 35

Figure 7

C. A Major Seismic Feature of Geographic Importance to Monitoring Soviet Seismic Events

It has long been suspected that large scale 3-dimensional features such as subduction zones might affect our ability to detect and characterize seismic events. Ordinarily, important seismic installations are not situated on such features in an effort to avoid the problem. In spite of these efforts, however, LASA and NORSAR were inadvertently located at less than ideal sites (Aki, 1973; Berteussen et al., 1975). Burdick and Langston (1977) and Langston (1977, 1978) have shown that many WWSSN stations are strongly affected by 3-dimensional structure at the receiver. A survey has been performed of the site characteristics of WWSSN stations in India and southern Eurasia to identify those which are transparent. In the course of the work, it was found that stations located near the collision boundary between India and Eurasia are all situated on strongly dipping structure. This has major implications for the monitoring effort because these stations and the new digital stations which are replacing many of them are geographically ideal for recording Novaya Zemlya and Kazakh events.

A survey of station site characteristics must generally proceed in two parts. First, the particle motion characteristics of the stations are examined to determined if three dimensional velocity variations are affecting the incoming waves. Then, in those instances where the velocity structure appears to be flat lying, plane layered models for the crust are constructed using P to S converted phases in teleseismic body waves. The stations considered in this survey are shown in Figure 8. The shaded region approximately shows the extent of the collision boundary between

India and Eurasia (Seeber et al., 1981). The stations located on the boundary are QUE, KBL and NIL. It is important to note that QUE is going to be upgraded to a digital WWSSN station and KBL already has an SRO.

If a teleseismic ($\Delta > 30°$) P wave impinges on a flat lying crustal column then the compressional motion will not couple to the tangential motion. This implies that the north component of motion must be just a constant times the east component.

$$N(t) = c\ E(T)$$

where c = cot (Back Azimuth).

At long times (t > 30 sec), energy scattered far from the station will cause this relationship to break down. At short times, however, serious breakdown of the relationship can only be caused by dipping structure at the station. The quality of a site can be determined by simply comparing the two horizontal components of motion for teleseismic P waves to each other.

Figure 9 shows some typical horizontal P wave components for stations in the survey. The column on the left shows some of the best stations; the column in the center, some intermediate stations and the column on the right the very poor ones which are those on the collision boundary. The tangential arrivals at the poor stations are very impulsive indicating a sharp velocity increase on a strongly dipping interface. It is not uncommon to find that the particle motion at any station is anomalous from certain azimuths. Figures 10 and 11 show additional comparisons of horizontal components of motion at KBL and QUE (NIL has a relatively short recording history). The particle motion is poor for all azimuths of

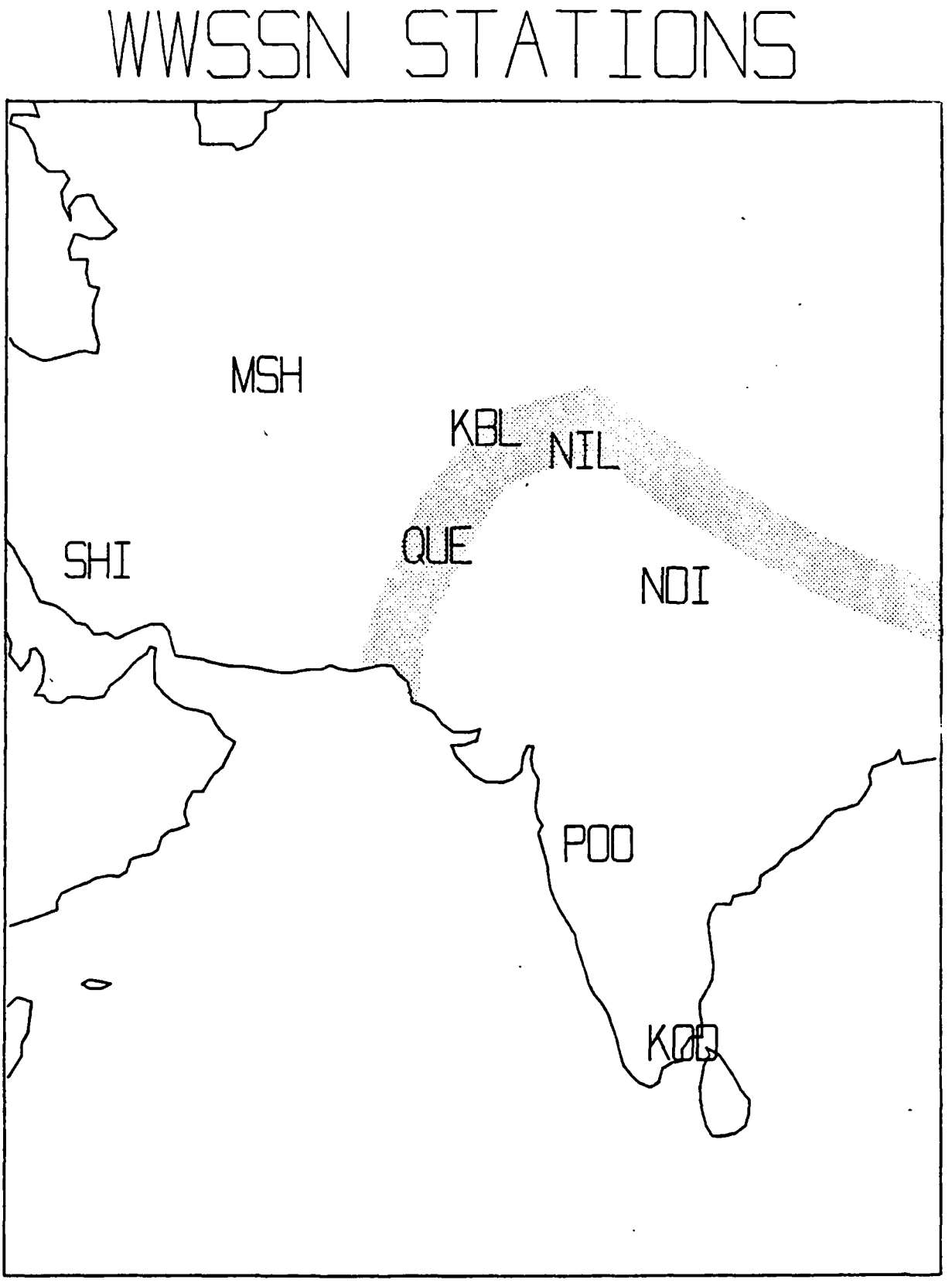

Figure 8

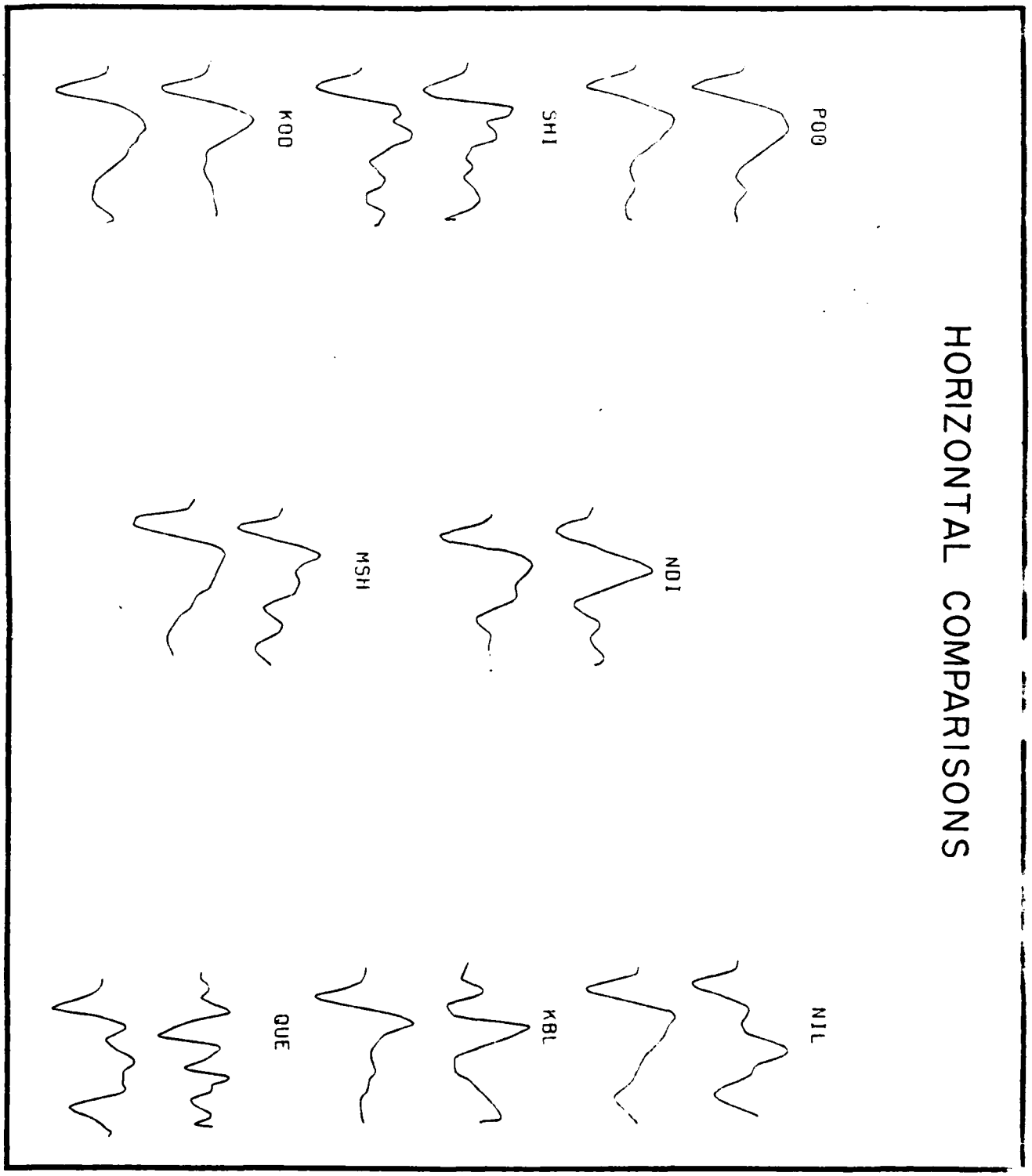

Figure 9

approach. The P waves coming from almost due north (Back Azimuth = 353.6 at QUE and Back Azimuth = 353.7 at KBL) are particularly interesting. They originated from a Soviet nuclear test at Novaya Zemlya. Because the station is nearly naturally rotated the east component is almost identical to the tangential or "SH" component. Note how the P wave bleeds onto the tangential component with time. This phenomenon is currently being investigated further, but from just this survey we can conclude that the continental collision boundary is a major three dimensional velocity structure which affects seismic recording in an adverse way.

The approach used in the second part of the survey to model the crustal structure at the good and intermediate quality sites is the one developed by Burdick and Langston (1977). The P to S converted phases in teleseisms are specifically identified and modeled using synthetic seismograms. Figure 12 shows theoretical seismograms for a plane wave incident from below on a layer over a half-space. The vertical component of motion is shown on the left and the horizontal on the right. The first order crustal reverberations are named and numbered using the notation of Bath and Steffanson (1966). The S phases, 4, 5 and 6, cause clear differences between the two components of motion. The largest arrival of the three is the first one, the Ps phase. We have been able to observe this phase in data from all of the good and intermediate quality stations in Figure 9. By modeling it, we have been able to constrain the crustal thickness in each case. Figure 13 compares data to synthetics for station SHI. The Ps arrival is clear in the radial components and is well matched by the synthetics. The crustal thickness is 33 km, very typical for continental crust. (We assume throughout that V_p = 8.1 km/sec in the lid.) Similar results for stations MSH, KOD, POO and NDI are shown in Figures 14-17. The

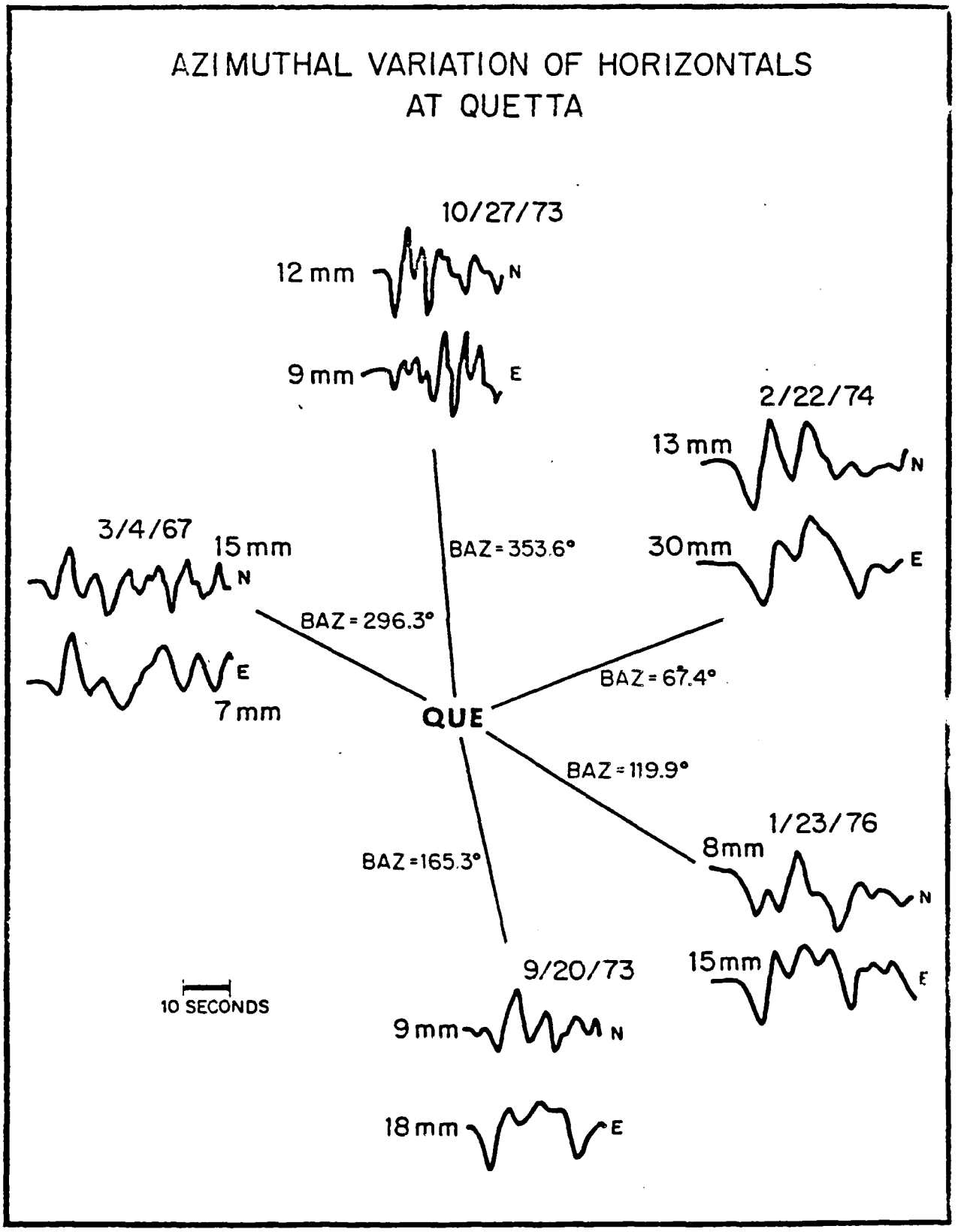
AZIMUTHAL VARIATION OF HORIZONTALS
AT QUETTA
10/27/73
12 mm
N
9 mm
E
2/22/74
13 mm
N
30mm
E
3/4/67
15 mm
N
E
7 mm
BAZ = 353.6°
BAZ = 296.3°
BAZ = 67.4°
QUE
BAZ = 119.9°
BAZ = 165.3°
1/23/76
8mm
N
15mm
E
9/20/73
9 mm
N
18 mm
E
10 SECONDS

Figure 10

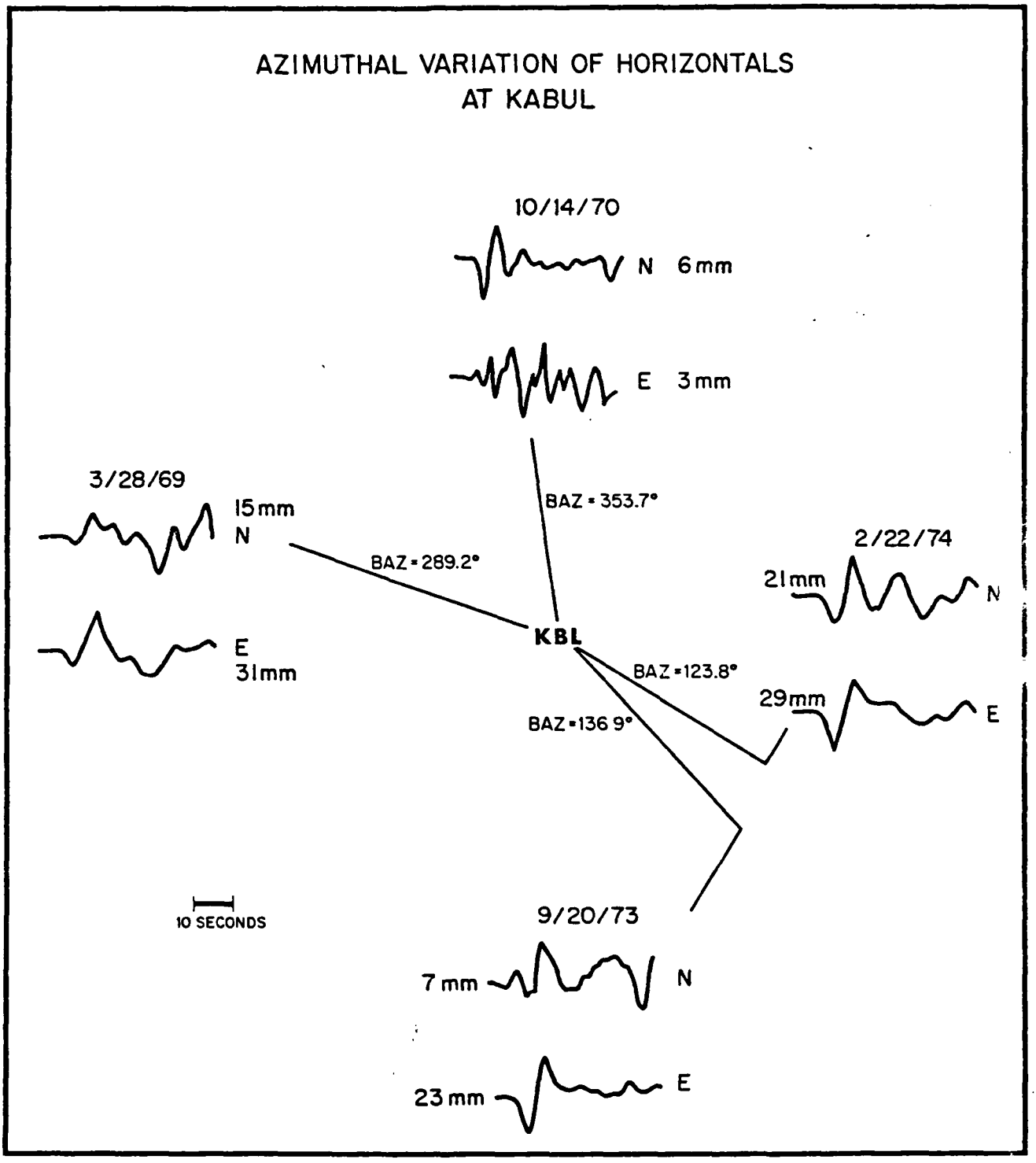
AZIMUTHAL VARIATION OF HORIZONTALS
AT KABUL
10/14/70
N 6mm
E 3mm
BAZ = 353.7°
3/28/69
15mm
N
BAZ = 289.2°
E
31mm
KBL
2/22/74
21mm
N
BAZ = 123.8°
29mm
E
BAZ = 136.9°
10 SECONDS
9/20/73
7 mm
N
23 mm
E

Figure 11

REFLECTED AND CONVERTED PHASES

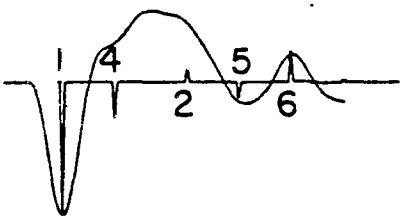

1) P
2) PpPmp
3) PpSmp

4) Ps
5) PpPms
6) PpSms

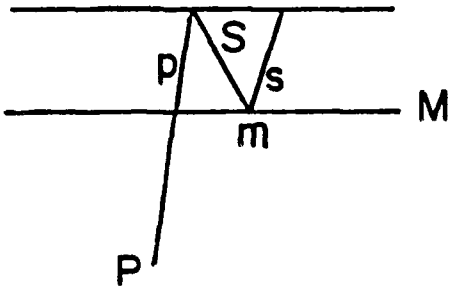

Figure 12

values for crustal thickness ranges from 30 to 50 km. There does not appear to be any systematic difference between the Indian and Eurasian plates.

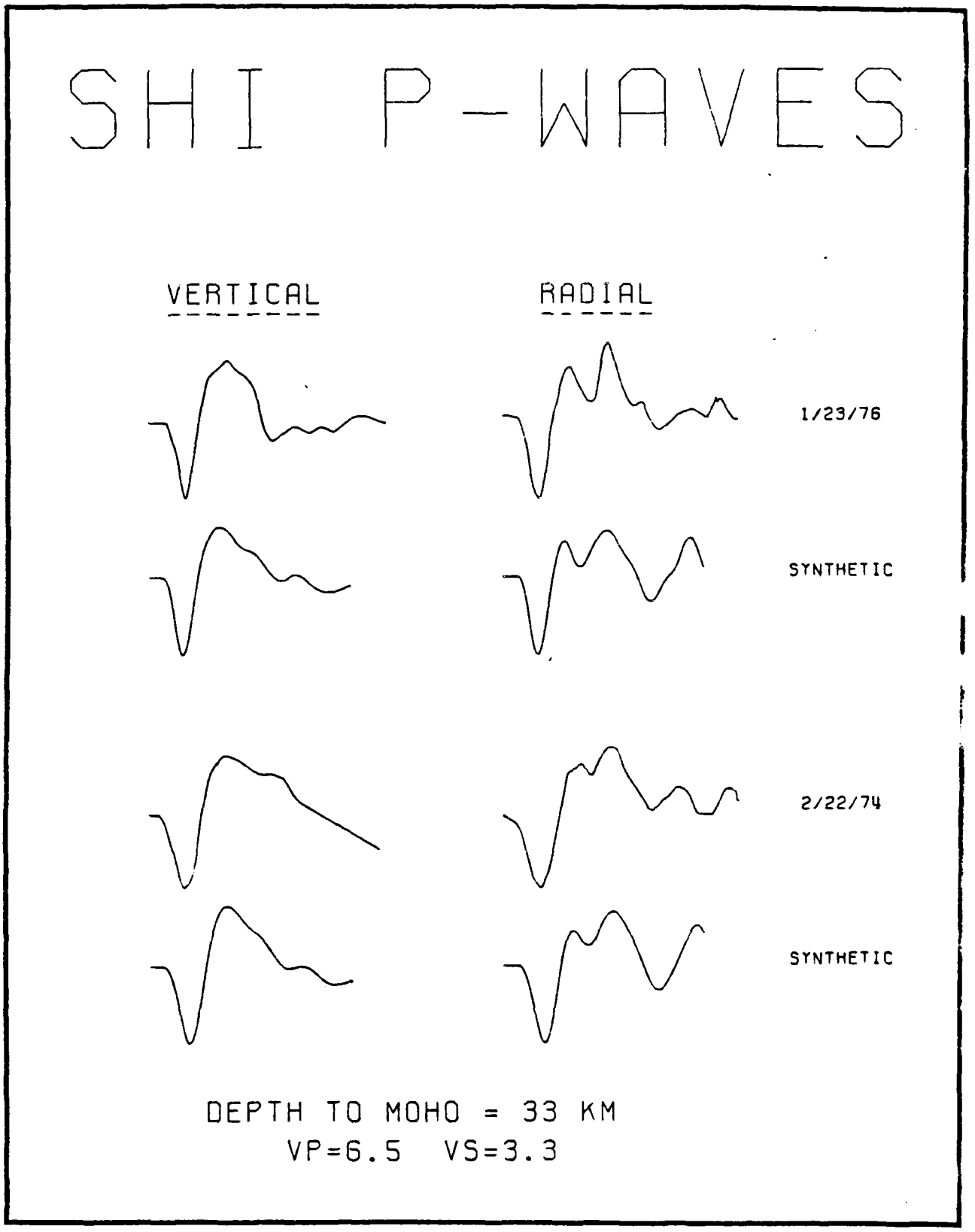
SHI P-WAVES
VERTICAL
RADIAL
1/23/76
SYNTHETIC
2/22/74
SYNTHETIC
DEPTH TO MOHO = 33 KM
VP=6.5 VS=3.3

Figure 13

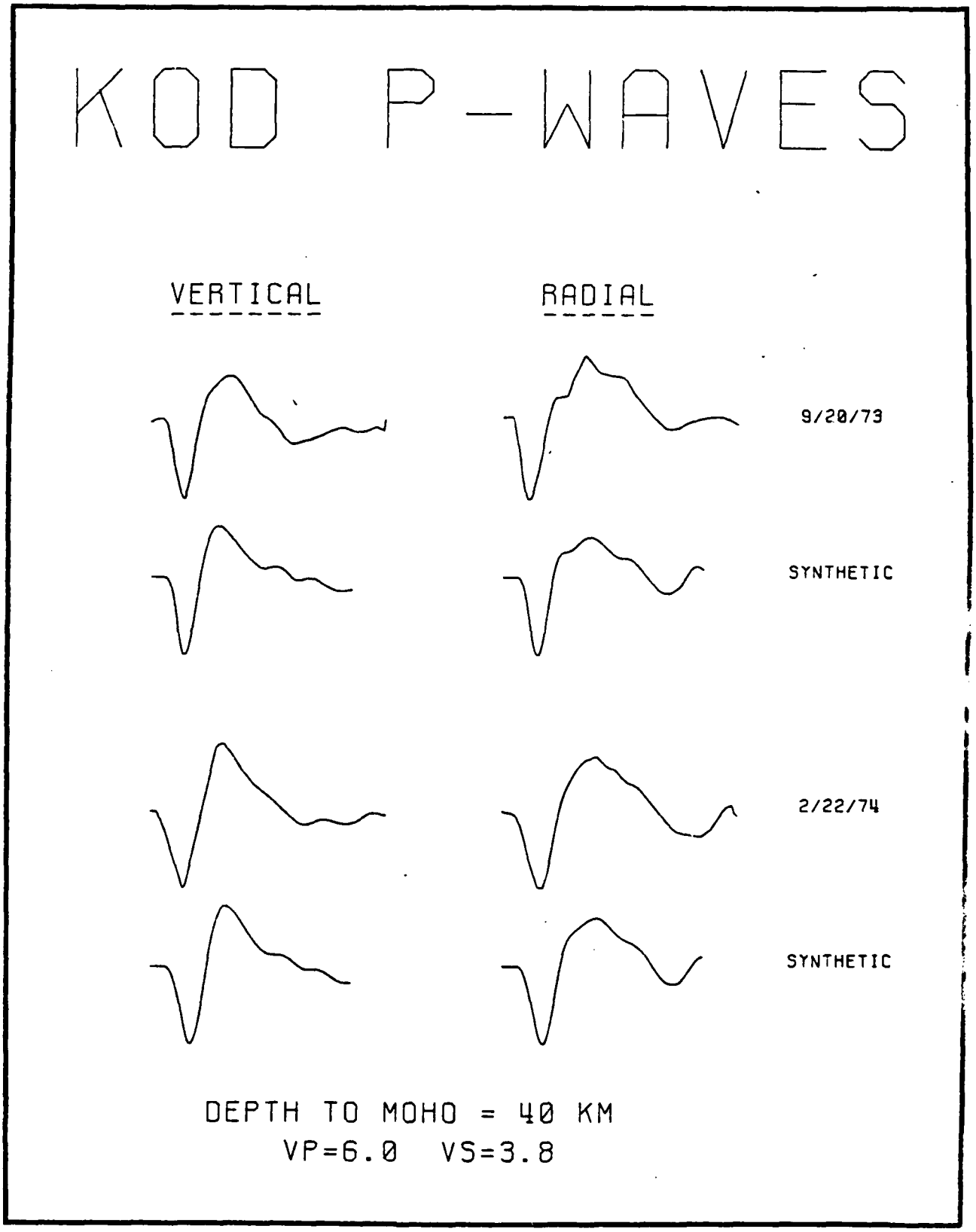
KOD P-WAVES
VERTICAL
RADIAL
9/20/73
SYNTHETIC
2/22/74
SYNTHETIC
DEPTH TO MOHO = 40 KM
VP=6.0 VS=3.8

Figure 14

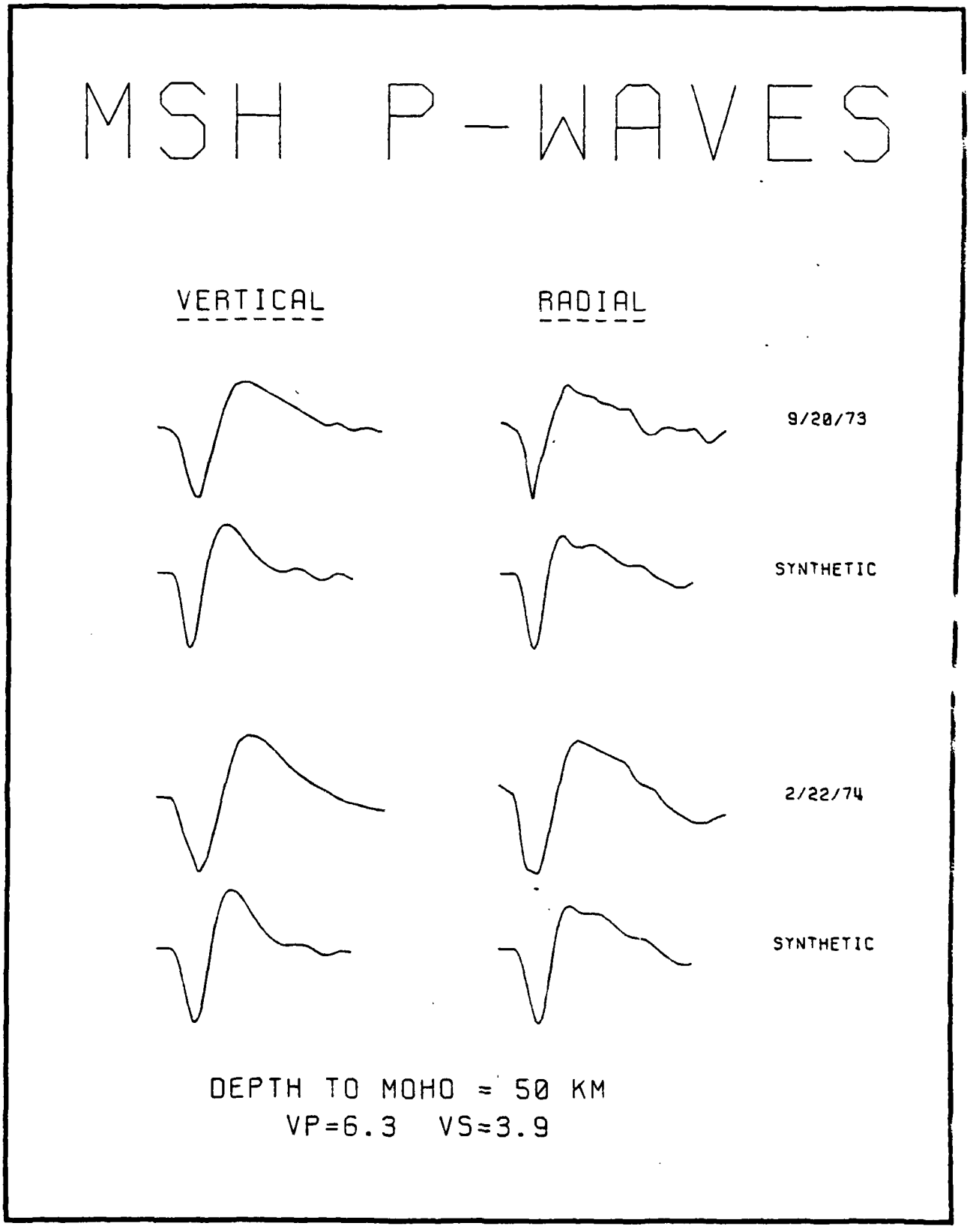
MSH P-WAVES
VERTICAL
RADIAL
9/20/73
SYNTHETIC
2/22/74
SYNTHETIC
DEPTH TO MOHO = 50 KM
VP=6.3 VS=3.9

Figure 15

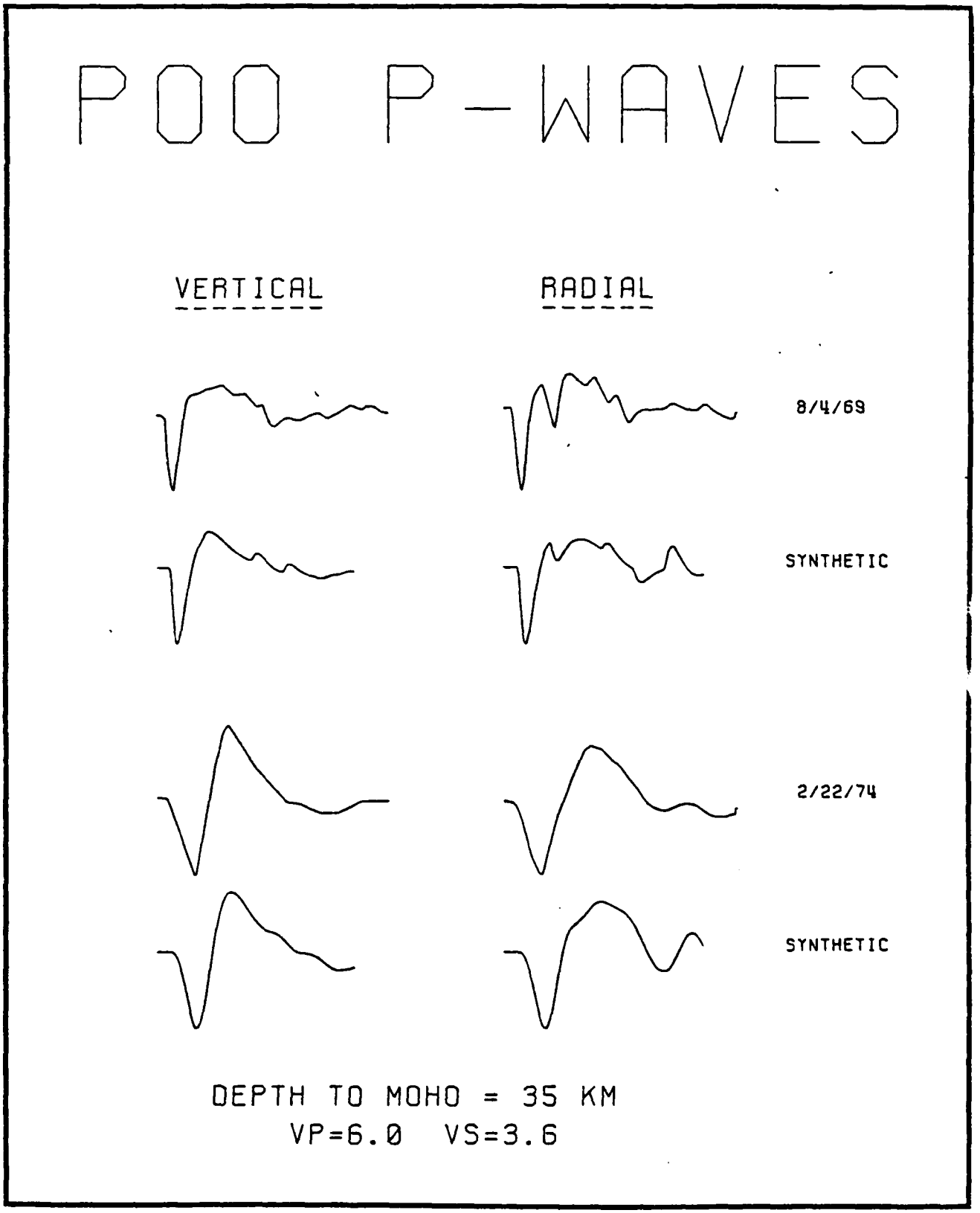
POO P-WAVES
VERTICAL
RADIAL
8/4/69
SYNTHETIC
2/22/74
SYNTHETIC
DEPTH TO MOHO = 35 KM
VP=6.0 VS=3.6

Figure 16

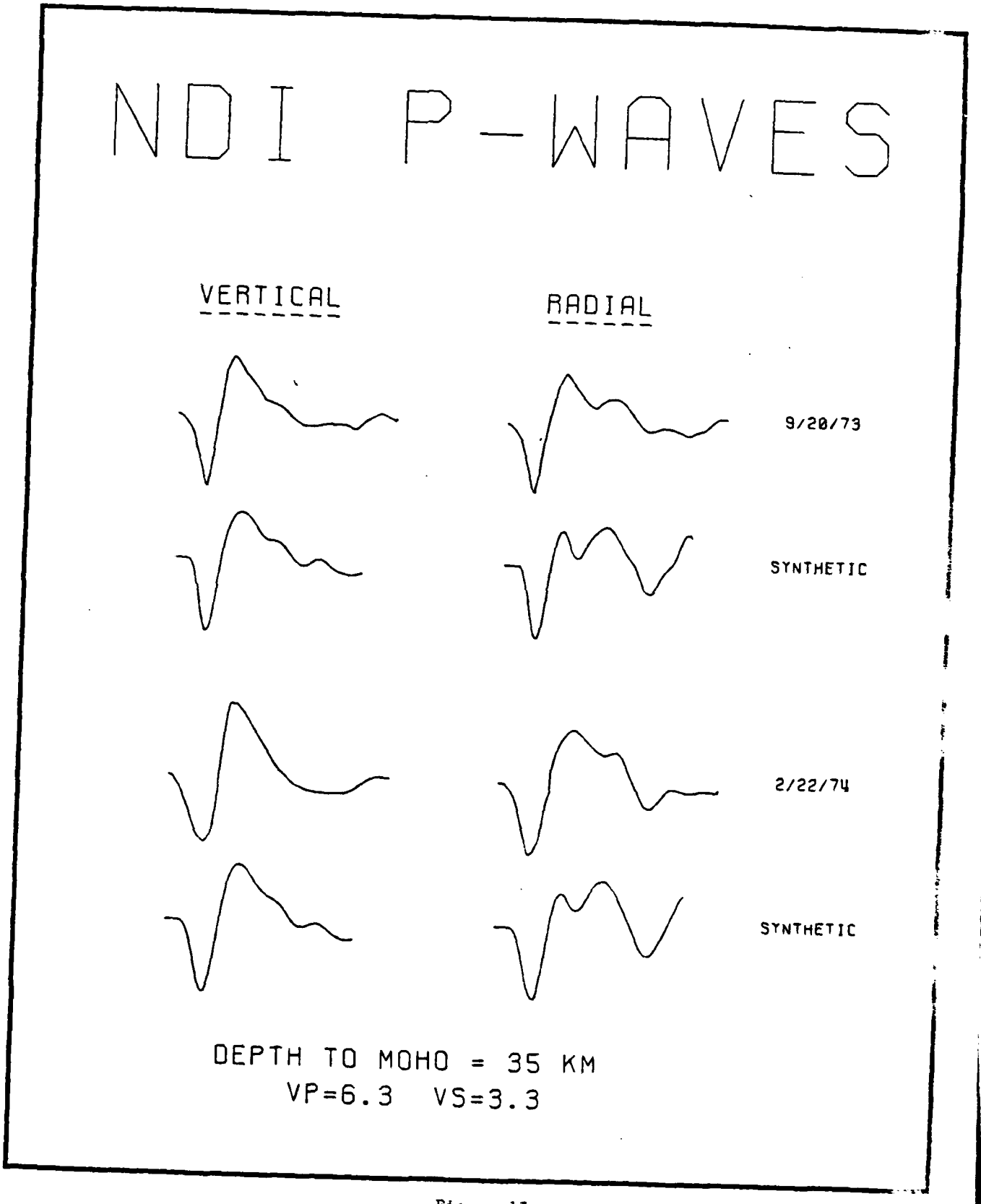
NDI P-WAVES
VERTICAL
RADIAL
9/20/73
SYNTHETIC
2/22/74
SYNTHETIC
DEPTH TO MOHO = 35 KM
VP=6.3 VS=3.3

Figure 17

D. Relative Attenuation of P and S Waves and the Frequency Dependence of Q

The recent attempts to correlate the results of body wave attenuation studies over a broad range of frequencies have produced evidence that Q must vary with frequency (Sipkin and Jordan, 1979). This raises two important questions. First, how does this affect the results of studies which had assumed a constant Q and second what is the frequency dependence of Q? Both of these questions are currently being investigated.

Some of the studies which have assumed that Q is independent of frequency have been the long period body wave modeling studies of Helmberger (1974), Burdick and Mellman (1976) and Langston (1976). It is important to establish whether or not these results would change if Q were assumed to depend on frequency. The procedure used in these investigations to correct for Q was to include a Futterman (1962) constant Q operator in the calculation of the synthetic seismograms. Sipkin and Jordan (1979) have suggested that an appropriate modification would be to use a standard linear solid (S.L.S.) Q operator (Minster, 1978). The S.L.S. operator has three adjustable parameters. One is just the minimum value of Q which is the equivalent of t* for a Futterman operator. The other parameters control the increase of Q at high and low frequencies. The low frequency behavior of Q is not important to body wave calculations, but the high frequency behavior is. The controlling parameter is τ_m. Sipkin and Jordan (1979) suggest that it should be between .1 and 1.0 sec, but as we show in the following section it is probably at the low end of this range.

Figure 18 is adapted from the work of Sipkin and Jordan and summarizes their arguments. The hatched areas show esimates of the average shear Q of the mantle ($\bar{Q}_\beta$) as determined from normal modes, ScS_n experiments and spectral decay measurements. It would seem reasonable on the basis of this evidence to adopt a value of $\tau_m = .5$. However, careful consideration of the results of measurements of the relative attenuation of P and S waves along raypaths where the source excitation is nearly constant show that this is not the case.

We begin by noting that the high frequency spectral decay measurements of Sipkin and Jordan are much less reliable then their low frequency ScS_n measurements. The spectral decay measurements are made by solving for the attenuation spectrum $A(\omega)$ from an observation $S(\omega)$ using

$$S(\omega) = A(\omega)\ R(\omega)$$

$R(\omega)$, the spectrum of the source is also unknown. The large vertical error bars on the spectral decay measurements in the figure were derived by testing a range of source models. The dark horizontal bars are based on the source parameter measurements of Wyss and Molnar (1972). Wyss and Molnar also solved an equation like (2), but they assumed a form for $A(\omega)$ and solved for $R(\omega)$. Their Q correction was based on the results of Julian and Anderson (1968) who used model MM8. The $\bar{Q}_\beta$ for this model is 580 which is very close to the value recovered by Sipkin and Jordan. That is to say, the source spectrum and attenuation spectrum determinations are self-consistant but totally non-unique. This does not invalidate Sipkin and Jordan's arguments for a lower bound for Q because seismic sources must have corner frequencies. It does show, however, how important it is to

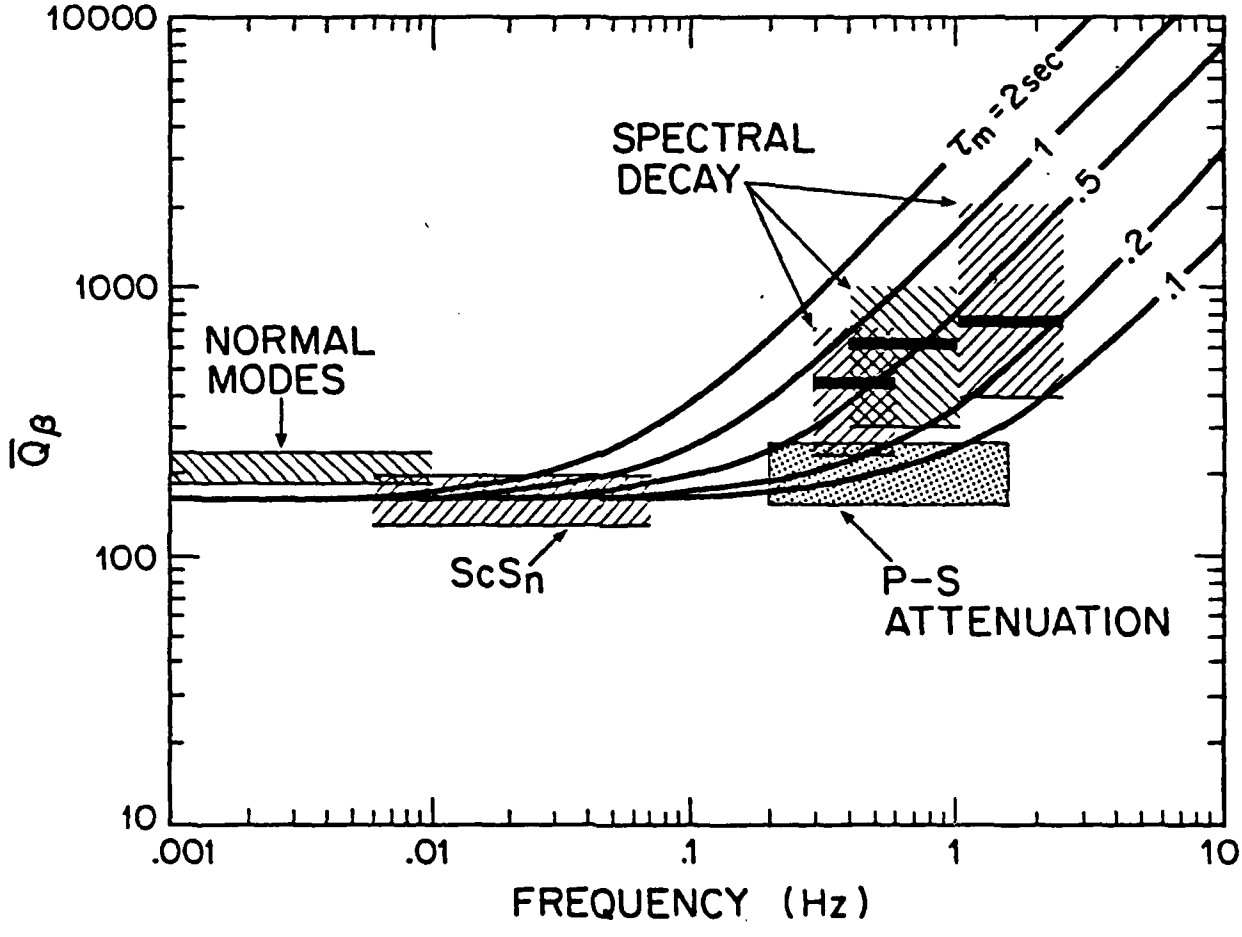

Figure 18 The measurements which had indicated that Q depends strongly on frequency (primarily the spectral decay measurements) are shown as hatched regions. The measurements which indicate that the increase of Q does not begin until frequency exceeds 1 Hz. (the source controlled measurements of the relative attenuation of P and S waves) are shown as a stipled region.

make measurements of attenuation in situations where the source excitation is controlled.

One way to measure attenuation so that the source excitation is controlled is to measure the relative attenuation of ScS with respect to ScP. In doing so, Kanamori (1967) measured $\bar{Q}_\beta$ for the mantle to be between 150 and 260 in the frequency range of .1 to .7 Hz. Sacks (1980) repeated the experiment and obtained a value of 250 between .3 and 1.5 Hz. Burdick (1978) compared sP to sS phases and obtained a value of $t_\beta^* = 5.2 \pm .7$ sec at a range of $\Delta = 40°$. The SL8 Q model (Anderson and Hart, 1979) predicts $t_\beta^* = 4.6$ sec at this distance and has an overall $\bar{Q}_\beta$ of 235. The Burdick (1978) measurement therefore scales to 210 ± 25 for WWSSN short period records low pass filtered at 1 Hz.

The relative S-P attenuation measurements are represented in Figure 19 as a stipled region of Q bounded between 150 and 260 over a frequency range of .2 to 1.5 Hz. The measurements clearly suggest that the rapid increase in Q with frequency does not begin to occur until after 1 Hz. The cutoff time τ_m might be appropriately chosen as .1 to .2 sec which reconciles as closely as possible the observations of Sacks (1980) with the lower bound of Sipkin and Jordan (1979). This would imply that $\bar{Q}_\beta$ rises to 1000 by 5 Hz. An appropriate constant $\bar{Q}_\beta$ approximation for all the data in the WWSSN band (.01 to 2 Hz) would be a value of 250. The important point here is that measurements of the relative attenuation of P and S waves in cases where the source excitation is controlled give a very self-consistent result. They appear to show that $\bar{Q}_\beta$ does not rise significantly above 300 at frequencies less than 1.5 Hz.

To determine the importance of the frequency dependence of Q to long period waveform studies, synthetic seismograms for the Borrego Mountain

earthquake (Burdick and Mellman, 1976) were computed using a Futterman and an S.L.S. operator (τ_m = .2 sec). The results are compared in Figure 19. The observed P wave from COL and the observed SH from OGD are shown at the top. Underneath them, superimposed on each other, are synthetics computed with the two different operators. The differences are almost invisible. From this and from other tests, we have concluded that the fact that Q does increase with frequency will have no effect on the results of the long period waveform modeling studies.

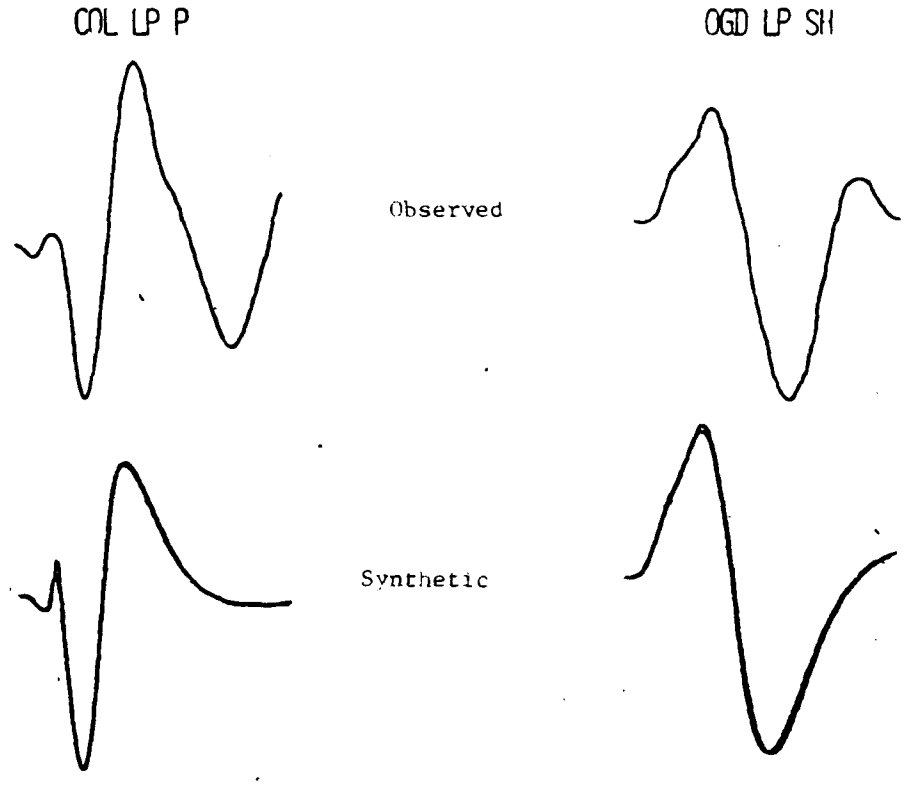

Figure 19 An observed P wave and an observed SH wave from the Borrego Mountain earthquake are shown on top. Beneath each are two synthetics superimposed on each other; one computed with a Futterman operator and one computed an S.L.S. operator.

CONCLUSIONS

The studies of the Gazli earthquakes and of the upper mantle show that we are becoming very proficient at predicting many of the features of long period body waves using simple point source approximations and plane layered earth structures. These approaches will undoubtedly continue to be of value to us. The results of the station survey, on the other hand, show that three dimensional velocity structures do have a significant effect on long period body waves in some instances. The effect will presumably be even larger on short period body waves. Likewise, the frequency dependence of Q will be important to the analysis of short period body waves. Since many small events are recorded only at short periods it will be important to continue our work in these areas.

REFERENCES

Aki, K., Scattering of P waves under the Montana LASA, J. Geophys. Res., 78, 1334-1346, 1973.

Anderson, D.L., and R.S. Hart, An earth model based on free oscillations and body waves, J. Geophys. Res., 81, 1461-1475, 1976.

Aptekman, Kh.Ya., V.M. Grazier, K.G. Pletnev, D.N. Rustanovich, N.V. Shebalin, and V.V. Shteinberg, Some data on processes in the epicentral zone of the 1976 Gazli earthquakes, in Epicentral Zones of Earthquakes; 19, Questions in Engineering Seismology, Nauka, Moscow, pp. 149-166 (in Russian).

Bath, M., and R. Stefansson, S-P conversions at the base of the crust, Ann. Geophis., 19, 119-130, 1966.

Berteussen, K.A., A. Christofferson, E.S. Husebye, and A. Dahle, Wave scattering theory in the analysis of P wave anomalies at NORSAR and LASA, Geophys. J. R. astr. Soc., 42, 403-417, 1975.

Burdick, L.J., and C.A. Langston, Modelling crustal structure through the use of converted phases in teleseismic body waveforms, Bull. Seism. Soc. Am., 67, 677-691, 1977.

Burdick, L.J., and G.R. Mellman, Inversion of the body waves of the Borrego Mountain earthquake to the source mechanism, Bull. Seism. Soc. Am., 66, 1485-1499, 1976.

Dey-Sarkar, S.K., and R.A. Wiggins, Upper mantle structure in western Canada, J. Geophys. Res., 81, 3619-3632, 1976.

England, P.C., and M.H. Worthington, The travel time of P seismic waves in Europe and western Russia, Geophys. J. R. astr. Soc., 48, 63-70, 1977.

England, P.C., B.L.N. Kennett, and M.H. Worthington, A comparison of the upper mantle structure beneath Eurasia and the North Atlantic and Arctic oceans, Geophys. J. R. astr. Soc., 54, 575-585, 1978.

Futterman, W.I., Dispersive body waves, J. Geophys. Res., 67, 5279-5291, 1962.

Given, J.W., and D.V. Helmberger, Upper mantle structure of northwestern Eurasia, J. Geophys. Res., 1980, in press.

Hales, A.L., The travel times of P seismic waves and their relevance to the upper mantle velocity distribution, Tectonophysics, 13, 447-482, 1972.

Helmberger, D.V., Generalized ray theory for shear dislocation, Bull. Seism. Soc. Am., 64, 45-64, 1974.

Johnson, L.R., Array measurements of P velocities in the upper mantle, J. Geophys. Res., 72, 6309-6325, 1967.

Kanamori, H., Spectrum of short-period core phases in relation to the attenuation in the mantle, J. Geophys. Res., 72, 2181-2186, 1967.

King, D.W., and G. Calcagnile, P wave velocities in the upper mantle beneath Fennoscandia and western Russia, Geophys. J. R. astr. Soc., 46, 407-432, 1976.

Langston, C.A., A body wave inversion of the Koyna, India earthquake of December 10, 1967, and some implicatins for body wave focal mechanisms, J. Geophys. Res., 41, 2517-2529, 1976.

Langston, C.A., Corvallis, Oregon crustal and upper mantle receiver structure from teleseismic P and S waves, Bull. Seism. Soc. Am., 67, 713-724, 1977.

Langston, C.A., Structure under Mt. Ranier Washington inferred from teleseismic body waves, EOS, 59, 1142, 1978.

Minster, J.B., Transient and impluse response of a one dimensional linearly attenuating medium, Part II. A parametric study, Geophys. J. R. astr. Soc., 52, 503-524, 1978.

Pearce, R.G., Fault plane solutions using relative amplitudes of P and surface reflections: Further studies, Geophys. J. R. astr. Soc., 60, 459-487, 1980.

Pomeroy, P.W., Regional seismic wave propagation, Rondout Associates Incorporated, Semi-annual Technical Report 5, 1980.

Sacks, I.S., Mantle Q_s from body waves - difficulties in determining frequency dependence, EOS, Trans. Am. Geophys. Un., 61, 298, 1980.

Seeber, L., J.G. Armbruster, and R.C. Quittmeyer, Seismicity and continental subduction in the Himalayan arc, Interunion Commission on Geodynamics, Working Group 6 Volume, 1981.

Sipkin, S.A., and T.H. Jordan, Frequency dependence of Q_{ScS}, Bull. Seism. Soc. Am., 69, 1055-1079, 1979.

Sykes, L.R., Intra-plate seismicity, reactiviation of pre-existing zones of weakness, alkaline magmatism and other tectonism postdating continental fragmentation, Rev. Geophys. Space Phys., 16, 621-688, 1978.

Wiggins, R.A., and D.V. Helmberger, Upper mantle structure of the western United States, J. Geophys. Res., 78, 1870-1880, 1973.

Wyss, M., and P. Molnar, Source parameters of intermediate and deep focus earthquakes in the Tonga arc, Phys. Earth and Planet. Inter., 6, 279-292, 1972.

Appendix I

A COMPARISON OF THE UPPER MANTLE STRUCTURE BENEATH NORTH AMERICA AND EUROPE[1]

L. J. Burdick

Lamont-Doherty Geological Observatory

of Columbia University

Palisades, New York 10964

ABSTRACT

The techniques of modeling upper mantle structure by matching long period waveforms with synthetic seismograms have been applied to observations from the tectonically stable part of North America and from Europe. The consistent differences which can be resolved by the long period data between Europe and North America can be interpreted in terms of variations in the crust, lid and low velocity zone. At epicentral ranges less than 15°, the effects of shallow lateral variations are strong and body wave propagation is regionally dependent. Between ranges of 15° and 20°, regional effects are still observed, but they can be explained in terms of variations above 250 km. Beyond 20°, wave propagation appears to be stable and independent of region. Most of the observed long period P waves from 20° to 30° are consistent with a single model. This indicates that the relative depths and sizes of the major discontinuities do not vary substantially. A comparison of the upper mantle models of this study with those of other studies indicates that the shape of the P velocity profile is fairly uniform through the transition region (300-700 km) though there

are differences in the absolute depth to the discontinuities. These differences may be the result of systematic errors in travel time data.

INTRODUCTION

Much recent interest in the problem of lateral variations in mantle structure has been caused by the suggestion of Jordan (1975) that the structural roots of continents extend down to 400 km or more. The primary support for this suggestion comes from studies of ScS travel times and surface wave dispersion [Sipkin and Jordan, 1975, 1976; Jordan, 1979]. Opposing evidence showing that continents are much shallower than 400 km has been presented by Okal and Anderson [1975] and Okal [1977, 1978]. The investigations of higher mode Rayleigh waves by Cara [1978] and of P wave travel times and apparent velocities by England et al. [1978] also indicate that major structural differences between continents and oceans are confined to depths above 250 km. The question is still very much under debate. An issue that is just as important in resolving the depth of continental roots is the depth of lateral variations between and within continents themselves [Jordan, 1979]. Both Sipkin and Jordan [1976] and England et al. [1977] have found evidence that structural differences within continents extend well below 250 km. At the current time, there appears to be at least as much evidence to support the idea of deep lateral variations between continents as there is to support variations between continents and oceans.

An unambiguous picture of the extent and magnitude of lateral variations in seismic velocity throughout the upper mantle will most certainly help in mapping the course of its geochemical and tectonic evolution.

However, such a picture is hard to derive from comparisons of the results of different types of studies in different regions of the world. It is difficult to sort out true variations in structure from apparent variations caused by differences in methodology. Here we present the results of an effort to compare the P velocity structures of North America and Europe in the depth range of 250 to 1000 km using the single method of modeling waveforms with synthetic seismograms.

The problem of resolving large scale lateral variations in the 250 km to 1000 km depth range is severely complicated by the fact that there are substantial variations above 250 km in the crust, lid and low velocity zone. Waveform data usually come from sources in tectonically active regions and are recorded at stations in both active and stable regions. The process of distinguishing deep variations in structure from shallow is a very difficult one. In this investigation, we have attempted to find the distance range over which clear evidence for lateral variation in structure persists. We have attempted to find whether observed variations in wave propagation can be explained in terms of shallow structural differences alone or whether deeper differences are indicated. Finally we have attempted to define a set of models which can explain the different wave propagation characteristics of P waves within the regions studied.

SYNTHETIC SEISMOGRAM METHODS

The techniques for modeling upper mantle velocity structure using synthetic seismograms have been described and used by Wiggins and Helmberger [1973], Dey Sarkar and Wiggins [1976] and by Burdick and Helmberger [1978]. The procedure consists of two parts. First accurate

source models for moderate sized earthquakes or explosions are determined using data from ranges where earth structure does not significantly affect the wave shape (30° to 90°). Then synthetics are computed to match waveform observations from ranges where upper mantle structure has a strong effect (15° to 30°). A starting model is chosen for the upper mantle structure, and its response for a given range is computed using the Cagniard-de Hoop technique [Wiggins and Helmberger, 1974]. The response is convolved with the source, instrument and attenuation operators to produce the synthetic. If the final synthetic does not match the data, the starting model is perturbed by trial and error until a satisfactory fit is attained.

A more detailed discussion of the methods for computing synthetics is unnecessary in light of the previous contributions. However, some recent studies have raised some issues that need to be mentioned. One possible difficulty has been brought to light by the investigations of Burdick and Orcutt [1979] who compared the results of the Cagniard-de Hoop method to those of the reflectivity method for upper mantle structures. They showed that the primary ray approximation breaks down in the Cagniard-de Hoop method for thin transition zones. The primary ray sum is adequate only for models with moderate gradients and first order discontinuities. The extended ray sum which is necessary for thin transition zones has not yet been established and the general behavior of the seismic wave field in the presence of high gradients is not well understood. Both of these questions must be answered by future research, so only appropriately simple models will be discussed here.

A second point which has received some attention recently involves the accuracy of the correction for attenuation. In most cases a Futterman

[1962] operator has been used. New work by Sipkin and Jordan [1979] among others has shown that Q may begin to increase with frequency at some point within the seismic band. These effects are most important for short period body waves, however, and here we will be concerned with long period data. Both Kennett [1975] and Burdick and Helmberger [1978] have considered the importance of the depth dependence of Q on synthetic calculations. The latter showed that the current method is adequate if the Q distribution in the earth falls within a rather broad range. However, they investigated a specific velocity model with a relatively thin lithosphere. Rays which traveled in this high Q region were too slow to be of significance beyond 10°. In a model with a thicker, faster lithosphere, these unusually high Q paths become much more important. Such regional phases as PL and P_n may contaminate the waveform out to much greater ranges. In this study, the data set has been limited to observations from beyond 14° to minimize these possible problems.

THE REGIONS OF STUDY

The distribution of WWSSN stations and active seismic zones in the world make the U.S. and Europe the two regions that are most suitable for modeling mantle structure with the synthetic seismogram approach. The central and eastern U.S. can be studied using sources in the intermountain seismic belt on one side and in the Caribbean on the other. Central and southern Europe can be studied using sources in the North Aegean region with stations in Scandinavia or western Europe. Much is already known about the basic character of the mantle in both regions because careful studies of the travel times have been made for each.

Hales [1972] has summarized the work on travel times in the U.S. Observations from the GNOME explosion in eastern New Mexico and the Early Rise explosions in Lake Superior show that the stable part of the North American continent is very fast out to 20°. The tectonically active western U.S. is as much as 6 seconds slower in this range for P. Figure 1 shows the locations of the seismic events used in this study with respect to the stations in the U.S. and Canadian networks. The first event, the 3/28/75 Pocatello, Idaho earthquake, occurred on the eastern edge of the intermountain seismic belt [Smith and Sbar, 1974]. It had a simple impulsive source which produced a large quantity of teleseismic upper mantle data. Many of the raypaths from the source to the eastern and northeastern stations remain exclusively in the tectonically stable part of the continent. It should be noted that a few of the paths to stations in the south or northwest (DAL, JCT, FSJ) do sample the tectonic part of the continent modeled by Burdick and Helmberger [1978] (Model T7). We will show that along these paths the mantle response is somewhat different than it is in the east. The second event, the 3/24/78 Bermuda earthquake, is also well located for sampling the seismic structure of the eastern part of the continent. In this case, of course, the beginning of the raypath is always in an oceanic regime. For those paths actually used in the study, the ray bottoming points are primarily under the continent or the continental shelf. The location of the 4/9/68 Borrego Mountain earthquake in California is also shown in Figure 1 since data from it will also be considered.

Figure 2 shows the sources and stations used in studying the mantle structure of Europe. The travel times for this same combination of source regions and stations were studied by England and Worthington [1977]. They

found that the times were generally much slower out to ranges of 20° than they are in central and eastern North America. In this sense the region should perhaps be classified as tectonically active continent, but some of the WWSSN stations to the north are situated in areas which have been stable since Hercynian times. (In classifying areas as tectonically active or stable we will generally adopt the map given by Jordan [1975]). So, as in the North American study, some of the raypaths traverse mixed tectonic regimes. The two North Aegean earthquakes selected for use are moderate sized normal events which are very comparable to the Idaho event in North America. They produced simple clear P wave records at all ranges from 15° to 90°.

THE SOURCE MODELS

The earthquake sources are modeled as simple point shear dislocations buried in a layered half space. The far field time function is assumed to be a triangular pulse specified only by a rise and fall-off time which is independent of azimuth and take-off angle [Langston and Helmberger, 1975]. The final source models based on fits to the P and SH waveforms from = 30° to 90° are given in Table 1.

The Pocatello, Idaho earthquake source was modeled independently by both Burdick [1978] and Bache et al. [1980]. The first motion data alone constrained the fault plane solution and as shown in Figure 3, the source model fits the WWSSN records from the greater distances. An accurate source model for the Bermuda earthquake was first presented by Stewart [1979]. (The model used here was modified slightly to fit additional first motion data from South America.) It was a thrust earthquake which occurred under about 5 km of water. The fits of the P waveforms are shown in Figure 4. The closely matched details later in the waveform are caused by

reverberations in the water layer. The two North Aegean events were previously studied by McKenzie [1972] using first motion data. His published source mechanisms were not accurate enough to fit the waveform observations, so some modifications were necessary. The new solutions still represent dipping normal faults, but the azimuths of the planes and the amount of strike-slip motion are different. Both P and SH waveforms were used to constrain the solutions. The final waveform fits are shown in Figures 5 and 6.

The quality of fit of synthetics to data in Figures 3 through 6 should give some measure of the accuracy with which the effects of the source and the instrument on the waveforms can be predicted. Though the fit is generally good, it is not exact. The degree of misfit of synthetics at upper mantle ranges must be compared to the misfit from these greater ranges in deciding whether it results from failure of the upper mantle model or failure of the source model.

MODELS FOR SHALLOW VARIATION IN STRUCTURE

The problem of resolving deep lateral variations in structure in the presence of strong shallow variations is a difficult one. It is made even more difficult by the fact that the synthetic seismogram methods to be used are appropriate for purely radial structures. The simple approach we have taken is to define a model that we take to be an average for tectonically active regions and a model that is an average for stable regions. The differences in the models above 250 km are designed to satisfy observed differences in travel time and vertical delay and to be qualitatively consistent with surface wave regionalization results. From these two

models, we have attempted to establish the magnitude of the effect of the shallow lateral variations on long period P wave propagation, and the distance range to which it extends. We have then compared the results with the observed properties of wave propagation in North America and Europe to see if variations occur which fall outside of these bounds.

The models tested are shown in Figure 7 and listed in Table 2. Tectonic continent model, T9, is a variant on the western U.S. model T7 of Burdick and Helmberger [1978]. (We adopt the convention of showing layers as homogeneous in both the radial and flat-lying case.) The only difference is that the lower discontinuity has been raised slightly for reasons to be discussed later. The model has a well developed low velocity zone which is appropriate for a tectonically active continent [Johnson, 1967; Helmberger, 1973]. Stable continent model S8 has a thicker crust and no low velocity zone. Below 250 km, models S8 and T9 are identical.

Figure 8 compares the travel time curves for the two models. The predominant effect of the low velocity zone in model T9 is to slow it down with respect to S8. The crosses in the figure are travel times along stable continent paths in North America. They include the Early Rise times along the Texas and Arkansas profiles, times from Early Rise to some other selected stations, times from Salmon and also times from the GNOME explosion along the eastern profile [Romney et al., 1962; Jordan et al., 1966; Iyer et al., 1969]. Green and Hales (1968) used this data in constructing their stable continent model ER1. The circles are travel times from tectonic continent paths and mixed regime paths. They include the data set of NTS travel times considered by Burdick and Helmberger [1978] and the average travel times for Europe given by England and Worthington [1977]. The two data sets clearly define the travel time differences between stable

and active continent, and models S8 and T9 are shown to be representative of the two types of behavior. The difference in vertical delay time is 1 second between the two models. This corresponds with the measured average residual difference between the eastern and western U.S. of Carder et al. [1966]. The qualitative differences between the models are consistent with the well known results of surface wave regionalization work [Knopoff, 1972]. The differences in the theoretical responses of the models should provide an estimate of the average effects of shallow differences in structure between stable and tectonic continent.

Burdick and Helmberger [1978] observed that at distances less than 15° shallow lateral variations in structure have a large effect. The characteristics of the propagation of long period body waves are so regionally dependent that modeling waveforms with an average earth model is not productive. The same is true at short ranges in the regions considered here. The effects of shallow lateral variations are less severe beyond 15°, but they exist nonetheless. Figure 9 compares the delta function responses for S8 and T9 at ranges between 15° and 19°. Even though the direct ray is turning below 250 km and the large reflection comes from 400 km, the variations above 250 km have a significant effect. The relative time and amplitude of the two arrivals are measurably different. We can expect, therefore, that variations in lid and low velocity zone structure will continue to have an effect in these ranges. The magnitude of the effect will typically be of the order of the differences in Figure 9, but because S8 and T9 are average rather than extremal models it could be even larger. Given and Helmberger [1980] show that if the lid velocities are slightly higher than in S8, the first arrival will be in the lid shadow zone out to 19°. It will be very fast but very small. Alter-

natively, some ray paths may pass through an even more substantial low velocity zone than the one in T9, so that the two arrivals will be moved still closer together. Thus, if we find in the data variations in the relative amplitude and time of the two arrivals at ranges between 15° and 19°, we can attribute the effect to lateral varitions above 250 km. The interpretation will not be unique, however, and we cannot preclude variations from 250 to 400 km.

By 19° in Figure 9, the responses of the two models have become similar. The lateral variations above 250 km still do have a residual effect beyond this range because the distance, Δ, for a given ray parameter will be shifted. Figure 8 shows that the triplications of model T9 are just those of S8 shifted to shorter range by about half a degree. In real data we can expect to sometimes find that the triplications are shifted to different ranges for different raypaths simply because of lateral variations above 250 km.

THE UPPER MANTLE TRIPLICATIONS

The two discontinuities in models S8 and T9 cause two major triplications. The first begins at about 14° and ends at 23°, and the second extends roughly from 17° to 26°. Past experience has shown that given branches of the triplications are best observed over selected distance ranges. These are the ranges where the triplication branch is about 5 to 10 seconds behind the first arrival. Then the secondary arrival is far enough behind the first so that it is clear of it but not so far back that it is lost in the noise of the coda. In the following, we will consider the data in groups by distance range according to which triplication branches have the largest effect.

Figure 10 compares data to synthetics for ranges where the first arrival comes from above the 400 km discontinuity, and a strong second arrival is caused by the forward branch of the first triplication. As Figure 9 shows, there are substantial differences between S8 and T9 at these ranges, so in Figure 10 synthetics are shown for each. The large two-sided arrival in the delta function responses is the 400 km discontinuity reflection and the small one-sided third arrival is the narrow angle reflection from the 650 km discontinuity. The MNT and OTT records from Bermuda show a clear feature associated with the triplication arrival as indicated by the small arrows. Model S8, without the low velocity zone, fits this feature much better than T9. All of the Bermuda records are more consistent with S8 indicating that this model is more appropriate for eastern North America. The data from the Idaho event are not more consistent with one model than the other, but as shown in Figure 1 many of the raypaths traverse partially tectonic and partially stable areas. The records from the European events are more consistent with the S8 model, but again the raypaths involved traverse mixed regions.

Evidence for some type of lateral variation in structure is abundant in data from less than 19°. A good example in Figure 10 can be found in a comparison of the records from DAL and JCT for the Idaho event. Both stations are at the same distance (15.5°) and are at very nearly the same azimuth from the source (Figure 1), but the waveforms are different. It will be shown that in this instance, as in several others, the discrepancy can be explained by a slight shift in the arrival time of the reflected energy. The records can be modeled with the upper mantle response of T9 or S8 from a shifted range which is less than 1° away from the true range.

Between 19° and 22° there are five critically reflected ray arrivals causing a quintuplication. Figure 11 compares the observations to the synthetics for these ranges from model S8. [Model T9 gives almost identical results.] The delta function responses show the strong interaction between the various arrivals. The fit between the data and synthetics indicates that the model responses are accurate at these very sensitive ranges. The arrows show a small secondary arrival which appears at 19.3°, 19.6° and 19.8°. This feature has been modeled as the forward branch of the second triplication. If this interpretation is correct, these are among the first observations of this branch which have been modeled in long period waveform data. To match the timing of this phase, it was necessary to move the lower discontinuity up to 650 km. The velocity gradient beneath the discontinuity was reduced to compensate for the change. This keeps the model responses of T7 and T9 the same at greater distances. The only significant differences in the T7 and T9 responses occur from 19° to 22° where the arrival time of the lower discontinuity reflection is different. Burdick and Helmberger [1978] did not have any observations of this reflection so T7 was unconstrained with regard to this triplication branch. The match of the timing and amplitude of the small arrival is good at 19.3° and 19.6°, but the fit at MAL at 19.8° is relatively poor. Nonetheless, the arrival is clear in the data and some possible reasons for the misfit are discussed in the following.

The data from ranges between 15° and 20° contained many indications of lateral variation in mantle response. Figure 12 shows some specific examples in which the fit to the waveforms can be much improved by using the theoretical responses from a shifted range. The first and second arrivals vary in relative timing and amplitude by about a second, but there

is no evidence for anomalously large or anomalously small second arrivals and no evidence for additional arrivals. Also shown in Figure 12 is the record from 19.8° which contains an arrival from the lower discontinuity. The duration of the source time function in the synthetic has been shortened which improves the fit substantially. This indicates that source directivity may have been an important factor. Attempts to improve the fit further by perturbing the upper mantle structure were unsuccessful. However, the amplitude of the arrival appears to be nearly correct, and at this range the interference between arrivals is very delicate. A small change in the triplication arrival times might account for the effect, but a major change in the size of the discontinuity is not suggested by the data. Further complications in the source or structure at the station may also have had an effect.

Figure 13 shows data and synthetics for ranges 22° to 24.5° where the back branch of the first triplication causes some clear features as indicated by the arrows. Records from both the European events and the Idaho event are fit well by the model. Figure 14 compares data to synthetics for Δ = 24.5° to 28°. The model fits all of the observations from the U.S. and Europe reasonably well. The records of the 4 new events being studied did not contain clear features associated with the back branch of the second triplication. For this reason two records from the Borrego Mountain earthquake which do contain such an arrival were modeled. The records are marked "BO" in the figure and the arrival is indicated by the arrows. This arrival was originally modeled with T7 by Burdick and Helmberger [1978], but T9 fits it just as well. Thus we have included in the data set clear features associated with the forward and back branches of both triplications and have modeled them with models S8 and T9. No strong evidence

has been found that the sizes of the discontinuities or the basic shape of the triplication curves vary systematically in North America and Europe.

RESULTS AND DISCUSSION

The process of searching for large scale lateral variations in upper mantle structure using the synthetic seismogram method has only begun. Many continental as well as oceanic areas have not yet been studied by any method. However, there are some important results which are true for this particular comparison. There is no consistent evidence for broad scale differences in such features as the size of the major discontinuities, their relative locations or the strength of the velocity gradients between them. There is no evidence for additional discontinuities. In the quintuplication region, where the effect of the upper mantle discontinuities is strongest, we find very similar upper mantle delta function responses for North America and Europe (Figure 7). Most of the evidence for lateral variations in upper mantle structure can be explained in terms of differences above 250 km.

Given and Helmberger [1980] completed a waveform analysis study for northwestern Eurasia which gave results very similar to the ones presented here. Figure 15 compares their preferred model K8 with S8 of this study. The sizes of the discontinuities, their relative separation and the strengths of the gradients between them are virtually the same. The inset shows that the shape of the triplications in the travel time curve are nearly the same for the two models. However, there is a difference in the absolute depth to the discontinuities of about 20 km causing a relative shift in the triplications of about 1°. The differences in depth to the

discontinuities may not be significant. Different structures were adopted in the two studies for the crust and lid. The apparent variations in absolute depth could be partially or completely absorbed in the top portions of the models. The shift in the distance range of the triplication by 1°, on the other hand, is grounded directly in the observations. It also corresponds with the types of lateral variations found in this study. There is a definite possibility that systematic variations in absolute depth to the transition zones do occur at about the level indicated in Figure 13. The studies of Jordan [1979] may have resolved this type of variation. If the absolute depth to the major discontinuities does change on a broad scale, but their relative shape and position remains constant, then vertical delay times would change, but the shapes of the triplication curves would not. This type of lateral variation model could reconcile all the observations, although it would imply lateral density gradients. The differences in the depths to the discontinuities would also have to be larger than those in Figure 15 to explain the magnitude of the S wave residual differences between continents and oceans. A final important point is that the S wave vertical travel time residuals cited by Jordan [1979] varied by only about 1.5 seconds between stable and active continent. In P waves, this would correspond to a difference of only about 1 second. Models S8 and T9 can account for this difference.

One possible shortcoming of the upper mantle models for northwestern Eurasia of both Given and Helmberger [1980] and King and Calcagnile [1976] is that they are based on travel time data that may be inaccurate. Both models were constrained to fit ISC travel times from Soviet nuclear tests. These observations dictate that travel times from 25° to 30° should be very close to JB. Rodean [1979] points, however, that the estimated origin

times for these events are always 2 or 3 seconds before the minute. He concludes that the distribution of stations around the USSR combined with the use of JB travel time curves by ISC in locating events has caused this systematic error in origin time. Many studies show that stable continental travel times are faster than JB from 25° to 30° [Hales, 1972; Carder et al., 1976], and S8 has been designed to fit this criterion. Figure 13 shows that if model K8 was adjusted so that it was 2 seconds faster for rays that bottom below 800 km, it would begin to resemble S8 even more.

The previous work of King and Calcagnile [1976] and England et al. [1977, 1978] suggested that major lateral variations in the sizes of the upper mantle discontinuities existed in the continental regions surrounding NORSAR. Waveform analysis studies have failed to substantiate this result. The King and Calcagnile model, KCA, contained an unusual low gradient zone above the first discontinuity and a relatively large (7%) jump in velocity for that transition. The work of Given and Helmberger [1980] has shown that these unusual features are not all representative of the mantle structure of northwestern Eurasia. The synthetics from KCA do not even satisfy waveform observations from WWSSN stations very close to NORSAR. The low gradient zone above 420 km is either a very localized feature or an artifact caused by some peculiarity of the shallow structure beneath NORSAR. England et al. [1977] concluded that major differences existed between Europe and northwestern Eurasia because they also failed to find evidence of the unusual structure in KCA above 420 km. Since this structure represents at best a very local feature and since very similar models have been found for the two regions from waveform studies (Figure 15), few reasons remain to suspect deep lateral variations in

structure exist between them. It would appear from these comparisons at least that the relative shape of the velocity profile through the transition region is approximately as shown in Figure 15 beneath North America, Europe and northwestern Eurasia. The predominant type of lateral variation in wave propagation is a shifting of the triplications in distance caused by laterally varying structure above 250 km (Figure 8) or variation in the depth to the transitions (Figure 15).

ACKNOWLEDGEMENTS

This manuscript has been improved substantially by the helpful comments of Lynn R. Sykes and Paul G. Richards. The work has been supported by the Advanced Research Projects Agency of the Department of Defense and was monitored by the Air Force Office of Scientific Research under Contract Number F49620-79-C-0021. Lamont-Doherty Geological Observatory Contribution Number 0000.

REFERENCES

Bache, T.C., D.G. Lambert, and T.G. Barker, A source model for the March 28, 1975 Pocatello Valley earthquake from time domain modeling of teleseismic P waves, Bull. Seism. Soc. Am., 70, 405-418, 1980.

Burdick, L.J., Reflections from upper mantle discontinuities beneath the central U.S. [Abst.], EOS, Trans. Am. Geophys. Un., 59, 1142, 1978.

Burdick, L.J., and D.V. Helmberger, The upper mantle P velocity structure of the western United States, J. Geophys. Res., 83, 1699-1712, 1978.

Burdick, L.J., and J.A. Orcutt, A comparison of the generalized ray and reflectivity methods of waveform synthesis, Geophys. J. R. astr. Soc., 58, 261-278, 1979.

Cara, M., Lateral variations of S velocity in the upper mantle from higher mode Rayleigh waves, Geophys. J. R. astr. Soc., 57, 649-670, 1979.

Carder, D.S., D.W. Gordan, and J.N. Jordan, Analysis of surface foci travel times, Bull. Seism. Soc. Am., 56, 815-840, 1966.

Dey-Sarkar, S.K., and R.A. Wiggins, Upper mantle structure in western Canada, J. Geophys. Res., 81, 3619-3632, 1976.

England, P.C., and M.H. Worthington, The travel time of P seismic waves in Euro e and western Russia, Geophys. J. R. astr. Soc., 48, 63-70, 1977.

England, P.C., M.H. Worthington, and D.W. King, Lateral variation in the structure of the upper mantle beneath Eurasia, Geophys. J. R. astr. Soc., 48, 71-79, 1977.

England, P.C., B.L.N. Kennett, and M.H. Worthington, A comparison of the upper mantle structure beneath Eurasia and the North Atlantic and Arctic oceans, Geophys. J. R. astr. Soc., 54, 575-585, 1978.

Given, J.W., and D.V. Helmberger, Upper mantle structure of northwestern Eurasia, J. Geophys. Res., 1980 [in press].

Green, R.W.E., and A.L. Hales, The travel times of P waves to 30° in the central United States and upper mantle structure, Bull. Seism. Soc. Am., 58, 267-289, 1968.

Hales, A.L., The travel times of P seismic waves and their relevance to the upper mantle velocity distribution, Tectonophysics, 13, 447-482, 1972.

Helmberger, D.V., On the structure of the low velocity zone, Geophys. J. R. astr. Soc., 34, 251-263, 1973.

Iyer, H.M., L.C. Pakiser, D.J. Stuart, and D.H. Warren, Project Early Rise: seismic probing of the upper mantle, J. Geophys. Res., 74, 4409-4441, 1969.

Johnson, L.R., Array measurements of P velocities in the upper mantle, J. Geophys. Res., 72, 6309-6325, 1967.

Jordan, J.N., W.V. Mickey, W. Helterbran, and D.M. Clark, Travel times and amplitudes from the Salmon explosion, J. Geophys. Res., 71, 3469-3482, 1966.

Jordan, T.H., The continental tectosphere, Rev. Geophys. Space Phys., 13, 1-12, 1975.

Jordan, T.H., Structural geology of the earth's interior, Proc. Nat. Acad. Sci. USA, 76, 4192-4200, 1979.

Kennett, B.L.N., The effect of attenuation on seismograms, Bull. Seism. Soc. Am., 65, 1643-1651, 1975.

King, D.W., and G. Calcagnile, P wave velocities in the upper mantle beneath Fennoscandia and western Russia, Geophys. J. R. astr. Soc., 46, 407-432, 1976.

Knopoff, L., Observation and inversion of surface wave dispersion, Tectonophysics, 13, 497-519, 1972.

Langston, C.A., and D.V. Helmberger, A procedure for modeling shallow dislocation sources, Geophys. J. R. astr. Soc., 42, 117-130, 1975.

McKenzie, D., Active tectonics of the Mediterranean region, Geophys. J. R. astr. Soc., 30, 109-185, 1972.

Okal, E., The effect of intrinsic oceanic upper mantle heterogeneity on regionalisation of long period Rayleigh wave phase velocities, Geophys. J. R. astr. Soc., 49, 357-370, 1978.

Okal, E.A., Observed very long period phase velocities across the Canadian Shield, Geophys. J. R. astr. Soc., 53, 663-668, 1979.

Okal, E.A., and D.L. Anderson, A study of lateral inhomogeneities in the upper mantle by multiple ScS travel-time residuals, Geophys. Res. Lett., 2, 313-316, 1975.

Rodean, H.C., ISC events from 1964 to 1976 at and near the nuclear testing ground in eastern Kazakhstan, Lawrence Livermore Laboratory Technical Report UCRL 52856, 1979.

Romney, C., B.G. Brooks, R.H. Mansfield, D.S. Carder, J.N. Jordan, and D.W. Gordan, Travel times and amplitudes of principal body phases recorded from Gnome, Bull. Seism. Soc. Am., 52, 1057-1074, 1962.

Sipkin, S.A., and T.H. Jordan, Lateral heterogeneity of the upper mantle determined from the travel times of ScS, J. Geophys. Res., 80, 1474-1484, 1975.

Sipkin, S.A., and T.H. Jordan, Lateral heterogeneity of the upper mantle determined from the travel times of multiple ScS, J. Geophys. Res., 81, 6307-6320, 1976.

Sipkin, S.A., and T.H. Jordan, Frequency dependence of Q_{ScS}, Bull. Seism. Soc. Am., 69, 1055-1079, 1979.

Smith, R.B., and M.L. Sbar, Contemporary tectonics and seismicity of the western United States with emphasis on the intermountain seismic belt, Geol. Soc. Am. Bull., 85, 1205-1218, 1974.

Stewart, G.S., The Grand Banks earthquake of November 18, 1929 and the Bermuda earthquake of March 24, 1978 -- a comparative study in relation to their intraplate location [Abst.], EOS, Trans. Am. Geophys. Un., 60, 312, 1979.

Wiggins, R.A., and D.V. Helmberger, Upper mantle structure of the western United States, J. Geophys. Res., 78, 1870-1880, 1973.

Wiggins, R.A., and D.V. Helmberger, Synthetic seismogram computation by expansion in generalized rays, Geophys. J. R. astr. Soc., 37, 73-90, 1974.

TABLE 1

Earthquake Source Models

Event	Strike*	Dip*	Rake*	Depth	T_1 †	T_2 †
N. Aegean 3/4/67	82°	49°	235°	12 km	2.0 sec	3.0 sec
N. Aegean 11/30/67	196°	49°	240°	12 km	2.5 sec	2.5 sec
Idaho 3/28/75	7°	61°	245°	6 km	1.0 sec	2.0 sec
Bermuda 3/24/78	138°	45°	65°	11 km	1.5 sec	1.5 sec

* For definitions see Langston and Helmberger [1975]

† Rise time and falloff time of triangular source pulse

TABLE 2

Velocity Models

Depth to Bottom of Layer (km)	α (km/sec)	Depth to Bottom of Layer (km)	α (km/sec)
	T9		S8
20.0	6.00	30.0	6.50
35.0	6.50	50.0	7.10
45.0	7.95	60.0	8.10
55.0	8.00	70.0	8.20
65.0	8.05	80.0	8.24
73.1	7.75	90.0	8.24
89.8	7.72	100.0	8.25
103.3	7.70	120.0	8.25
117.5	7.73	130.0	8.26
127.0	7.77	140.0	8.26
135.7	7.83	150.0	8.27
144.4	7.88	160.0	8.28
150.5	7.94	170 0	8.29
156.4	8.03	180.0	8.30
162.3	8.11	190.0	8.32
168.2	8.19	200.0	8.34
180.0	8.25	210.0	8.36
190.0	8.28	220.0	8.38
200.0	8.30	230.0	8.40
210.0	8.33	240.0	8.42
220.0	8.35	250.0	8.44
230.0	8.38		
240.0	8.41		
250.0	8.43		
	Both T9 and S8		
260.0	8.46		
270.0	8.48		
280.0	8.51		
290.0	8.54		
300.0	8.56		
310.0	8.59		
320.0	8.61		
330.0	8.64		
340.0	8.67		
350.0	8.69		

Depth to Bottom of Layer (km)	α (km/sec)	Depth to Bottom of Layer (km)	α (km/sec)
	Both T9 and S8		Both T9 and S8
360.0	8.72	805.0	11.06
370.0	8.74	815.0	11.08
380.0	8.77	825.0	12.00
386.0	8.79	835.0	11.12
395.0	8.81	845.0	11.14
400.0	9.24	855.0	11.16
410.0	9.27	865.0	11.18
420.0	9.31	885.0	11.22
430.0	9.35	905.0	11.26
440.0	9.39		
450.0	9.43		
460.0	9.46		
470.0	9.50		
430.0	9.54		
490.0	9.58		
500.0	9.62		
510.0	9.65		
520.0	9.69		
530.0	9.73		
540.0	9.77		
550.0	9.80		
560.0	9.84		
570.0	9.88		
580.0	9.92		
590.0	9.96		
600.0	10.00		
610.0	10.03		
620.0	10.07		
630.0	10.11		
640.0	10.18		
650.0	10.25		
655.0	10.76		
665.0	10.78		
675.0	10.80		
685.0	10.82		
695.0	10.84		
705.0	10.86		
715.0	10.88		
725.0	10.90		
739.0	10.92		
745.0	10.94		
755.0	10.96		
765.0	10.98		
775.0	11.00		
785.0	11.02		
795.0	11.04		

FIGUPE CAPTIONS

Figure 1: The locations of the seismic events (squares) used in the study of North America are shown with respect to the WWSSN and Canadian stations (circles). The shaded area is the previously modeled tectonic part of the continent.

Figure 2: The locations of the two seismic events (triangles) used in the study of Europe are shown with respect to the WWSSN stations (circles).

Figure 3: Observed records (heavy line) from the Idaho event from distance ranges between 30° and 90° are compared to the corresponding synthetics (light line). The data and synthetics shown here and throughout are normalized to peak amplitude.

Figure 4: Observed records (heavy line) from the Bermuda event from distance ranges between 30° and 90° are compared to the corresponding synthetics (light line).

Figure 5: Observed records (heavy line) from the first European event (E1) from distance ranges between 30° and 90° are compared to the corresponding synthetics (light line).

Figure 6: Observed records (heavy line) from the first European event (E1) from distance ranges between 30° and 90° are compared to the corresponding synthetics (light line).

Figure 7: The two layered velocity models representing stable and tectonic continental structure are compared. The only differences in the models occur above 250 km.

Figure 8: The triplication curves for the stable and tectonic continent models are plotted along with observed data.

Figure 9: The delta function responses for models S8 and T9 are compared in the distance ranges where the differences in the low velocity zone continue to have a large effect. The responses have been smoothed with a gaussian filter to remove the noise due to model layering.

Figure 10: The observed seismograms from ranges between 14° and 18° are shown in heavy line. To the left is shown the synthetic for the source except for the mantle response followed by the mantle model delta function response and then the final synthetic (all in light line) beneath the observed wave. Synthetics are shown for both S8 and T9. The arrows indicate clear features associated with the triplication arrival. B indicates records from the Bermuda earthquake, I from Idaho, E1 from the 3/4/67 European and E2 from the 11/30/67 European.

Figure 11: The observed seismograms (heavy line) from ranges between 19° and 22° are compared to synthetics (light line). The arrangement of data and synthetics is the same as in

Figure 10. The arrows indicate features associated with the arrival of the reflection from the lower discontinuity.

Figure 12: Observed P waves (heavy line) are compared to synthetics (light line) computed for a slightly shifted range. The source of the MAL record has been changed but the distance is correct. The arrangement of data and synthetics is the same as in Figure 10.

Figure 13: The observed seismograms (light line) from ranges between 22° and 25° are compared to synthetics (light line). The arrangement of data and synthetics is the same as in Figure 10. The arrows indicate features associated with the reflection from the upper discontinuity.

Figure 14: The observed seismograms (heavy line) are compared to the synthetics (light line) for ranges between 24° and 29°. The arrangement of data and synthetics is the same as in Figure 10. "BO" indicates records from the Borrego Mountain earthquake.

Figure 15: The layered velocity models for stable continent and northeast Eurasia are compared. The travel time curves in the inset are plotted on shifted time and distance scales.

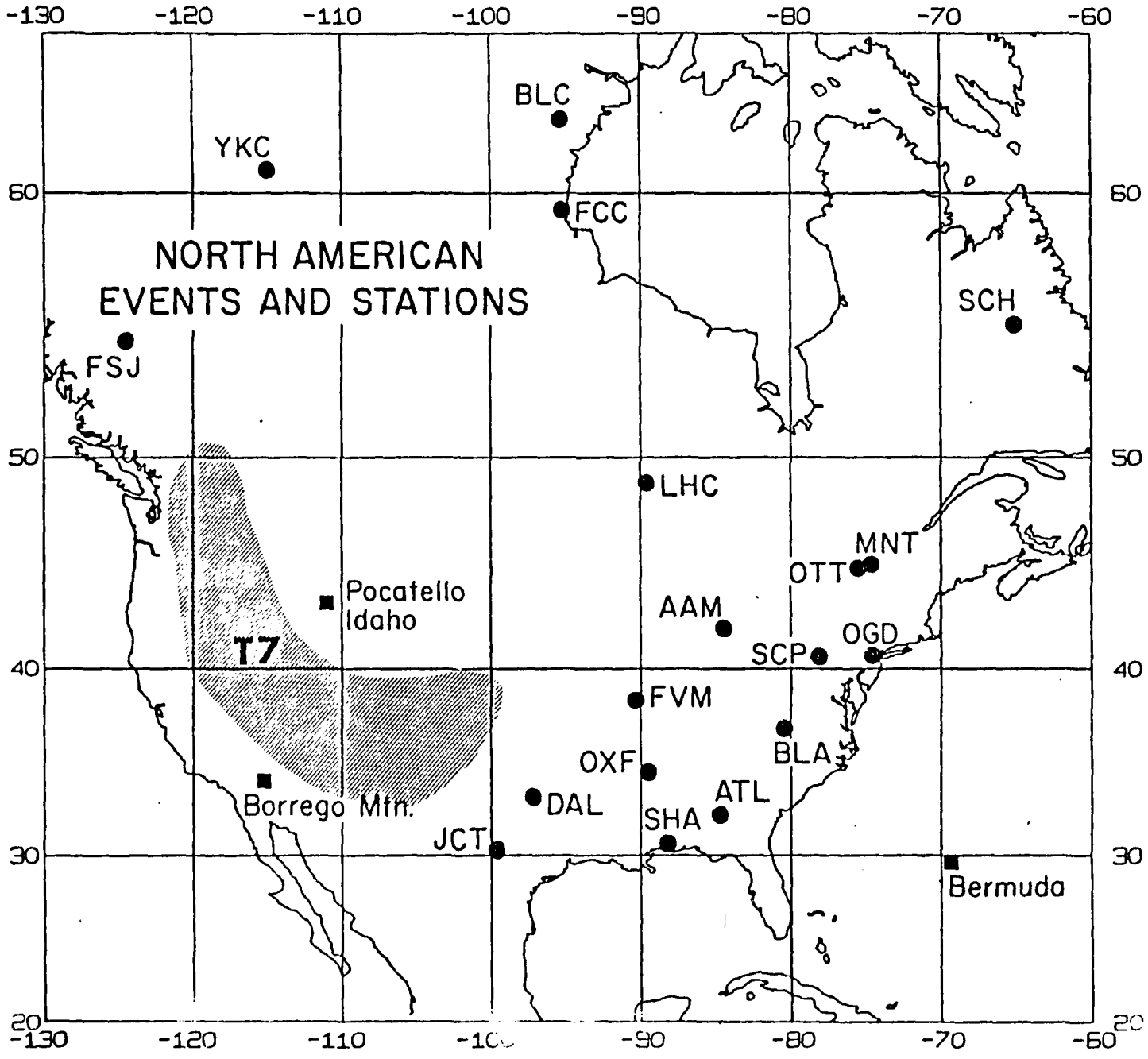
NORTH AMERICAN
EVENTS AND STATIONS
-130
-120
-110
-100
-90
-80
-70
-60
60
50
40
30
20
YKC
BLC
FCC
SCH
FSJ
LHC
MNT
OTT
Pocatello
Idaho
AAM
OGD
SCP
T7
FVM
BLA
OXF
ATL
DAL
SHA
JCT
Borrego Mtn.
Bermuda

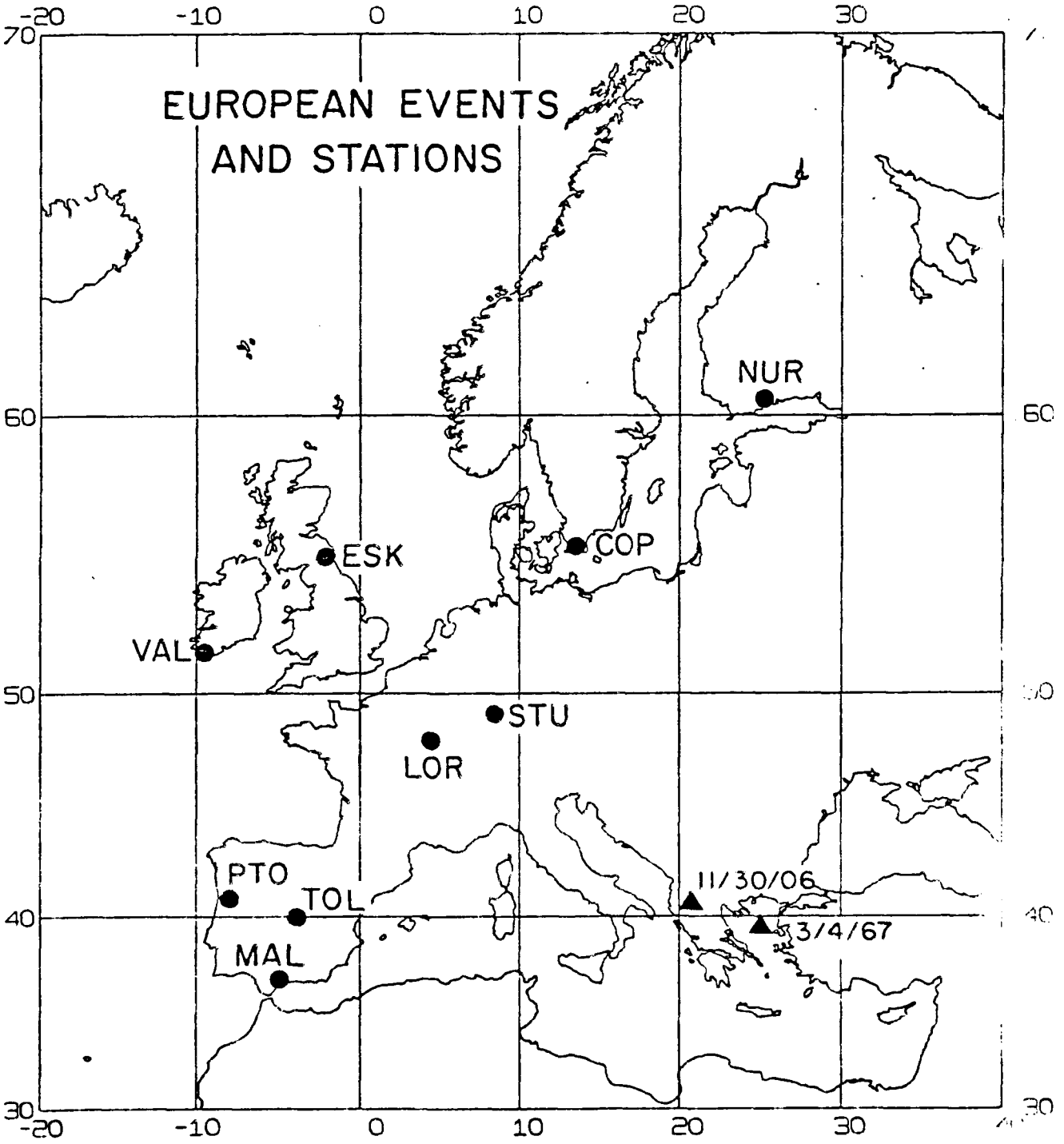
EUROPEAN EVENTS
AND STATIONS
-20
-10
0
10
20
30
70
60
50
40
30
NUR
ESK
COP
VAL
STU
LOR
PTO
TOL
MAL
11/30/06
3/4/67

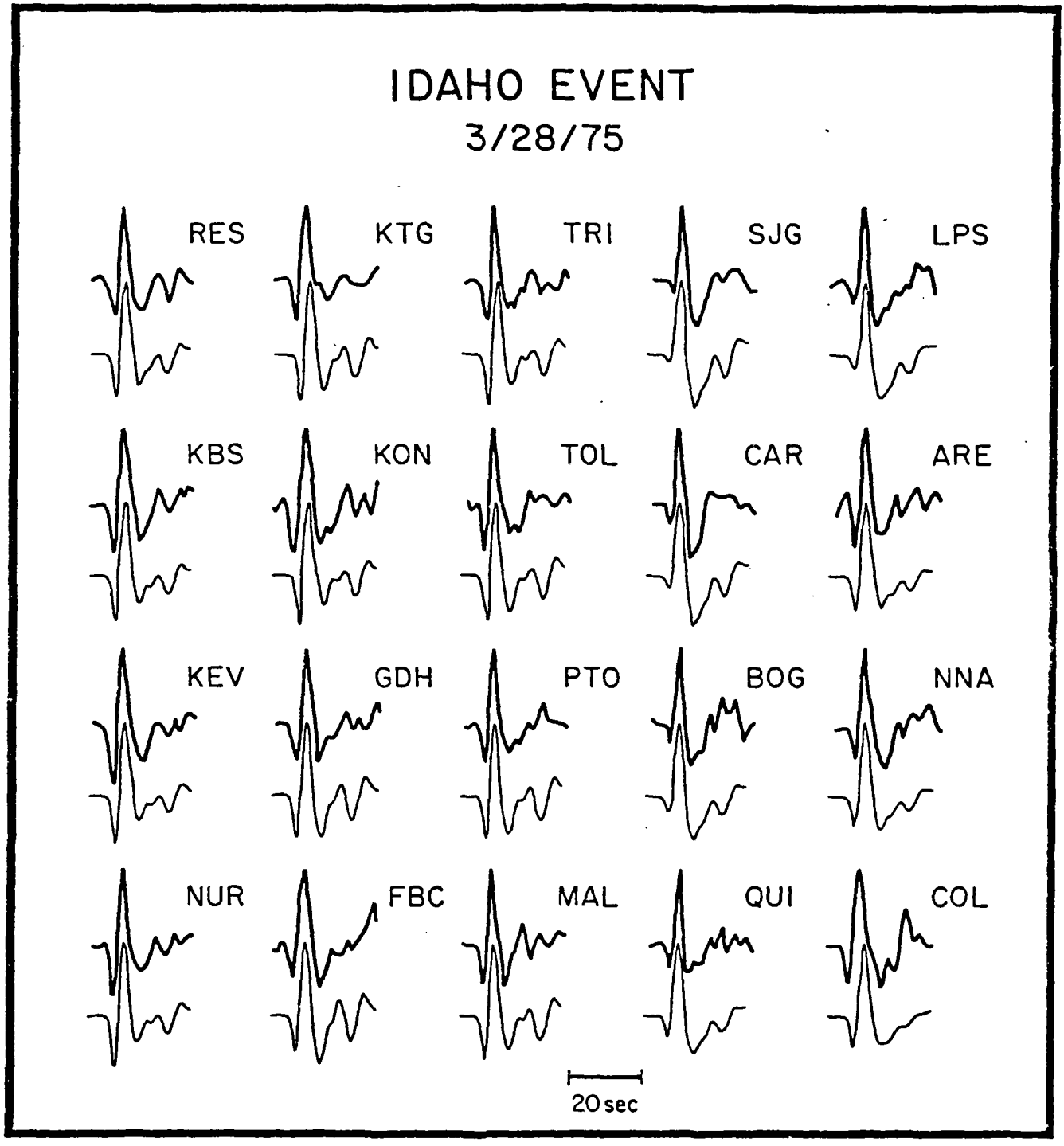
IDAHO EVENT
3/28/75
RES
KTG
TRI
SJG
LPS
KBS
KON
TOL
CAR
ARE
KEV
GDH
PTO
BOG
NNA
NUR
FBC
MAL
QUI
COL
20 sec

BERMUDA EVENT

3/24/78

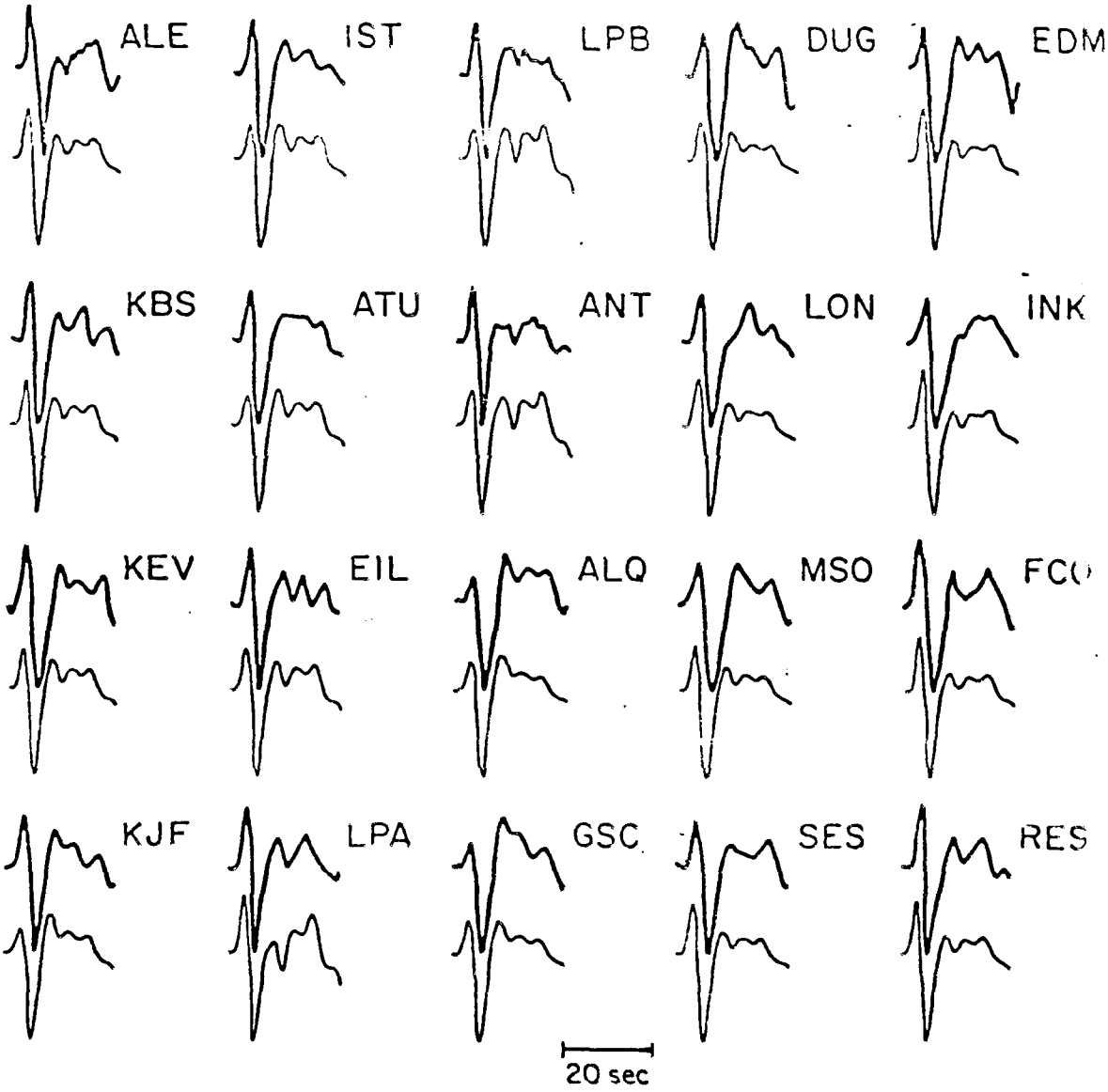

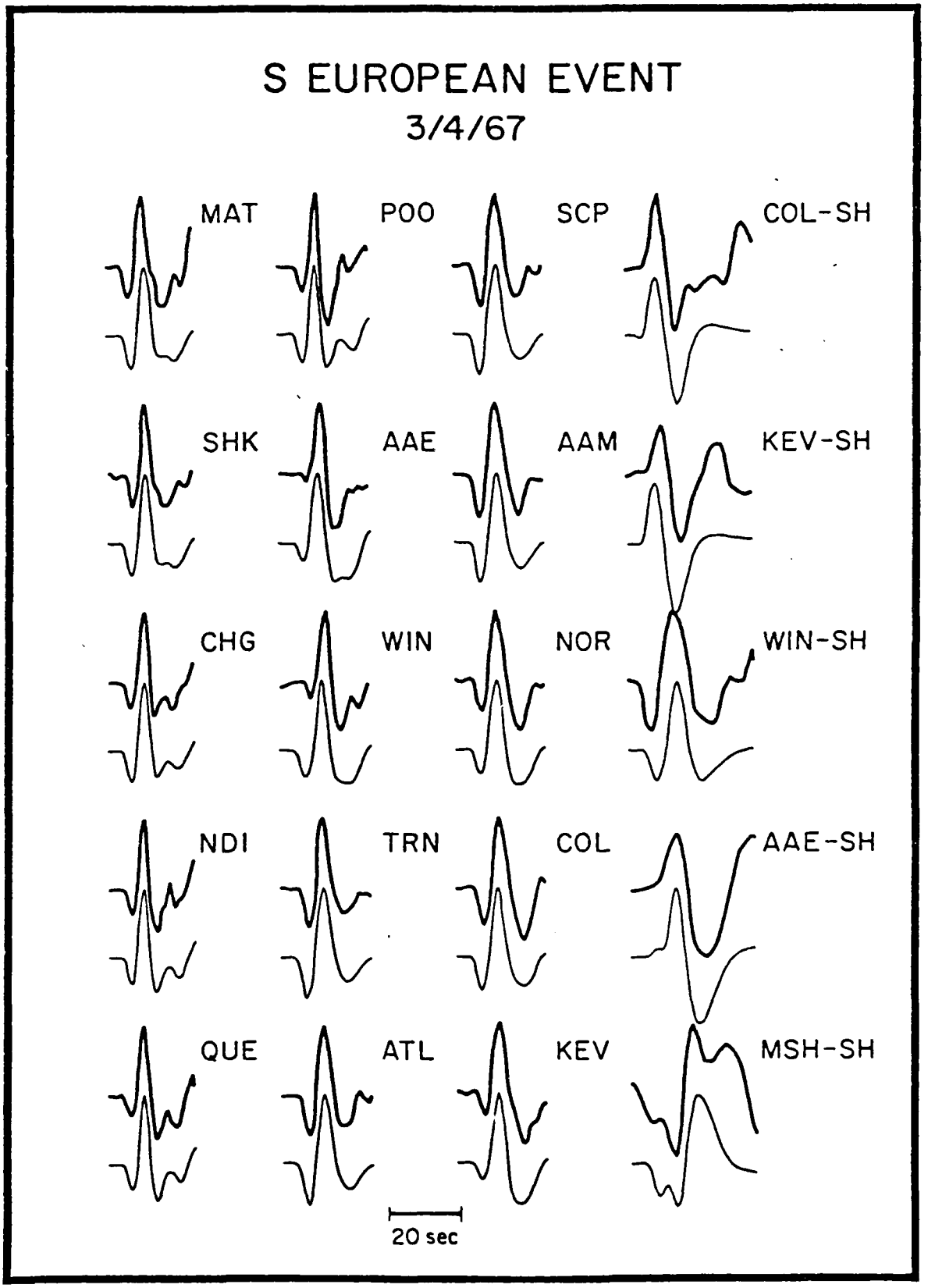
S EUROPEAN EVENT
3/4/67
MAT
POO
SCP
COL-SH
SHK
AAE
AAM
KEV-SH
CHG
WIN
NOR
WIN-SH
NDI
TRN
COL
AAE-SH
QUE
ATL
KEV
MSH-SH
20 sec

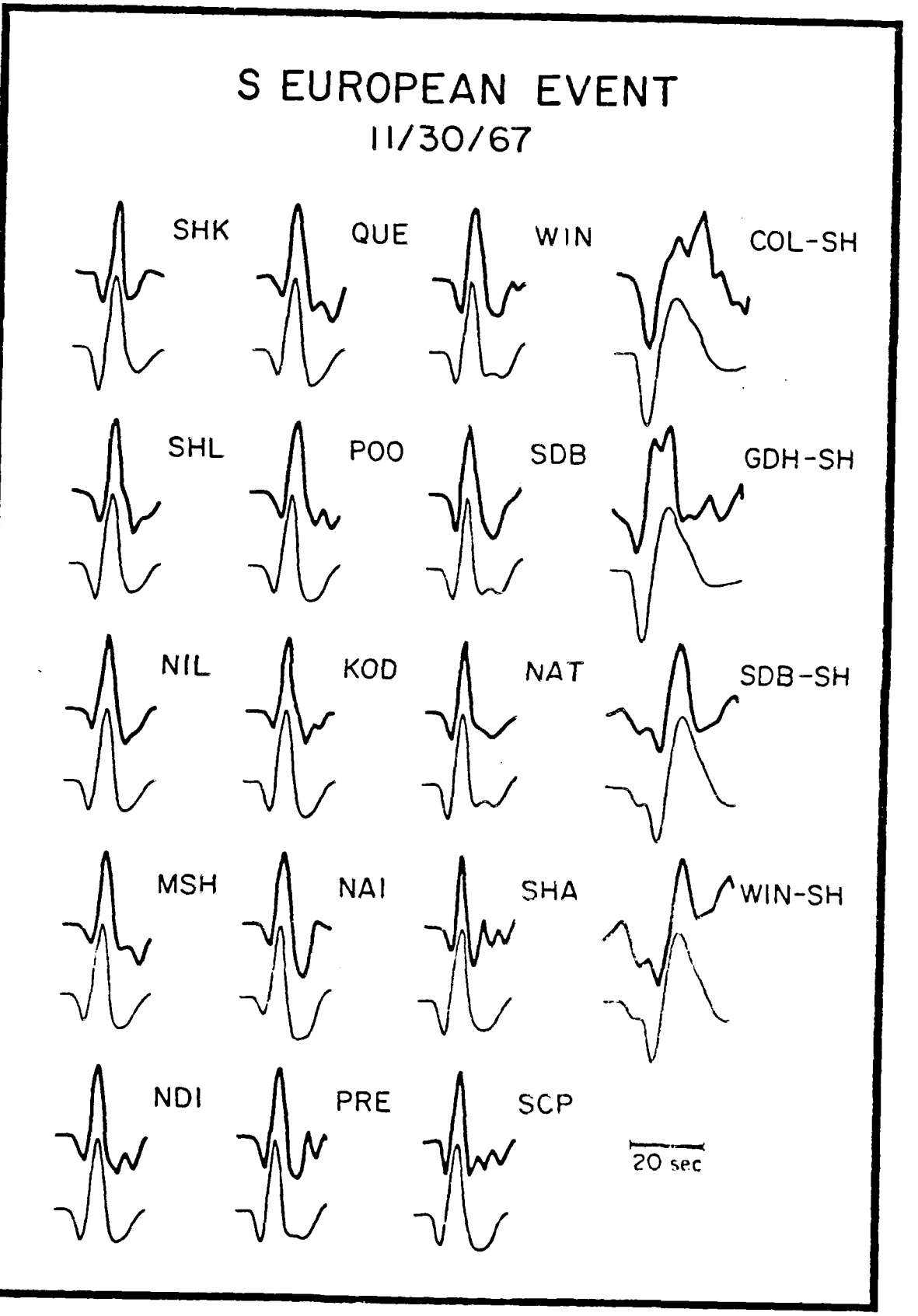
S EUROPEAN EVENT
11/30/67
SHK
QUE
WIN
COL-SH
SHL
POO
SDB
GDH-SH
NIL
KOD
NAT
SDB-SH
MSH
NAI
SHA
WIN-SH
NDI
PRE
SCP
20 sec

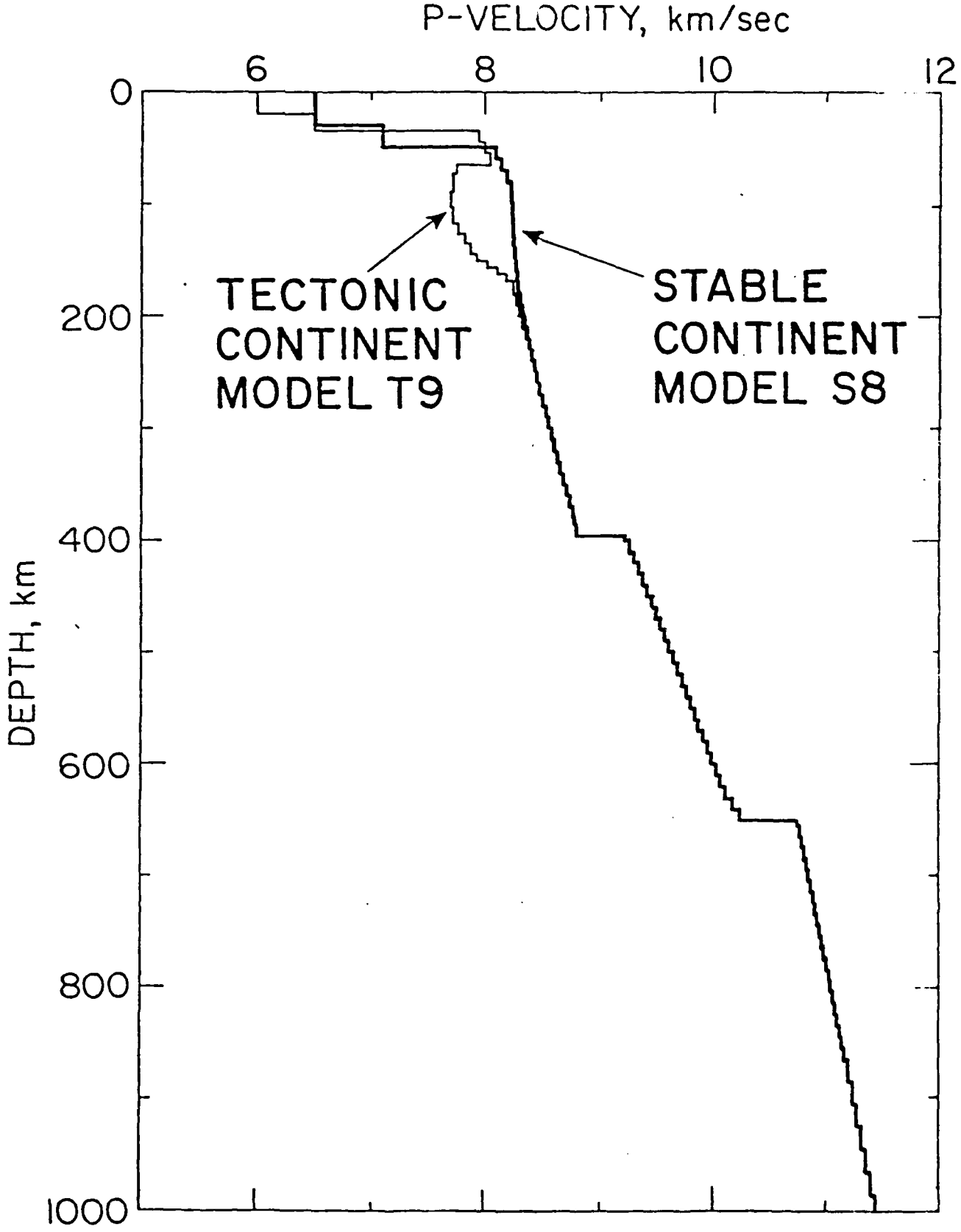
P-VELOCITY, km/sec
6
8
10
12
0
200
400
600
800
1000
DEPTH, km
TECTONIC CONTINENT MODEL T9
STABLE CONTINENT MODEL S8

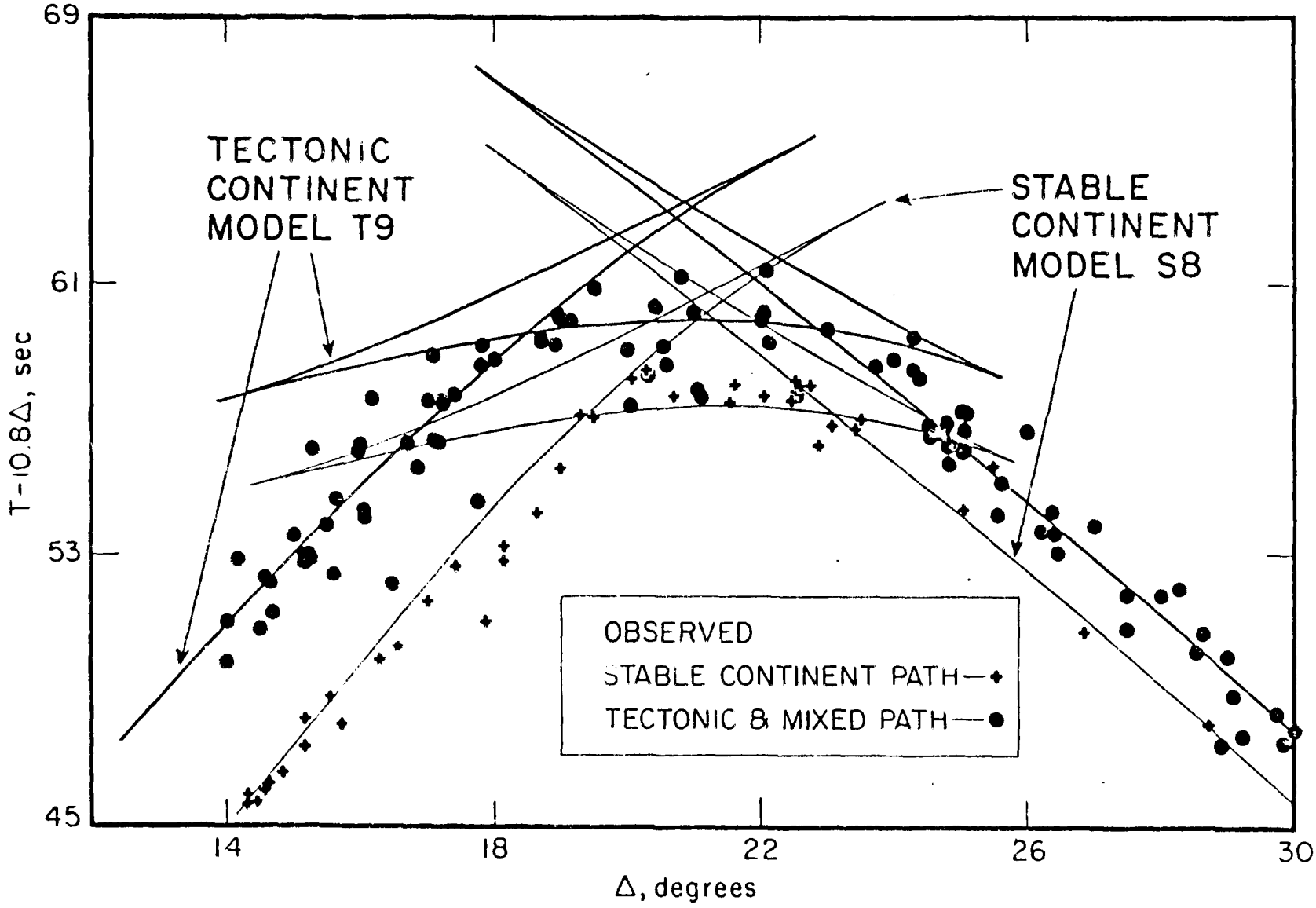
TECTONIC
CONTINENT
MODEL T9
STABLE
CONTINENT
MODEL S8
OBSERVED
STABLE CONTINENT PATH
TECTONIC & MIXED PATH
69
61
53
45
T-10.8Δ, sec
14
18
22
26
30
Δ, degrees

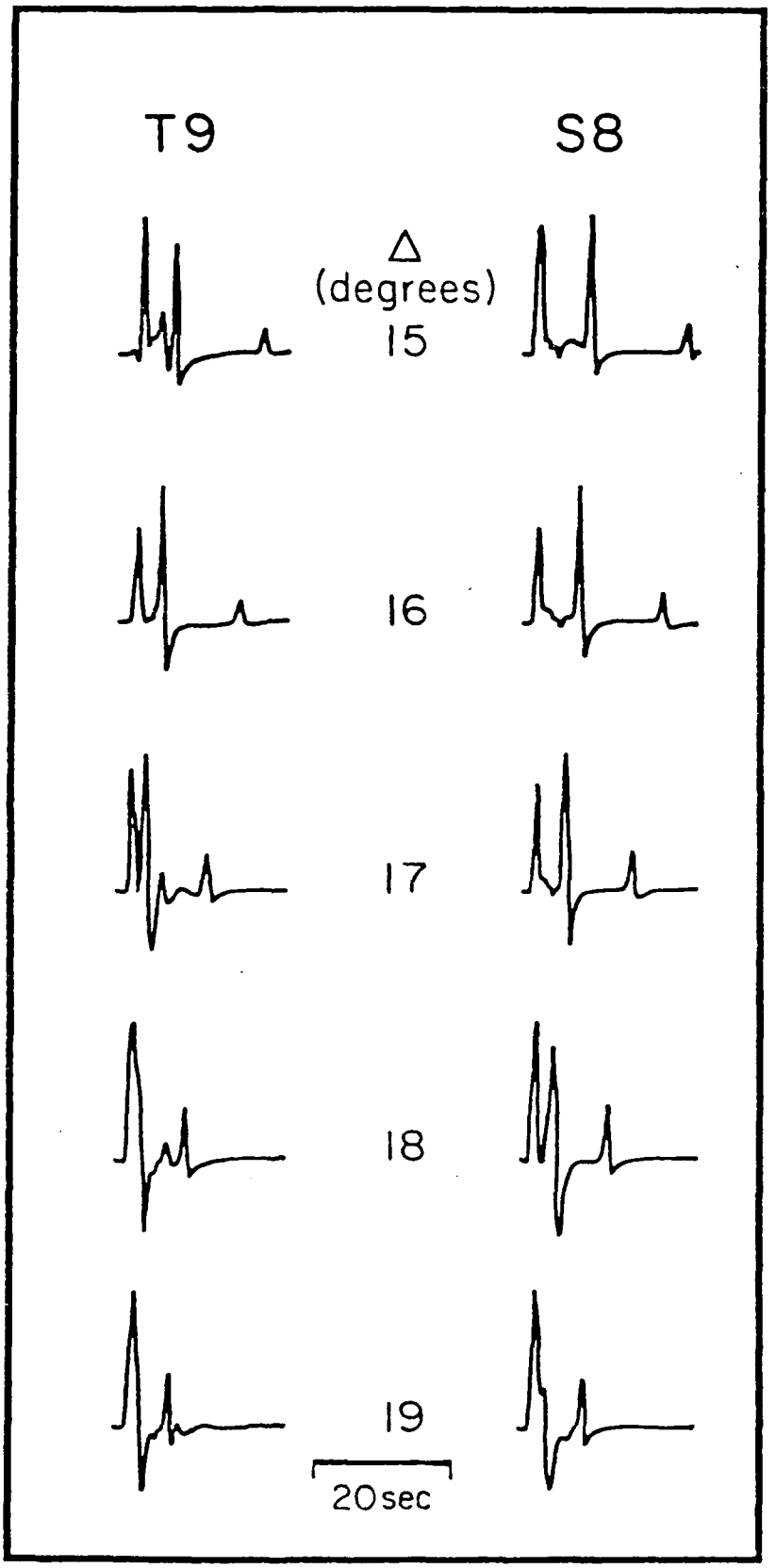
T9
S8
Δ
(degrees)
15
16
17
18
19
20sec

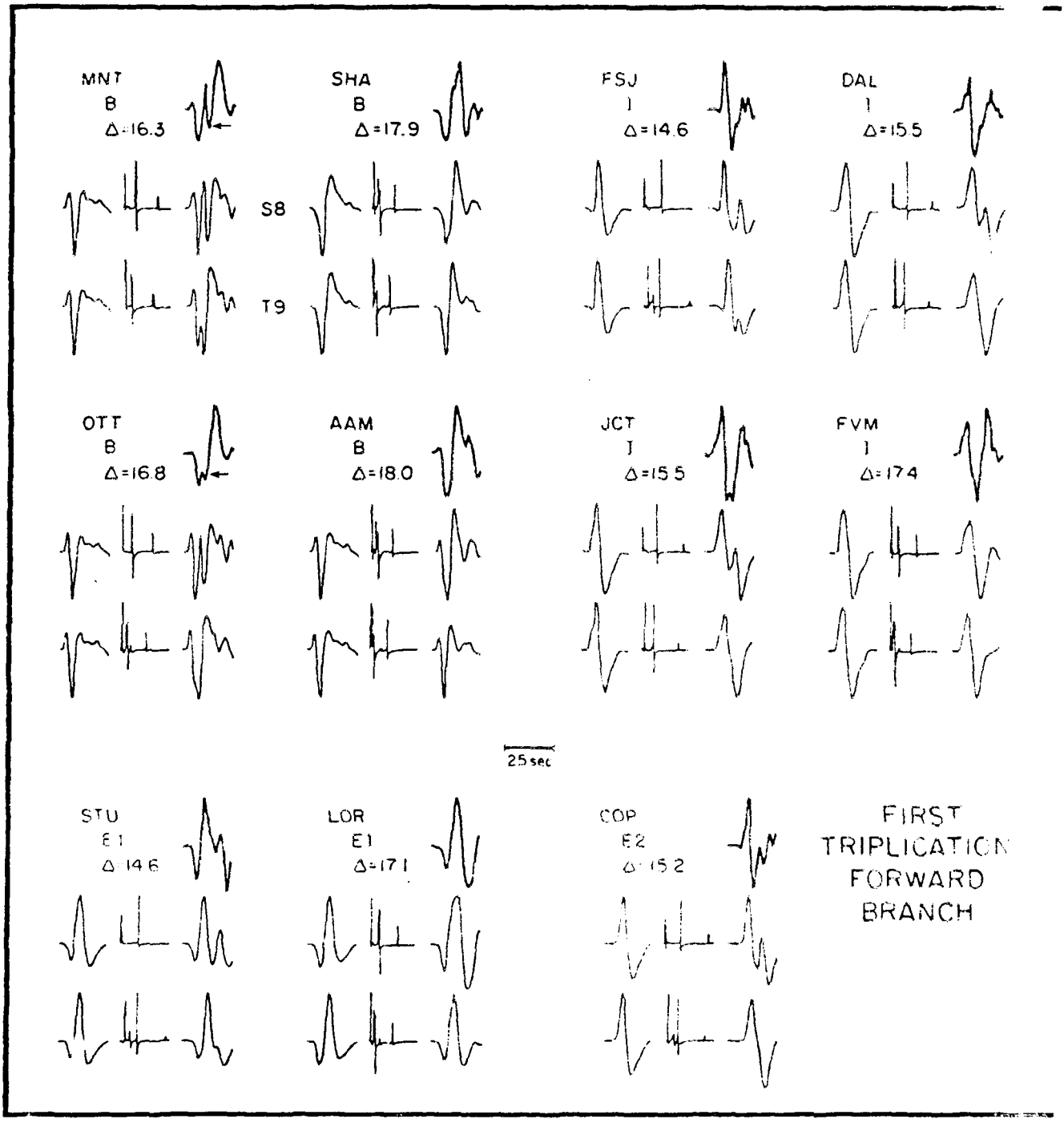
MNT
B
Δ=16.3
SHA
B
Δ=17.9
FSJ
1
Δ=14.6
DAL
1
Δ=15.5
S8
T9
OTT
B
Δ=16.8
AAM
B
Δ=18.0
JCT
1
Δ=15.5
FVM
1
Δ=17.4
25 sec
STU
E1
Δ=14.6
LOR
E1
Δ=17.1
COP
E2
Δ=15.2
FIRST
TRIPLICATION
FORWARD
BRANCH

THE QUINTUPLICATION

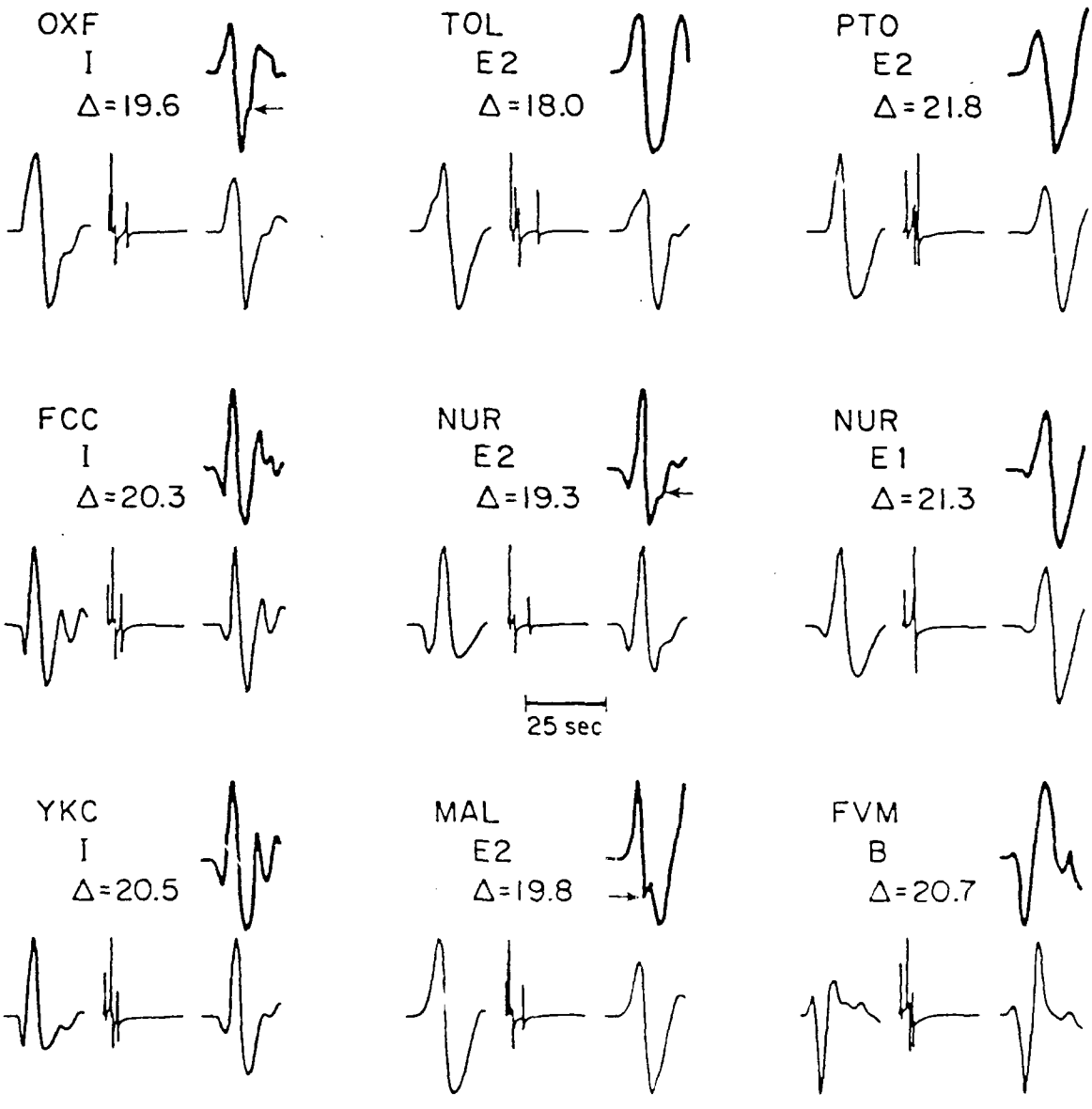

AD-A097 178 LAMONT-DOHERTY GEOLOGICAL OBSERVATORY PALISADES NY F/G 8/11
TECTONICS OF ASIA AND WAVEFORM STUDIES OF THE VELOCITY AND Q ST--ETC(U)
OCT 80 L R SYKES, L J BURDICK F49620-79-C-0021

UNCLASSIFIED AFOSR-TR-81-0285 NL

2 OF 2
AD A097 178

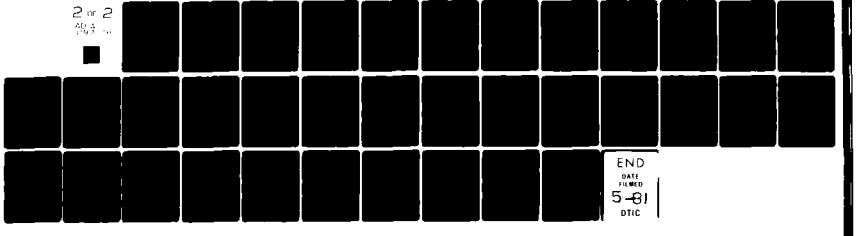

END
DATE FILMED
5-81
DTIC

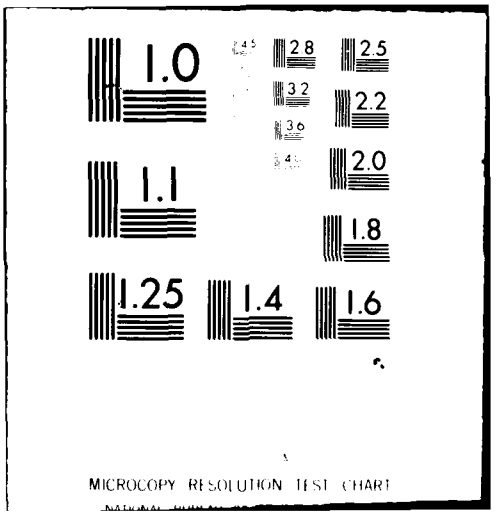
1.0
2.8
2.5
3.2
2.2
3.6
2.0
1.1
1.8
1.25
1.4
1.6
MICROCOPY RESOLUTION TEST CHART

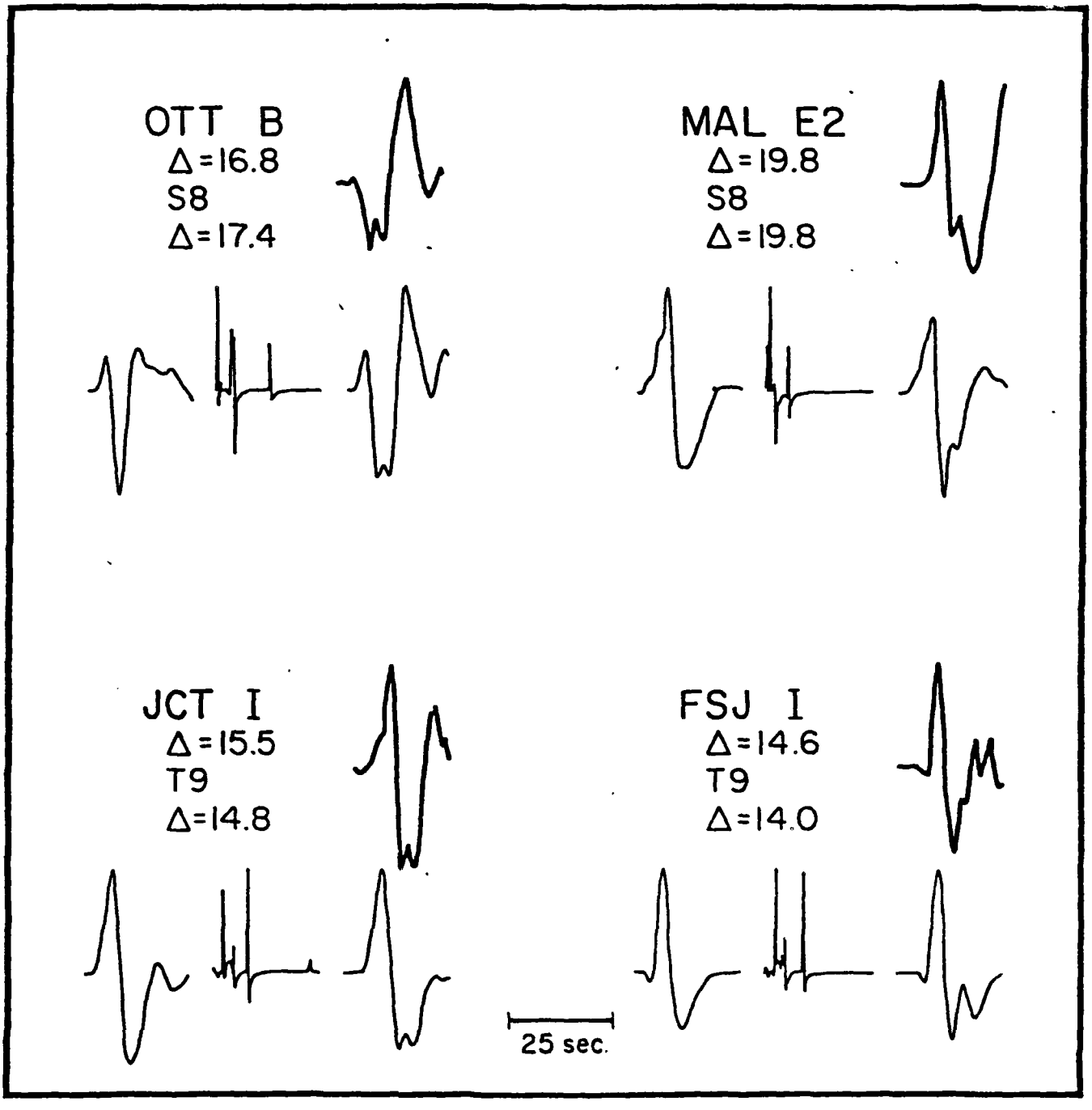
OTT B
Δ=16.8
S8
Δ=17.4
MAL E2
Δ=19.8
S8
Δ=19.8
JCT I
Δ=15.5
T9
Δ=14.8
FSJ I
Δ=14.6
T9
Δ=14.0
25 sec.

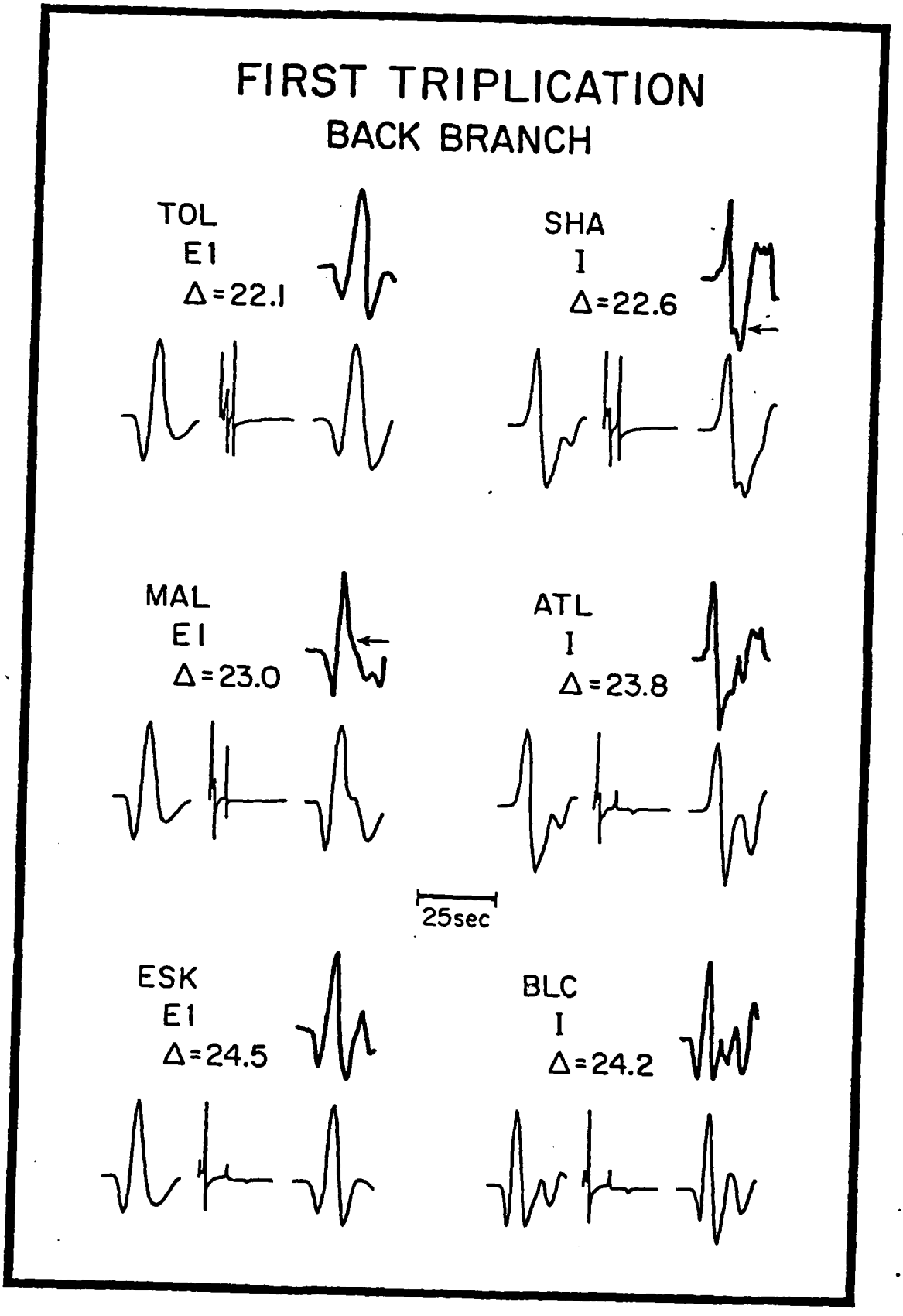
FIRST TRIPLICATION
BACK BRANCH
TOL
E1
Δ=22.1
SHA
I
Δ=22.6
MAL
E1
Δ=23.0
ATL
I
Δ=23.8
25sec
ESK
E1
Δ=24.5
BLC
I
Δ=24.2

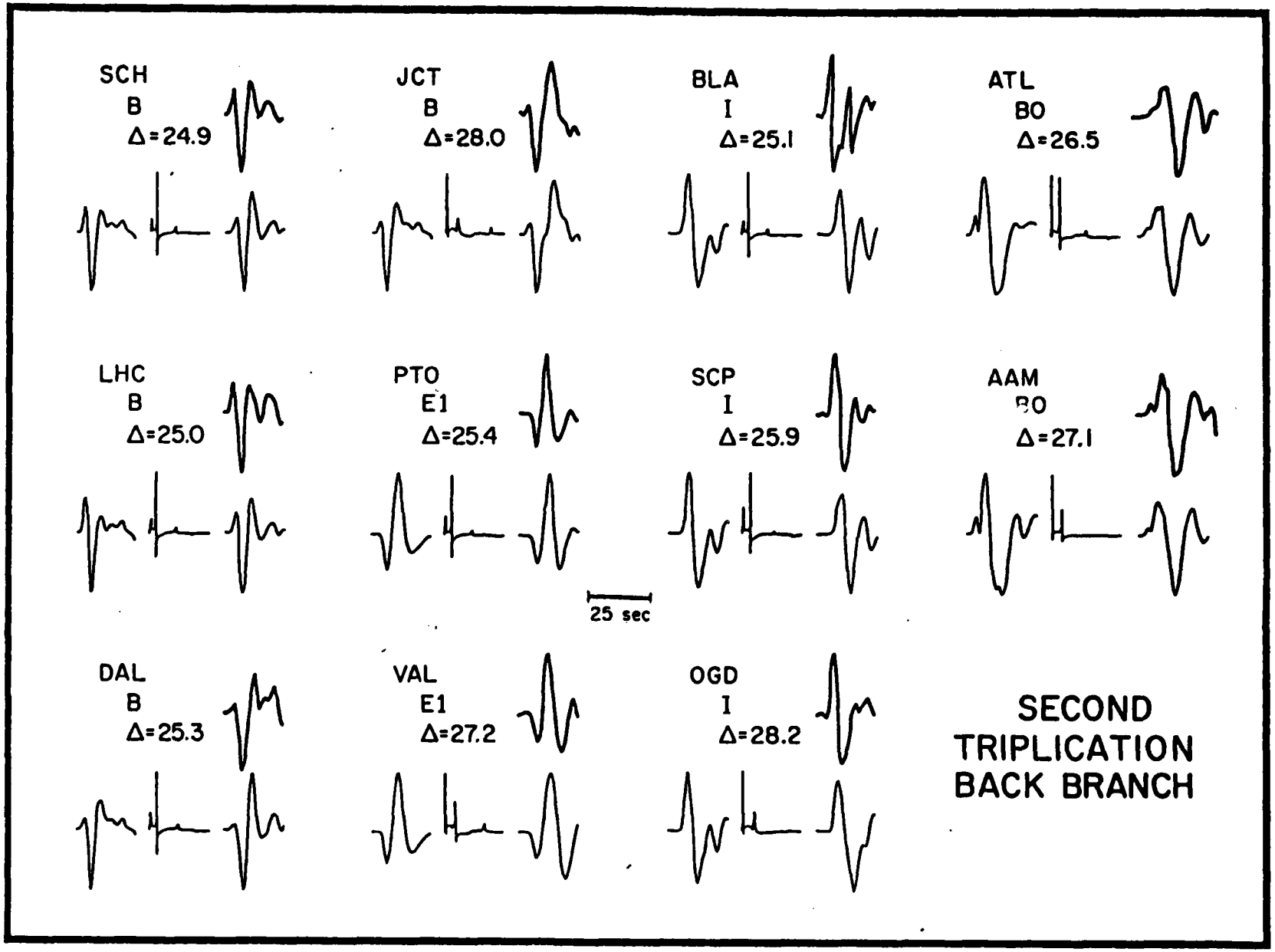
SCH
B
Δ=24.9
JCT
B
Δ=28.0
BLA
I
Δ=25.1
ATL
BO
Δ=26.5
LHC
B
Δ=25.0
PTO
E1
Δ=25.4
SCP
I
Δ=25.9
AAM
BO
Δ=27.1
25 sec
DAL
B
Δ=25.3
VAL
E1
Δ=27.2
OGD
I
Δ=28.2
SECOND
TRIPLICATION
BACK BRANCH

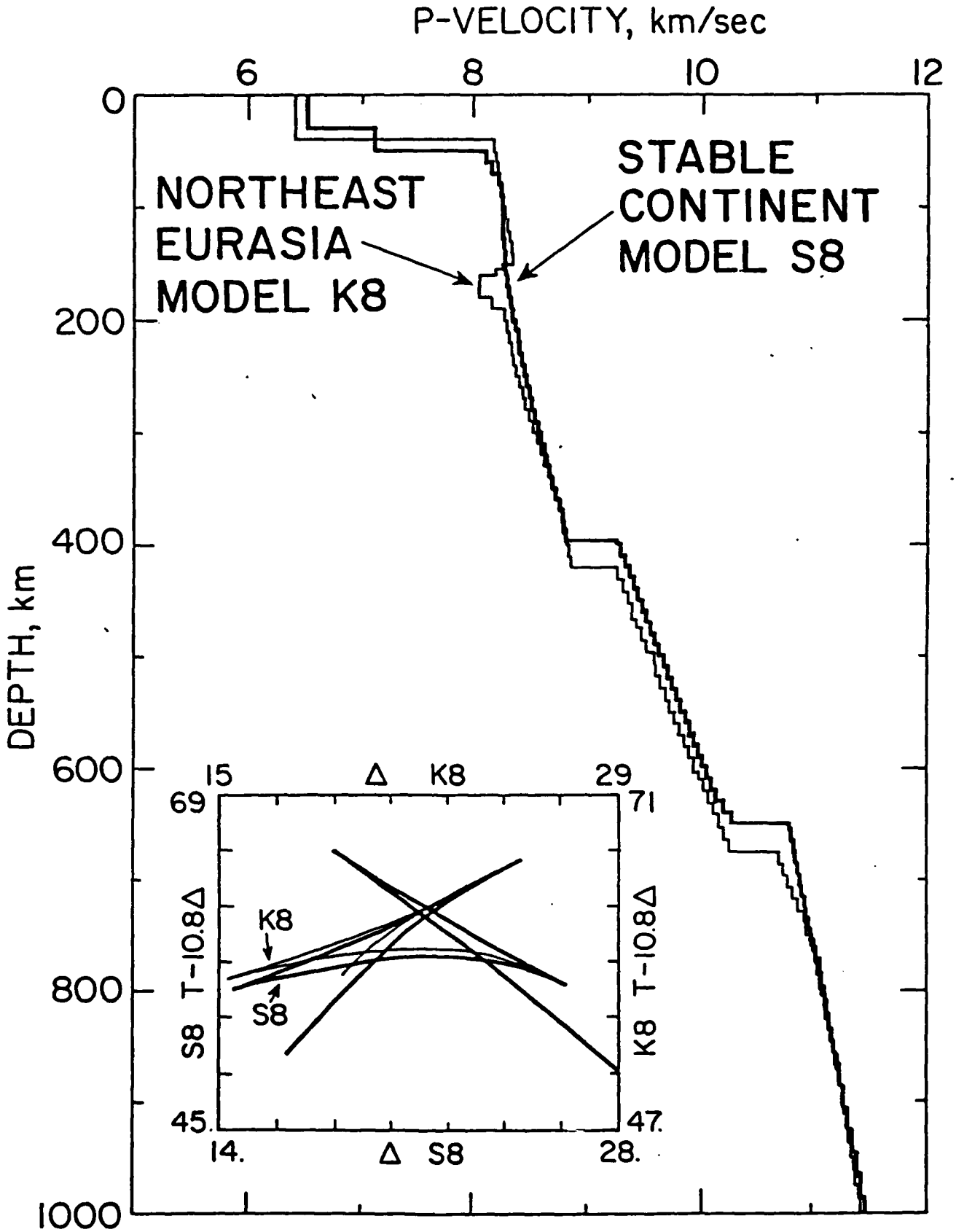
P-VELOCITY, km/sec
6
8
10
12
0
200
400
600
800
1000
DEPTH, km
NORTHEAST
EURASIA
MODEL K8
STABLE
CONTINENT
MODEL S8
15
Δ K8
29
69
71
S8 T-10.8Δ
K8 T-10.8Δ
K8
S8
45.
47.
14.
Δ S8
28.

Appendix II

THE FOCAL MECHANISMS OF THE GAZLI, USSR EARTHQUAKES[1]

M. J. Kristy[2], L. J. Burdick and D. W. Simpson

Lamont-Doherty Geological Observatory

of Columbia University

Palisades, New York 10964

ABSTRACT

Two $M_S = 7$ earthquakes struck in April and May of 1976 near the town of Gazli, Uzbekistan in the Soviet Union causing extensive damage. The focal mechanisms of the two events have been determined by modeling the long period body waves with synthetic seismograms. Both events have large components of thrust faulting, but they vary measurably in azimuthal orientation. The moment of the first event was 2.1×10^{26} dyne-cm and of the second was 2.4×10^{26} dyne-cm. The stress drops were around 50 bars which is typical for intraplate events.

The surrounding region had been assigned a low seismic risk based on recent patterns of seismicity. Historic records from the ancient city of Bukhara show that earthquakes in the magnitude range 6 to 7 had actually occurred in the region several times prior to the turn of the century. The Gazli events appear to have occurred on a pre-existing zone of weakness that is evidenced by the geologic record.

INTRODUCTION

Two large earthquakes occurred in April and May 1976 in the Kyzyl-Kum desert of western Uzbekistan, USSR, approximately 400 km southwest of Tashkent (Figure 1). The first event of 2:40:23.9 April 8, 1976 was located at 40.3°N, 63.72°E (ISC) about 30 km northeast of the small town of Gazli. It had a magnitude $M_s = 7.1$ (PAS). At 2:58:41.1 May 17, 1976, the second event occurred 20 km west of the first at 40.35°N, 63.45°E with a magnitude $M_s = 7.1$ (PAS). Deaths apparently occurred and extensive damage was reported at Gazli and in nearby gas fields (Aptekman et al., 1978; Pletnev et al., 1977).

The Gazli earthquakes have several unusual aspects that are of special interest. The occurrence of two large earthquakes of the same magnitude at essentially the same location within six weeks of one another does not fall into any of the usual foreshock-mainshock-aftershock patterns. A high level of activity occurred between and after the two shocks, but the active area was small compared to earthquakes of similar magnitude (Aptekman et al., 1978).

These earthquakes occurred in an intraplate region that had previously exhibited relatively low seismic activity. Figure 2a shows all of the events from the Kondorskaya and Shebalin (1977) catalogue with magnitudes greater than 7 from the years 1900 to the present. There was certainly little evidence from these events that large earthquakes would occur so far westward in the Eurasian block. Figure 2b shows the current pattern of smaller seismicity including all shallow (<100 km) events from the ISC catalogue from 1964 to 1977 that were located with more than 10 stations. This seismicity again gave little indication of the potential of the Gazli area. Also shown in 2a are the seismic zoning contours that had been adopted prior to the earthquake. The area was assigned a low seismic risk

Medvedev, 1976) with a maximum expected intensity of V as measured on the 1964 MSK scale (roughly equivalent to the Modified Mercalli scale). The actual intensities experienced during the 1976 earthquake were near X, and an accelerograph installed before the May 17 event recorded a maximum vertical acceleration of 1.3 g (Pletnev et al., 1977).

Even though the two earthquakes are separated by only 20 km (Aptekman et al., 1978), we present data below showing that the focal mechanisms are substantially different. In agreement with most other fault plane solutions for this region (e.g., Shirkova, 1967; Das and Filson, 1975; Nowroozi, 1972; Molnar et al., 1973; Ni, 1978), the main component for both events is thrusting; however the azimuth of the nodal planes differs by more than 60°. Much of the broad, diffuse zone of intraplate seismicity north of the India-Eurasia plate boundary can be interpreted as occurring along pre-existing zones of weakness separating stable continental blocks (e.g., Molnar and Tapponnier, 1975; Das and Filson, 1975). In some areas, these zones can be identified based on geological data and background seismicity. Such correlations are difficult in the Gazli area because of the Quaternary cover of the Kyzyl Kum sands and of the paucity of recent seismicity. Historical data from the ancient city of Bukhara do show that large earthquakes have occurred in the region over the last 800 years. We later show evidence that this activity may be associated with the westward extension of a zone of Hercynian deformation which, farther to the east in the southern Tien Shan, follows one of the most seismic zones in Central Asia.

The Gazli earthquakes are located near a site of active gas production. This connection raises the possibility that they may have been induced. Confirmation of this must await further details on the extent and location of the pumping. If the connection is real, however, the Gazli earthqukes would be the largest known induced events.

THE SOURCE MODELS

The fault plane solutions for the two main shocks were determined by matching the WWSSN long period records of the P and SH waves with synthetic seismograms. A full description of the techniques involved is given by Helmberger and Burdick (1979). Some recent applications of the methods to similar problems include the work of Cipar (1980), Bache et al. (1980) and Ebel et al. (1978). Fundamentally, a long period synthetic seismogram is computed by convolving together a series of linear time dependent operators. The first and most important represents the response for a point double couple source of given orientation (fault plane solution) buried in a layered half space. The computations make use of Haskell propagator matrices. The time function of the source is assumed to be a simple triangular pulse independent of azimuth and ray parameter. Other operators that are convolved in represent the effects of attenuation and the recording instrument. The records used are selected from the ranges 30° to 90°. This avoids complications caused by earth structure because the bottoming point for the rays is in the smooth lower mantle. There are no discontinuities to cause triplications or other features in the travel time curve. The records modeled were also selected on the basis of their signal to noise ratio and their azimuthal coverage of the source. Perturbations of the source orientation, the time function and the depth in the half space are made by trial and error until the synthetic seismograms provide a satisfactory fit to the observed data. The observed long period P waves are simply digitized and windowed at 30 seconds. The observed S waves on the other hand, must be rotated into SH and SV components. This is a difficult and unstable process. SH waves which were small with respect to the corresponding SV signal were not weighted heavily in the trial and error fitting.

Figures 3 and 4 show the P and SH waveforms respectively for the April 8 earthquake. Figures 5 and 6 show those for the May 17 event. The April 8 event was 15 km deep and was modeled with a triangular source pulse with rise time 2 seconds and fall off time 3 seconds. The May 17 event was also 15 km deep and the source pulse model had a rise time of 3 seconds and a fall time of 4 seconds. Both events were thrust with a small but resolvable component of strike slip. The azimuthal orientation of the fault planes, however, was definitely different for the two events. The P waves in Figure 3 are fit well by the model but they do not vary strongly with azimuth. The P wave data constrain the mechanism to be a dipping reverse event in that no focal planes pass through the center of the sphere. The strikes of the planes, however, are not well constrained. Neither the data or synthetics vary strongly with azimuth, so the theoretical solution can be rotated about a vertical axis without seriously deteriorating the fit. As is usual for dip slip events, the SH data provide a much stronger constraint on the strike of the fault plane. Figure 4 shows the S data displayed around the lower focal hemisphere for SH. The nodal lines for this case are not planes intersecting the sphere, but they do divide the focal sphere into positive and negative sections. The equations for the SH nodes are given in Burdick (1977). As the figure shows, there must be a nodal line between stations PTO and BUL and also between GDH and MAT. This constrains the azimuthal orientation of the solution. The precise values for the fault strike and the rake were chosen to give the best match to the details of the waveform. For the P waves this amounts to matching the relative sizes of the P, pP and sP phases as they vary with azimuth. For the S waves the relative sizes of S and sS are matched.

The fault planes for the May 17 event are constrained by the data in much the same way. The P waves show the mechanism to be a dipping thrust and the SH waves constrain the strike. Since it may be surprising to some that the two shocks

had substantially different mechanisms, the evidence that shows this is worth covering carefully. In Figure 3, the P wave observations to the east (SEO, SHK, BAG, MAN, DAV) show a relatively strong first motion upward caused by a strong direct P phase. The corresponding stations in Figure 5 show a nodal first motion, particularly MAT, SEO, HKC, DAV and LEM. In the fault plane solution in Figure 6 these stations are very close to the P node, so the synthetics match the effect quite well. The evidence from the SH waves that the two focal mechanisms were different is even stronger. The waveforms at KTG, GDH and PRE in Figure 4 are much different than the corresponding ones at KTG, COL and PRE in Figure 6. The comparison between GDH and COL is not strictly as valid as the other comparisons, but we argue that since they are so close in location on the focal sphere their waveforms should be very similar.

Aptekman et al. (1978) and Bezrodny (1979) present fault plane solutions for the Gazli events based on first motion data from teleseismic stations and local Soviet networks. Although there are major differences between the two papers they agree that the two Gazli events had substantially different mechanisms. Their focal mechanisms are consistent for the most part with the results of this investigation with the exception of Bezrodny's solution for the April event. However, his result is very inconsistent with the SH waveform data. A very thorough investigation of the mechanism of the May 17 event has recently been completed by Hartzell (1980). His fault plane solution is similar to the one in Figure 5 but rotated clockwise by 15°. He found that the slight rotation was required by the surface wave data. He used a finite fault model to further improve the fit. A careful comparison of his finite fault synthetics with those in Figure 5 indicates how difficult it is to resolve the effects of source finiteness from long period data. Pearce (1980) has modeled one of the aftershocks of the April event. He found that the mechanism was a near 45° dip slip reverse fault with a strike slip component.

The depths of the events were constrained by matching the relative timing of the depth phases. A good discussion of the relative sizes and polarities of the depth phases for dipping thrust events can be found in Langston and Helmberger (1975). Briefly, in all the P waves modeled here, the direct P is a small positive arrival followed by strong pP and sP arrivals which are negative. This causes the small first swing - large second swing shape of the P waves in Figures 3 and 5. The interaction of the S and sS phases is much more variable, but the KTG record in Figure 6 shows a case where the S arrival is just a small negative arrival followed by a strong positive sS arrival. The relative timing of the phases is well matched in the synthetics. The actual values of depth obtained depend of course on the crustal model used. Some information on the velocity structure near Gazli is available from the work of Rodriguez (1969) and Zunnonov et al. (1974). We adopted the model of Kosminskaya et al. (1969) since it seems fairly representative (Table I).

The moments of the events were determined from the observed P wave amplitudes at each station (Langston and Helmberger, 1975). Figures 4 and 6 show the moment value determined from each station next to the corresponding waveforms. The observed values for the April 8 event range from 0.7×10^{26} to 3.9×10^{26} dyne-cm. The average value is 2.1×10^{26} dyne-cm with a standard deviation of 0.9 dyne-cm. The average observed value of seismic moment for the May 17 event was 2.4 dyne-cm with a range of 0.4 to 4.8 x 10^{26} dyne-cm and a standard deviation of 0.9 dyne-cm.

Kanamori and Anderson (1975) show that interplate and intraplate earthquakes segregate on a moment-magnitude diagram. The Gazli events fall in the center of the distribution of intraplate events. Assuming that the corresponding interpretation of stress drop from Kanamori and Anderson (1975) is correct, we find stress drop values of 50 bars for both events. It is important to note, however, that the relationships between stress drop and other fault parameters are still a point of controversy. A full summary of the source models is given in Table 2.

The largest uncertainties in the source model are in the time function since it trades off directly with the Q operator. We have assumed a Futterman (1962) operator with a t^*_α of 1.0 s and a t^*_β of 4.0 s. We could have used different values and absorbed the difference directly into the source function. Minster (1978) has pointed out that, for realistic rheologies, Q must have some frequency dependence. We find that our synthetics are virtually unchanged if we use his standard linear solid Q operator with τ_m of .2 s, $t^*_\alpha = 1.0$ s, and $t^*_\beta = 4.0$ s. These values are consistent with the observations of Sipkin and Jordan (1979). If we assume the above values for t* we find that the time function duration is resolved to within about 50% and the values of rise time versus fall time trade off with the source depth.

TECTONICS AND SEISMICITY

The Gazli earthquakes are well removed from any major plate boundary (Figure 1). The Arabian and Indian plates are converging on the Eurasian plate, but almost 1000 km to the south of Gazli. More sophisticated interpretations of the tectonics involving several additional plates were presented by Morgan (1968), Le Pichon (1968) and Nowroozi (1972) among others. A consistent feature in all of these models is that the convergence is basically north-south and that the Gazli region is not associated with a plate boundary.

Much of southern and eastern Asia shows a high level of intraplate seismicity, and several theories have been proposed to explain this phenomenon. Molnar and Tapponnier (1975) compared the sense and orientation of faulting in Asia to the slip lines for a rigid identor in a plastic medium and found many similarities. Molnar et al. (1973) and Das and Filson (1975) suggest that zones of weakness separate Asia into blocks with relatively stable interiors. Sykes (1978) observed that in many intraplate areas seismicity tends to concentrate along zones of pre-existing

weakness and suggested that a similar phenomenon is occurring in Asia. This concept is at least applicable in Soviet Central Asia were Nersesov (personal communication) has found the seismicity can be best explained in terms of the movement of a few blocks.

The seismicity and major faults of southwest Asia are shown in Figure 2. Most of the faults shown in 2a are evident in the seismicity pattern. These include the Kopet Dag fault, the southern Tien Shan fault system, the Sharud fault, and the Herat fault (Yanskin, 1966). The seismicity between the Herat and southern Tien Shan faults is associated with the Hindu Kush. The segment of the Talas-Fergana fault, shown in Figure 2a does not appear to be seismically active at present, but an extension of the fault to the southeast is active, with one known earthquake greater than magnitude 7 on it.

The most active zones of seismicity in Figure 2b follow the northern boundary of the Alpine orogenic belt (Figure 7) through the Caspian Sea, along the Kopet Dag and Herat faults and north of the Pamirs. In many parts of the Tien Shan, concentrated zones of seismicity can be related to edges of zones of Hercynian deformation, e.g., along the Gissar-Kokshal fault in the southern Tien Shan (Gubin, 1967) and along the Talas-Fergana and main Tien Shan faults in the northern Tien Shan (Simpson et al., 1980). Scattered exposures of Hercynian age continue in outcrops northwest of the southern Tien Shan but become increasingly covered by Neogene and Quaternary sands (Markovskii, 1975; Yanskin, 1966). Major structural features, however, extend northwestward through Samarkand and Bukhara. Near Gazli these split into two trends, one continuing along the same azimuth and passing through the northern Caspian Sea (Figure 7); the other turning northward to join the Hercynian structures of the Ural Mountains, north of the Aral Sea (Beloussov, 1976).

The Gazli earthquakes occurred along the southern boundary of the Kyzyl-Kum uplift (Lukina, 1978). Ulomov (1974, 1979) has stressed the importance of structural trends in controlling the seismicity of the Kyzul Kum. In 1974, based on surface deformation near Tamdu-Bulak (100 km northeast of Gazli) and temporal changes in seismicity in western Uzbekistan, he had identified the Kyzul Kum area as the likely site for a large earthquake in the near future (Ulomov, 1974). From geophysical data, several faults with east-west to northeast-southwest orientation have been proposed for this region (Lukina, 1978; Hamrabaev et al., 1976; Zunnonov et al., 1974). The Kyzyl-Kum uplift provides the link between the Hercynian deformation in the Urals and the Hercynian deformation in the southern Tien Shan (Burtman, 1975; Beloussov, 1976; Kravchenko et al., 1977). As observed in Figure 7, Hercynian structures in the southern Tien Shan have an east-west orientation and the Ural Hercynian belt, north of the Aral Sea, is oriented along a north-south trend. The connection of these two sections of the Hercynian orogeny has subsided and is an arcuate structure that continues west from the southern Tien Shan, northwest along the Kyzyl-Kum uplift and along the Aral Sea to the Urals (Beloussov, 1976). We propose, therefore, that the Gazli earthquakes occurred on this pre-existing zone of weakness that follows the belt of Hercynian deformation joining the Urals and Tien Shan. In addition, this zone is especially complex near Gazli where it undergoes a major change in azimuth.

DISCUSSION

The 1976 earthquakes were by far the largest events in the area in recent times. There was little evidence in the instrumentally recorded seismicity nor obviously in the more extensive data considered in the seismic zoning to indicate a high seismic potential for Gazli. The large shocks since 1900 had all been located

well away from the region. The few earthquakes located near Gazli were small and occurred prior to 1960, when the locations were relatively inaccurate.

A somewhat different picture emerges if we consider the available information from before 1900. The city of Bukhara is an ancient one with historical accounts stretching back to before 1200 A.D. These records show that the city had been struck repeatedly by large earthquakes. Figure 8 shows their locations as given by Kondoroskaya and Shebalin (1977). They have been assigned magnitudes from 6 to 7 based primarily on intensity data from Bukhara. A comparison of Figures 2 and 8 shows the importance of the historical data. There is a clear indication that the zone of seismicity west of the Tien Shan fault system reaches several hundred kilometers farther into the Eurasian block than shown by the recent data. The Bukhara data indicate that earthquakes as large as magnitude 6 to 7 may occur along this zone as frequently as every 150 years. Sykes (1978) stresses the importance of identifying such zones of weakness in the contiental crust in the determination of seismic risk.

The fact that the two Gazli events had substantially different mechanisms is well resolved by the data. As methods of determining fault mechanisms have improved, however, this type of behavior in multiple shocks has been found quite commonly. Some particularly analogous cases include the double shock thrust events in Friulli, Italy studied by Cipar (1980), the sequence north of the Pamirs studied by Jackson et al. (1979) and the 1966 Karatag earthquakes in Tadjikistan, west of Dushanbe (Gubin, 1967). Shebalin (see Aptekman et al., 1978) suggests that such double shocks are characteristic of regions in which tectonic structures do not follow simple linear trends. In fact, following the April 8 Gazli earthquake, Shebalin had identified the region as one susceptible to multiple shocks and predicted, based on comparisons with double shocks in other areas, that a second large earthquake would occur during the second half of May (Aptekman et al., 1978).

Sykes (1978) points out that many intraplate earthquakes occur along pre-existing zones of weakness; especially where these zones are oriented favorably with respect to the current stress direction. In regions of high stress where no such "favorably-oriented" weak zones exist, stress may be relieved in pairs of earthquakes or complex single events rupturing along conjugate zones, oblique to the current stress direction. We note that the nodal planes for the Gazli earthquakes are approximately parallel to the strike of the two trends in the structural fabric of the Gazli area (Figure 7). Other studies (Shirokova, 1967; Nowroozi, 1972; Molnar et al., 1973; Das and Filson, 1975) show a general northwest compression along the USSR-Afghanistan border and northeast compression between Iran and the USSR (Figure 2a). The difference in stress directions inferred from the two Gazli earthquakes reflects the strong control on the fault planes imposed by local geological structure. Hence, although the thrusting mechanisms are indicative of strong horizontal compression and are in agreement with previous studies, the inferred directions of maximum compression from Gazli are less reliable indicators of regional trends than the more consistent directions found from earthquakes to the south.

ACKNOWLEDGEMENTS

The authors gratefully acknowledge the helpful reviews and comments of S. Hartzell, L. Seeber, L. Sykes and C. Scholz. This work was supported by the U.S. Geological Survey under Grant USGS 14-08-0001-16844 and by the Advanced Research Projects Agency of the Department of Defense and was monitored by the Air Force Office of Scientific Research under Contract Number F49620-79-C-0021.

REFERENCES

Aptekman, Kh.Ya., V.M. Graizer, K.G. Pletnev, D.N. Rustanovich, N.V. Shebalin, and V.V. Shteinberg (1978). Some data on processes in the epicentral zone of the 1976 Gazli earthquakes, in "Epicentral Zones of Earthquakes", vol. 19, Questions in Engineering Seismology, Nauka, Moscow, 149-166 [in Russian].

Bache, T.E., D.G. Lambert, and T.G. Barker (1980). A source model for the March 28, 1975 Pocatello Valley earthquake from time domain modeling of teleseismic P waves, Bull. Seism. Soc.Am., 70, 405-418.

Beloussov, V.V. (1976). Mountain formation in the history of the Earth's tectonosphere, in "Geotectonics of the Kashmir Himalaya Karakorum-Hindu Kush--Pamir Orogenic Belts, Accademia Nazionale dei Lincei. Rome, 165-184.

Bezrodny, E.M. (1979). The mechanism of the Gazli earthquakes from seismological data, in "Seismological Research in Uzbekistan", V.G. Katrenko and I.B. Yakovleva, eds., FAN Press, Tashkent, 42-53 [in Russian].

Burdick, L.J. (1977). Broad-band seismic studies of body waves, Ph.D. Thesis, California Insitute of Technology, Pasadena, California.

Burtman, V.S. (1975). Structural geology of Variscan Tien Shan, USSR, Am. J. Sci., 275-A, 157-186.

Cipar, J. (1980). Teleseismic observations of the Friulli earthquake sequence, Bull. Seism. Soc. Am., in press.

Das, S., and J. Filson (1975). Tectonics of Asia, Earth Planet. Sci. Lett., 28, 241-253.

Ebel, J.E., L.J. Burdick, and G.S. Stewart (1978). The source mechanism of the August 2, 1966 El Golfo earthquake, Bull. Seism. Soc. Am., 68, 1281-1292.

Futterman, W.I. (1962). Dispersive body waves, J. Geophys. Res., 67, 5279-5291.

Gubin, I.E. (1967). Lecture Notes on Basic Problems in Seismotectonics, International Inst. of Seism. and Earthquake Eng., Tokyo, Japan, 195 pp.

Hamrabaev, I.H., V.A. Pack, and H.I. Yusuphodjaev (1976). The pecularities of geophysical fields and deep structure of the Pamirs and Tien Shan, in "Geotectonics of the Kashmir Himalaya Karakorum-Hundu Kush-Pamir Orogenic Belts", Accademia Nazionale dei Lincei, Rome, 77-86.

Hartzell, S.H. (1979). Faulting mechanism of the May 17, 1976 Gazli, USSR earthquake [Abst.], EOS, Trans. Am. Geophys. Un., 60, 894.

Helmberger, D.V., and L.J. Burdick (1979). Synthetic seismograms, Ann. Rev. Earth Planet. Sci., 7, 417-442.

Jacob, K.H., and R.L. Quittmeyer (1979). The Makran region of Pakistan and Iran: trench-arc system with active plate subduction, in "Geodynamics of Pakistan", A. Farah and K.A. DeJong, editors, Geological Survey of Pakistan, Quetta, 305-318.

Jackson, J., P. Molnar, H. Patton, and T. Fitch (1979). Seismotectonic aspects of the Markansu Valley, Tadjikistan, earthquake of August 11, 1974, J. Geophys. Res., 84, 6157-6167.

Kanamori, H., and D.L. Anderson (1975). Theoretical basis of some empirical relations in seismology, Bull. Seism. Soc. Am., 65, 1073-1095.

Kondorskaya, N.V., and N.V. Shebalin [editors] (1977). New Catalogue of Strong Earthquakes in the Territories of the USSR from Ancient Times to 1975. Nauka, Moscow, 535 pp.

Kosminskaya, I.P., N.A. Belyaevsky, and I.S. Volvovsky (1969). Explosion seismology in the USSR, in "The Earth's Crust and Upper Mantle", P.J. Hart, editor, Am. Geophys. Un., 195-208.

Kravchenko, K.N., N.Ye. Koshelev, N.Ye. Kravchenko, T.N. Kunitskaya, I.N. Polkanova, L.P. Polkanova, V.F. Roshchin, and N.S. Solovyeva (1977). Structural evolution of the Turan plate, Int. Geol. Rev., 20, 770-776.

Kravchenko, K.N. (1979). Tectonic evolution of the Tien Shan, Pamir and Karakorum, in "Geodynamics of Pakistan", A. Farah and K.A. DeJong, editors, Geological Survey of Pakistan, Quetta, 26-40.

Langston, C.A., and D.V. Helmberger (1975). A procedure for modeling shallow dislocation sources, Geophys. J. R. astr. Soc., 42, 117-130.

LePichon, X. (1968). Sea floor spreading and continental drift, J. Geophys. Res., 73, 3661-3697.

Lukina, N.V. (1978). The structure and deformation of the basement surface in the region of the Gazli earthquakes, Akad. Nauk SSR, Izv. Ser. Geol., 9, 110-118.

Markovskii, A.P. [editor] (1975). Geological Map of Eurasia (scale 1:5,000,000), Ministry of Geology, Moscow.

Medvedev, S.V. [editor] (1976). Seismic Zoning of the USSR, trans. by U.S. Dept. of Commerce.

Minster, J.B. (1978). Transient and impulse responses of a one dimensional linearly attenuating medium; Part I. Azimuthal results, Geophys. J. R. astr. Soc., 52, 479-501.

Molnar, P., T.J. Fitch, and F.T. Wu (1973). Fault plane solutions of shallow earthquakes and contemporary tectonics in Asia, Earth. Planet. Sci. Lett., 19, 101-112.

Molnar, P., and P. Tapponnier (1975). Cenozoic tectonics of Asia: effects of a continental collision, Science, 189, 419-426.

Morgan, W.J. (1968). Rises, trenches, great faults and crustal blocks, J. Geophys. Res., 73, 1953-1982.

Ni, J. (1978). Contemporary tectonics in the Tien Shan region, Earth Planet. Sci. Lett., 41, 347-354.

Nowroozi, A.A. (1972). Focal mechanisms of earthquakes in Persia, Turkey, W. Pakistan and Afghanistan and plate tectonics of the Middle East, Bull. Seism. Soc. Am., 62, 823-850.

Pearce, R.G. (1980). Fault plane solutions using relative amplitudes of P and surface reflections: further studies, Geophys. J. R. astr. Soc., 60, 459-487.

Pletnev, K.G., N.V. Shebalin, and V.V. Shteinberg (1977). Strong-motion records from the May 1976 Gazli USSR earthquakes, USGS Circular, 762-A, pp. 3-5.

Rodriguez, R.G. (1969). Atlas of Asia and Eastern Europe to Support Detection of Underground Nuclear Testing, Dept. of the Interior, U.S. Geol. Surv.

Shirokova, E.I. (1961). On stresses effective in the foci of earthquakes in Central Asia, Akad. Nauk SSSR, Izv., Ser. Geophys. [English translation], 6, 572-576.

Shirokova, E.I. (1967). General features in the orientation of principal stresses in earthquake foci in the Mediterranean-Asian seismic belt, Akad. Nauk SSR, Izv. Ser. Geophys. [English translation], 1, 12-22.

Simpson, D.W., M.W. Hamburger, V.D. Pavlov, and I.L. Nersesov (1980). Tectonics and seismicity of the Toktogul Reservoir region, Kirgizia, USSR, submitted to J. Geophys. Res.

Sipkin, S.A., and T.H. Jordan (1979). Frequency dependence of QScS, Bull. Seism. Soc. Am., 69, 1055-1079.

Sykes, L.R. (1978). Intra-plate seismicity, reactivation of pre-existing zones of weakness, alkaline magmatism and other tectonism postdating continental fragmentation, Rev. Geophys. Space Phys., 16, 621-688.

Ulomov, V.I. (1974). Dynamics for the Earth's Crust in Central Asia and Earthquake Prediction, FAN Press, Tashkent, 214 pp. [in Russian].

Ulomov, V.I. (1979). Dynamics of the Earth's crust and seismic zoning in western Uzbekistan, in "Seismological Research in Uzbekistan", V.G. Katrenko and L.B. Yakovleva, eds., FAN Press, Tashkent, 3-17 [in Russian].

Zunnonov, F.Kh., M.A. Akhmedzhanov, O.M. Borisov, and T. Ergeshev (1974). Geological and geophysical model of the crust in western Uzbekistan, Geotectnoica, 1, 28-34.

Yanskin, A.L. [editor] (1966). Tectonic Map of Eurasia, Nauka, Moscow.

FIGURE CAPTIONS

Figure 1: Major plate boundaries and their relationship to the Gazli earthquakes. Closed sawtooths represent ocean-continent convergence and the open teeth are continent-continent convergence. Single large arrows show the direction of relative motion between two plates. The star is the location of the Gazli earthquakes and the circle is the triple junction for the Indian, Arabian and Eurasian plates. Plate motions and boundaries are from Jacob and Quittmeyer (1979).

Figure 2: Compressive stress orientations and the relationship between the seismic activity and seismic zoning in the USSR. In Figure 2a, the solid circles are instrumentally located earthquakes with magnitude ≥ 7 from 1900 to 1976. The heavy solid lines are major faults: K - Kopet-Dag fault, ST - Southern Tien Shan fault system, S - Sharud fault, and H - Herat fault. Thin continuous lines show seismic zoning within the USSR (Medvedev, 1976). Bars in this figure show the orientation of P-axes from published focal mechanisms (Shirokova, 1967; Nowroozi, 1972) and from the Gazli focal mechanisms determined in this study (enclosed in the box). Figure 2b shows the same area and includes all of the shallow (<100 km) earthquakes from 1964 through March 1976 that were located by the ISC with 10 or more stations.

Figure 3: Fault plane solution (lower hemisphere) and corresponding P waveforms for the April 8, 1976 Gazli earthquake. Solid circles are compressions and open circles are dilatations. The top waveform at each station is the observed P wave and the lower one the synthetic waveform. In the lower right corner of each box is the body wave moment ($*10^{26}$ dyne-cm) for each station.

Figure 4: Fault plane solution and SH waveforms for the April 8, 1976 earthquake. The same convention is used as in Figure 3.

Figure 5: Fault plane solution and P waveforms for the May 17, 1976 earthquake. Notice the nodal character of the stations MAT, SEO, HKC, and DAV in comparison to similar stations for the April 8 earthquake, Figure 3.

Figure 6: Fault plane solution and SH waveforms for the May 17, 1976 earthquake. Notice that the station KTG is much more nodal than that observed for the April 8 earthquake, Figure 4.

Figure 7: The relationship between the Gazli earthquakes and faults as determined from geophysical data and surface outcrops of Hercynian age. Thick continuous lines are "deep" faults and lines with dotted interior delineate exposed basement of Hercynian age (Yanskin, 1966). The line shading represents Alpine deformation. Dashed box shows the area of the inset. Again the thick lines are faults from geophysical data (Zunnonov, 1974) and the lines with dashes outline local outcrops of Hercynian age.

Figure 8: Historic earthquakes located near Bukhara (hexagon) from intensity data (Kondorskaya and Shebalin, 1978). The triangle is the April 8, 1976 event and the square the May 17, 1976. The shaded areas are aftershock zones from ISC data. The solid line through the figure separates the region according to the seismic zoning (Medvedev, 1976). Roman numerals show the maximum expected intensity. The historic earthquakes shown: 942 (M = 6.7), 1390 (M = 6.1), 1822 (M = 6.4), 1822 (M = 7.0). Vertical and horizontal bars represent inaccuracy in location for each earthquake.

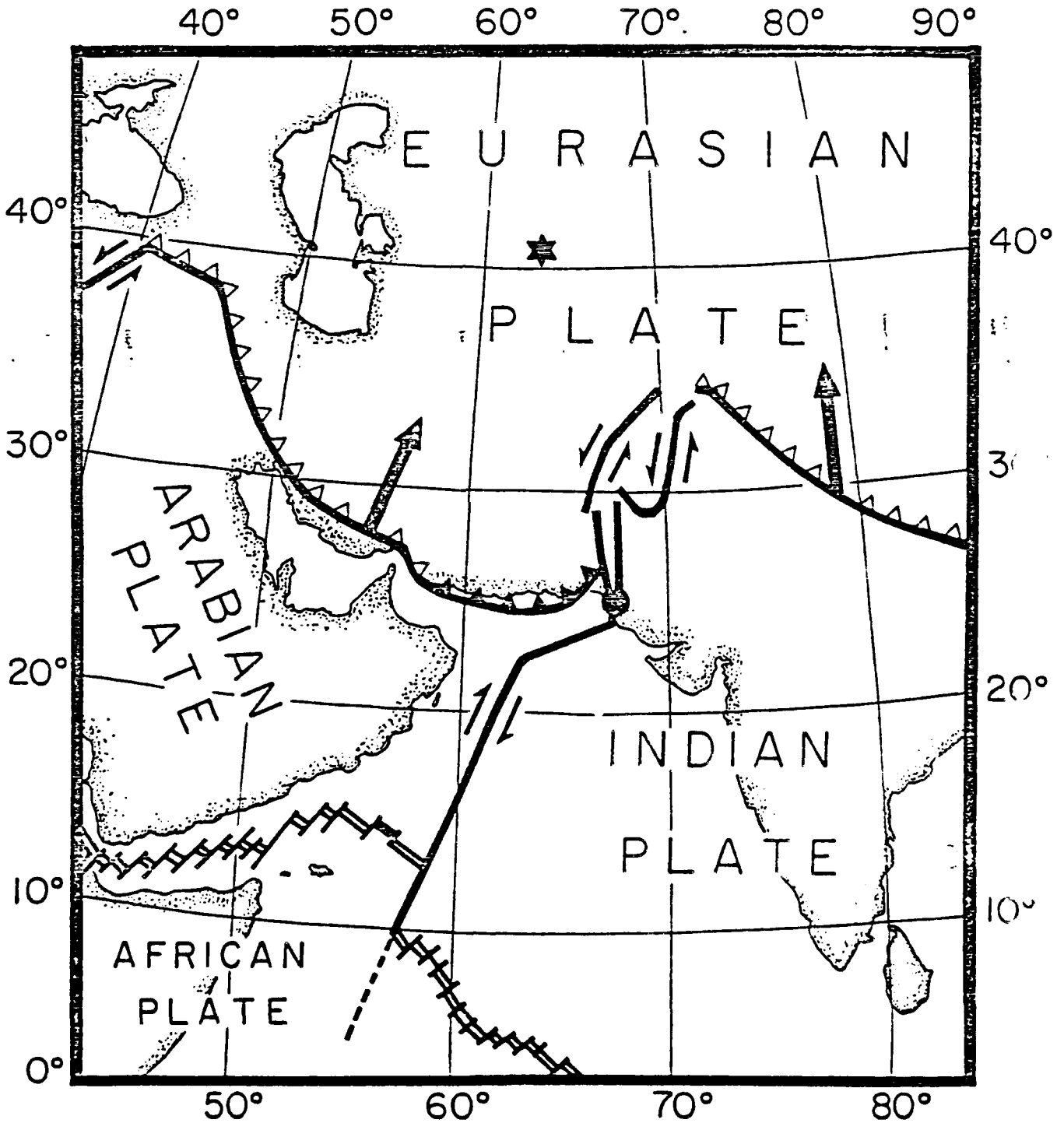
40°
50°
60°
70°
80°
90°
EURASIAN
PLATE
40°
30°
20°
10°
0°
ARABIAN
PLATE
INDIAN
PLATE
AFRICAN
PLATE
50°
60°
70°
80°

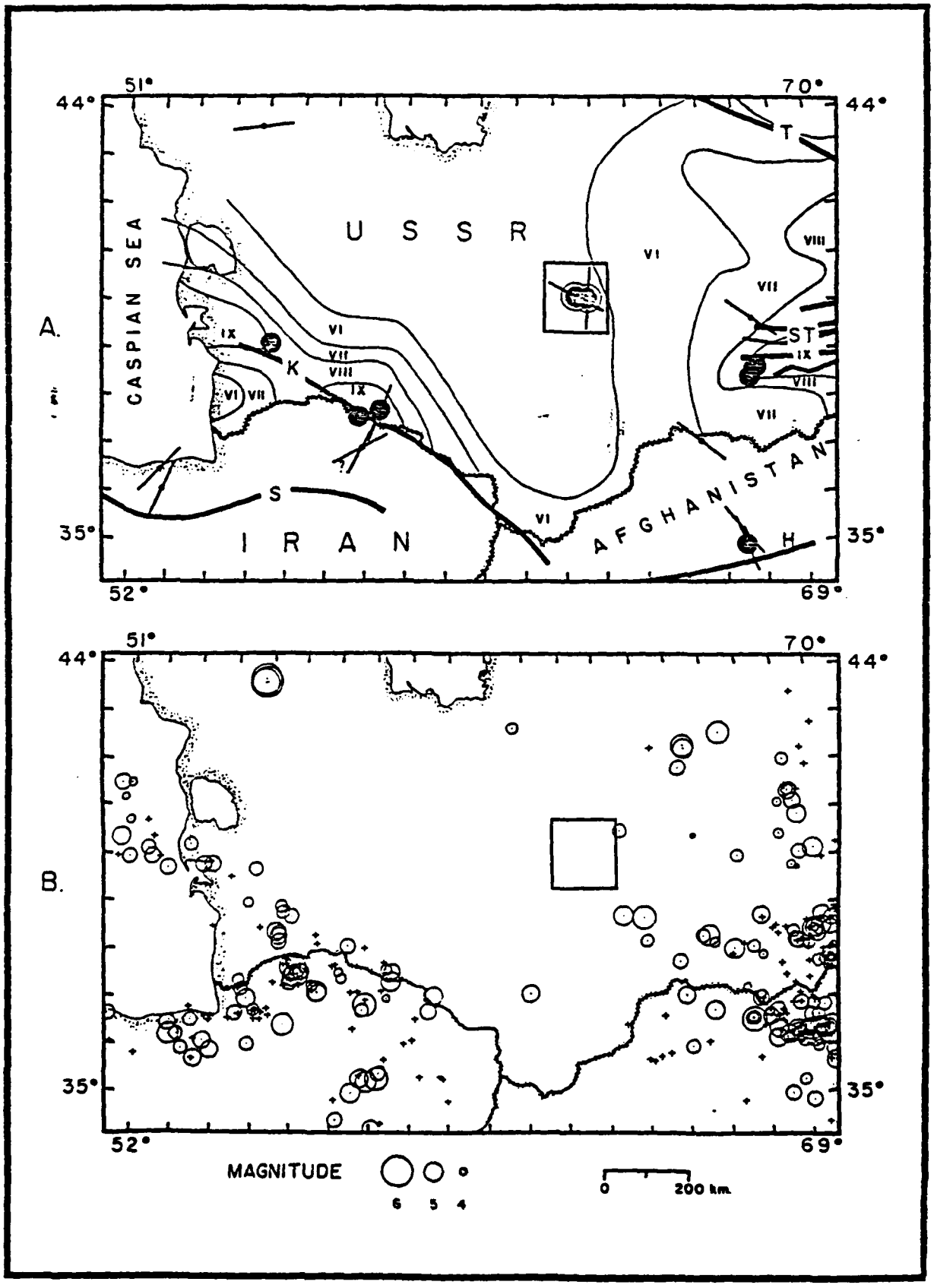
A.
51°
70°
44°
44°
U S S R
CASPIAN SEA
T
VIII
VII
VI
ST
IX
VIII
VII
IX
VIII
VII
VI
K
S
I R A N
AFGHANISTAN
H
35°
35°
52°
69°
B.
51°
70°
44°
44°
35°
35°
52°
69°
MAGNITUDE
6 5 4
0
200 km

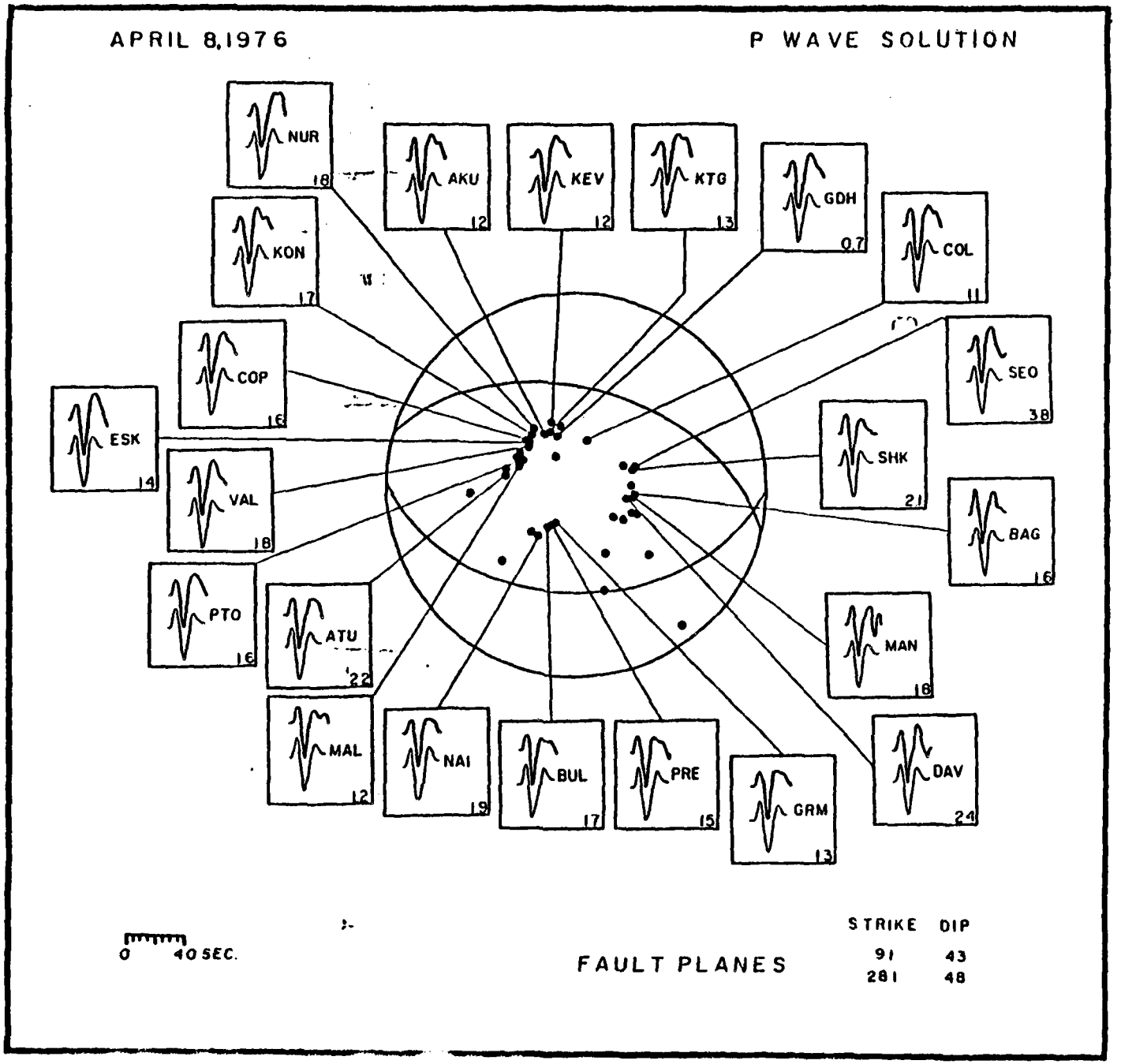
APRIL 8,1976
P WAVE SOLUTION
NUR 18
AKU 12
KEV 12
KTG 13
GDH 0.7
COL 11
KON 17
SEO 38
COP 16
ESK 14
SHK 21
VAL 18
BAG 16
PTO 16
ATU 22
MAN 18
MAL 12
NAI 19
BUL 17
PRE 15
GRM 13
DAV 24
0 40 SEC.
FAULT PLANES
STRIKE DIP
91 43
281 48

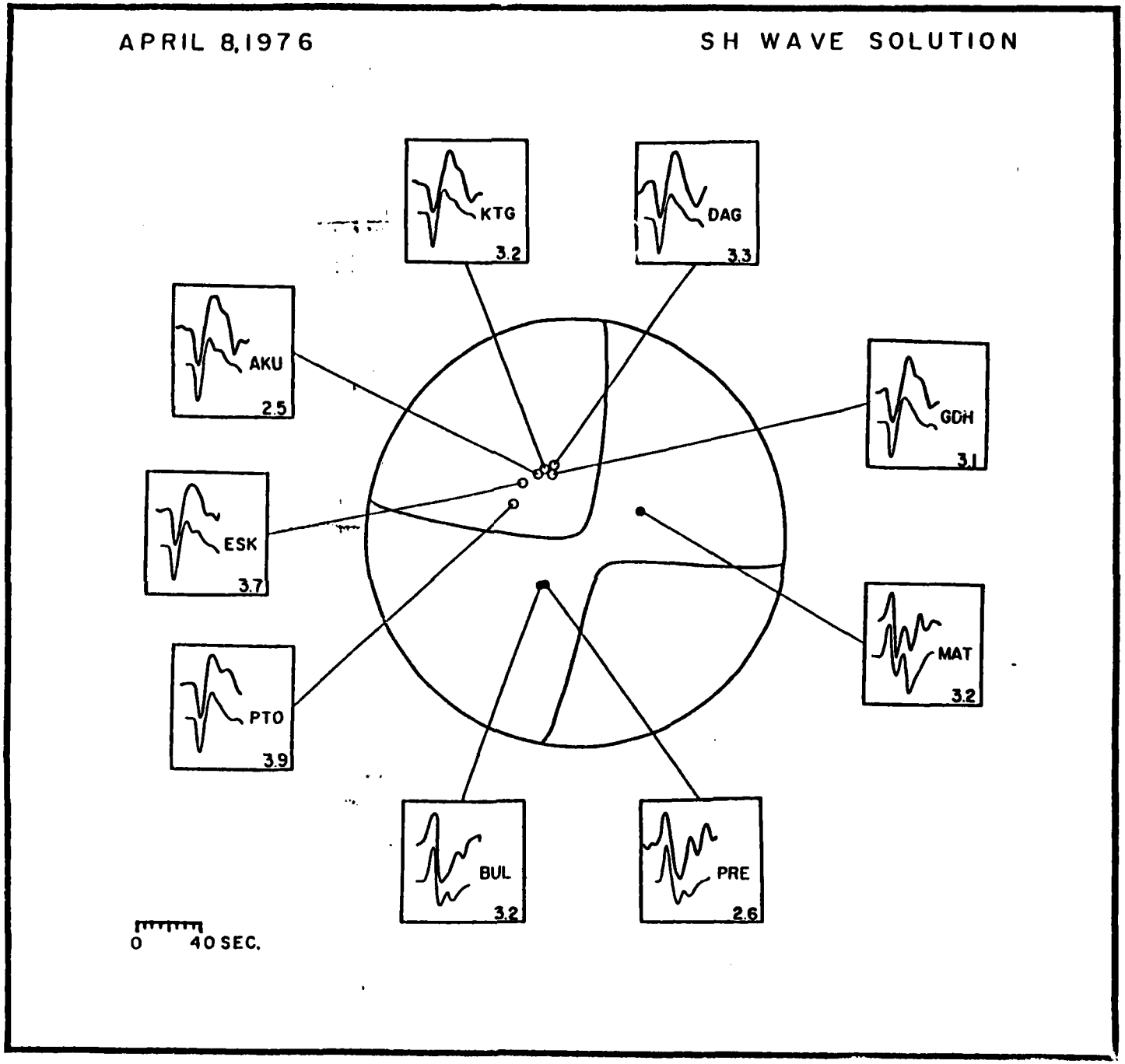
APRIL 8,1976
SH WAVE SOLUTION
KTG
3.2
DAG
3.3
AKU
2.5
GDH
3.1
ESK
3.7
MAT
3.2
PTO
3.9
BUL
3.2
PRE
2.6
0 40 SEC.

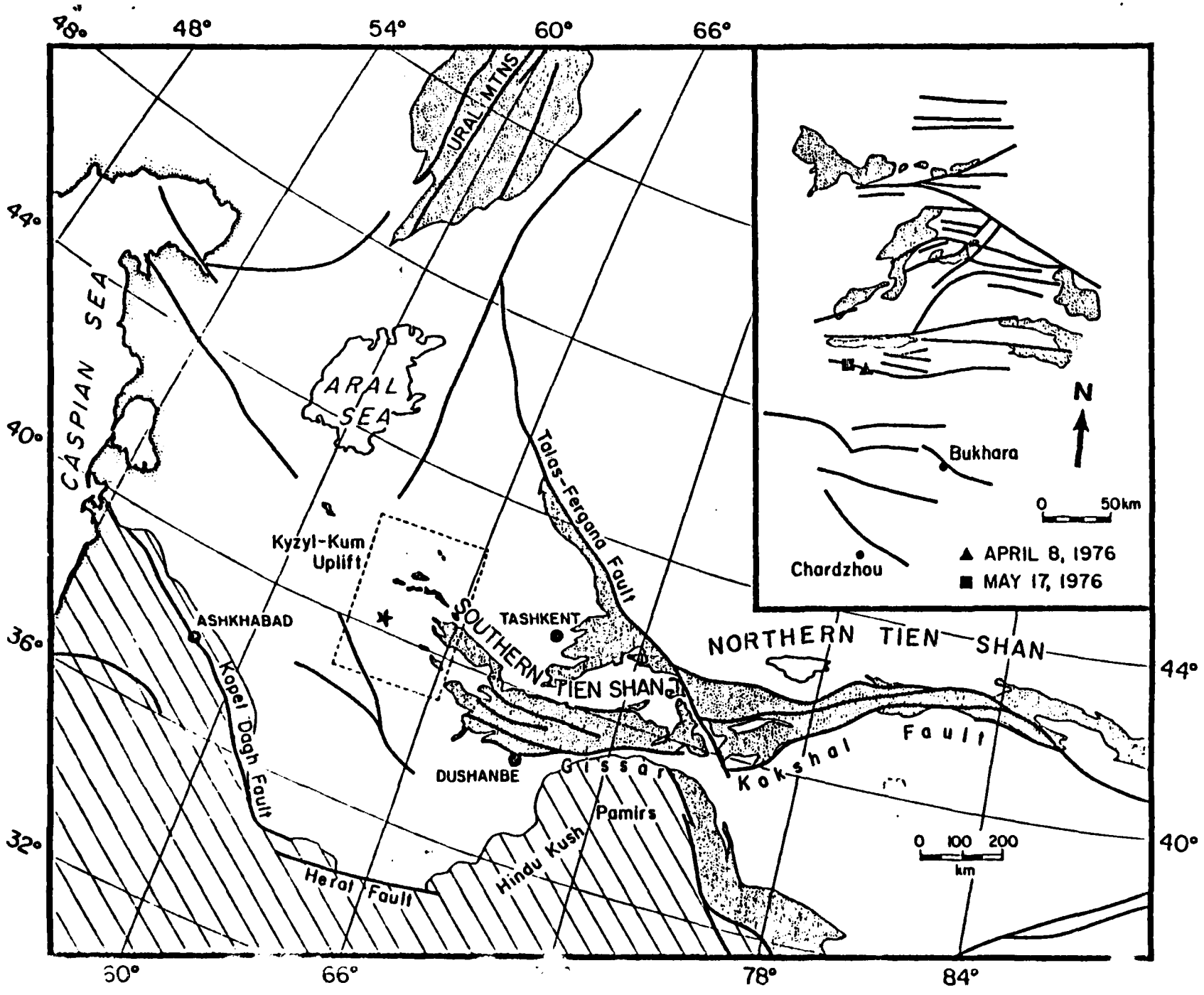
42°
48°
54°
60°
66°
44°
40°
36°
32°
30°
66°
78°
84°
CASPIAN SEA
ARAL SEA
URAL MTNS
Talas-Fergana Fault
Kyzyl-Kum Uplift
ASHKHABAD
Kopel Dagh Fault
Herat Fault
TASHKENT
SOUTHERN TIEN SHAN
NORTHERN TIEN SHAN
DUSHANBE
Gissar
Pamirs
Hindu Kush
Kokshal Fault
0 100 200
km
N
Bukhara
0 50km
Chardzhou
▲ APRIL 8, 1976
■ MAY 17, 1976

MAY 17, 1976

SH WAVE SOLUTION

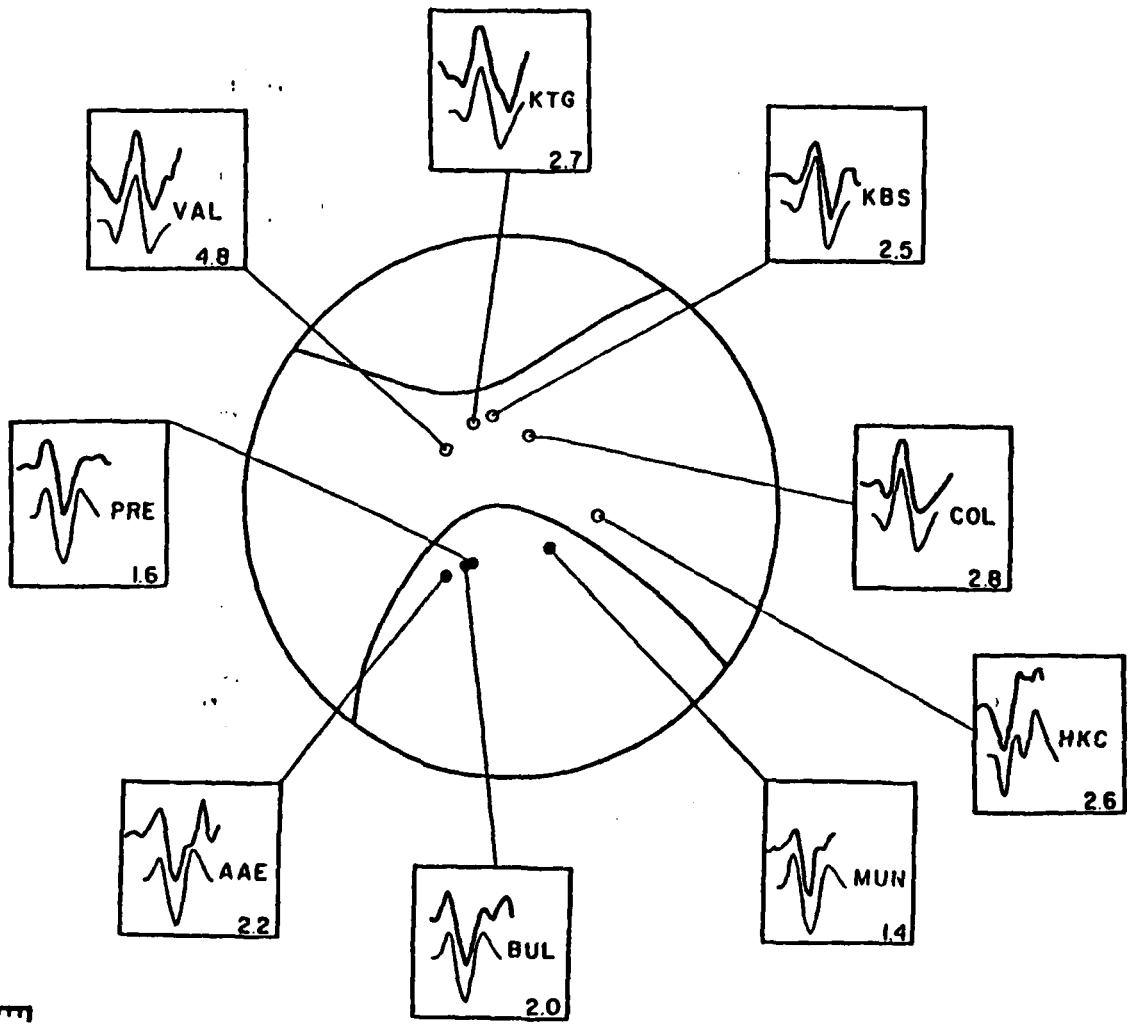

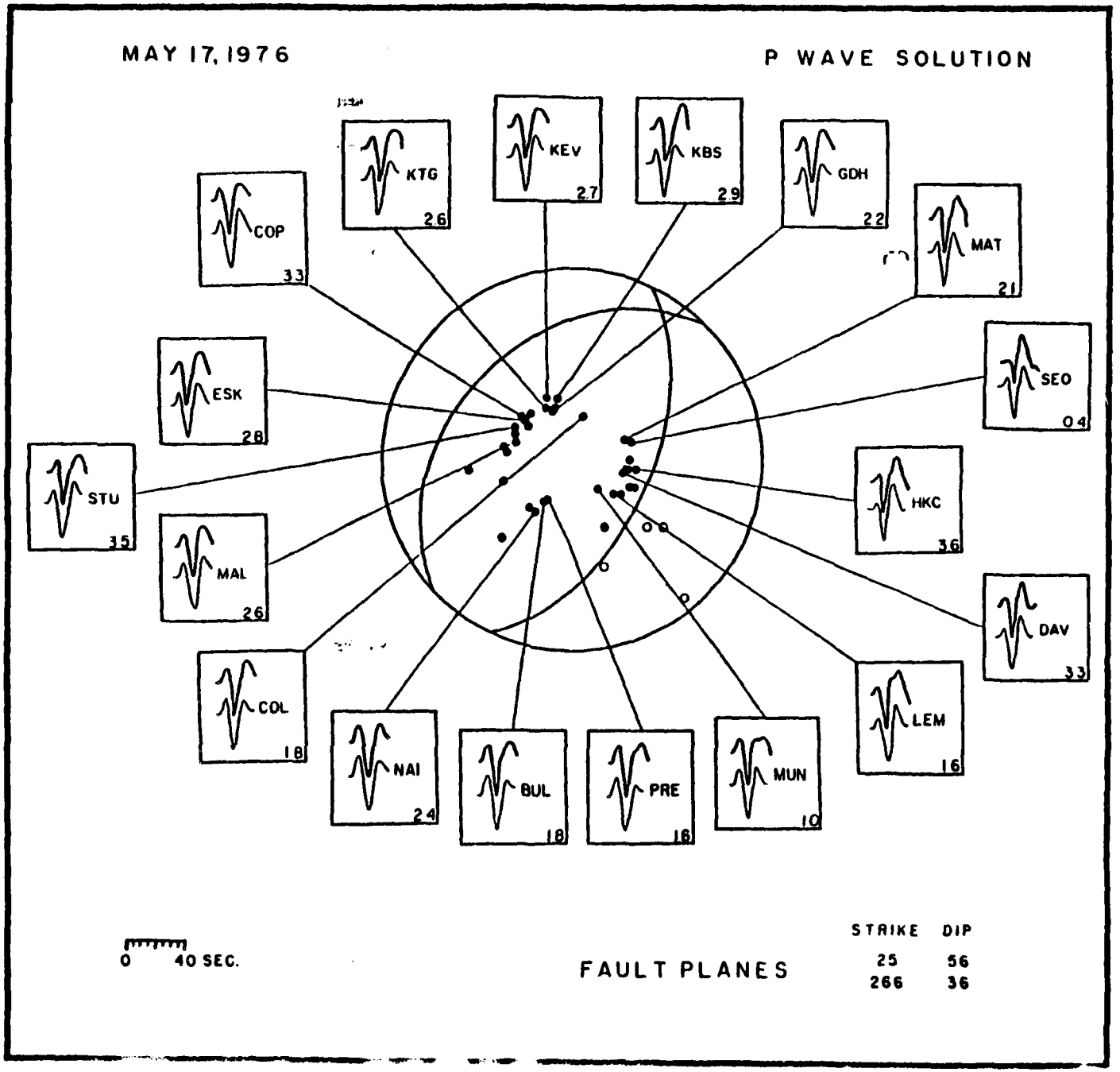
MAY 17, 1976
P WAVE SOLUTION
KTG 26
KEV 27
KBS 29
GDH 22
COP 33
MAT 21
ESK 28
SEO 04
STU 35
HKC 36
MAL 26
DAV 33
COL 18
LEM 16
NAI 24
BUL 18
PRE 16
MUN 10
0 40 SEC.
FAULT PLANES
STRIKE DIP
25 56
266 36

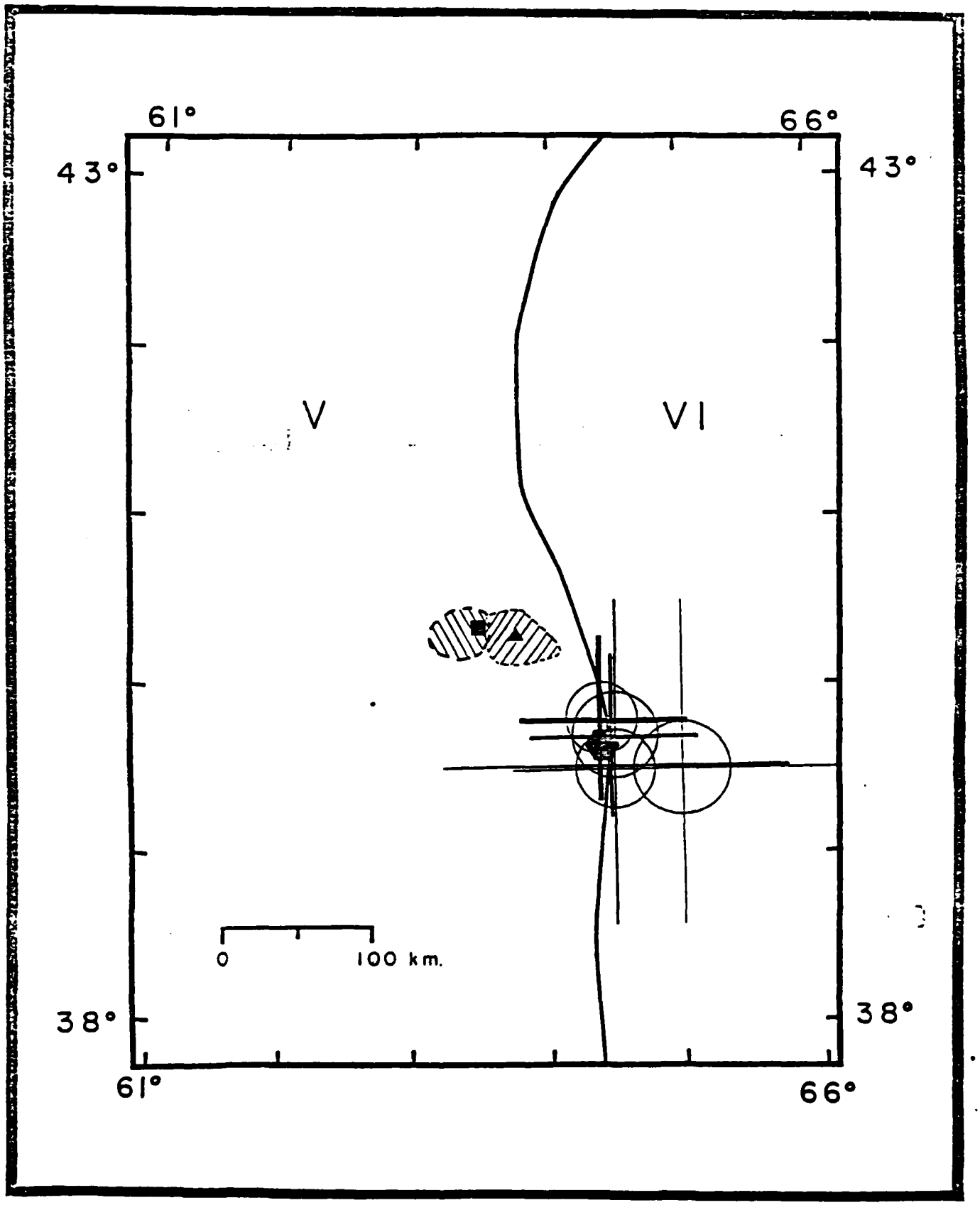
61°
66°
43°
43°
V
VI
0
100 km.
38°
38°
61°
66°

UNCLASSIFIED

SECURITY CLASSIFICATION OF THIS PAGE (When Data Entered)

REPORT DOCUMENTATION PAGE

READ INSTRUCTIONS BEFORE COMPLETING FORM

1. REPORT NUMBER: AFOSR-TR-81-0285	2. GOVT ACCESSION NO: AD A097178
3. RECIPIENT'S CATALOG NUMBER	
4. TITLE (and Subtitle): Tectonics of Asia and Waveform Studies of the Velocity and Q Structure of the Mantle.	5. TYPE OF REPORT & PERIOD COVERED: Interim, 1 Sept. 1979-31 Oct. 1980
	6. PERFORMING ORG. REPORT NUMBER
7. AUTHOR(s): Lynn R. Sykes, Laurence J. Burdick	8. CONTRACT OR GRANT NUMBER(s): F49620-79-C-0021
9. PERFORMING ORGANIZATION NAME AND ADDRESS: Lamont-Doherty Geological Observatory of Columbia University, Palisades, New York 10964	10. PROGRAM ELEMENT, PROJECT, TASK AREA & WORK UNIT NUMBERS: 61102F 3291/32
11. CONTROLLING OFFICE NAME AND ADDRESS: AFOSR/NP, Bolling AFB, DC 20332	12. REPORT DATE: Oct 1980
	13. NUMBER OF PAGES: 128
14. MONITORING AGENCY NAME & ADDRESS (if different from Controlling Office)	15. SECURITY CLASS. (of this report): Unclassified
	15a. DECLASSIFICATION/DOWNGRADING SCHEDULE

16. DISTRIBUTION STATEMENT (of this Report)

Approved for Public Release; Distribution Unlimited

17. DISTRIBUTION STATEMENT (of the abstract entered in Block 20, if different from Report)

18. SUPPLEMENTARY NOTES

19. KEY WORDS (Continue on reverse side if necessary and identify by block number)

earthquake mechanisms
lateral variations
Himalayas
Gazli earthquakes
upper mantle structure
synthetic seismograms
waveform modeling

20. ABSTRACT (Continue on reverse side if necessary and identify by block number)

During the term of this contract work on Tectonics of Asia (P.I. Lynn R. Sykes) was carried out in the following areas:

1) A study of the focal mechanisms of small magnitude earthquakes in Central Asia using surface waves.

(over)

DD FORM 1 JAN 73 1473 EDITION OF 1 NOV 65 IS OBSOLETE

UNCLASSIFIED 404497

SECURITY CLASSIFICATION OF THIS PAGE (When Data Entered)

20. (con't.)

Work on Waveform Studies of the Velocity and Q Structure of the Mantle (P.I. Larry J. Burdick) has been carried out in the following areas:

1) Waveform modeling studies of the structure of the upper mantle have been carried out in both the U.S. and Europe. The results are compared to those of other regions to form a composite picture of lateral variations in upper mantle structure.

2) A study of the seismicity patterns in the region of the Gazli earthquakes in the Soviet Union was carried out to attempt to understand why these unusual earthquakes occurred where they did. The focal mechanisms of the two main shocks were determined by analysis of the body waveforms.

3) A site quality survey of WWSSN stations in India and Southern Asia has been made. It was found that all stations near the continental collision boundary are situated on dipping structure that strongly distorts particle motion.

4) An analysis is presented of the importance of measurements of the relative attenuation of P and S waves to determination of the frequency dependance of Q.


DATE
ILME